2019-03-06

Partial Upgrading of Oilsands Bitumen and Heavy Oil: Kinetic Modeling and Reactor Design

Balaghi, Vahideh Arabi

UNIVERSITY OF CALGARY

Partial Upgrading of Oilsands Bitumen and Heavy Oil: Kinetic Modeling and Reactor Design

by

Vahideh Arabi Balaghi

A THESIS

SUBMITTED TO THE FACULTY OF GRADUATE STUDIES

IN PARTIAL FULFILMENT OF THE REQUIREMENTS FOR THE

DEGREE OF MASTER OF SCIENCE

GRADUATE PROGRAM IN CHEMICAL ENGINEERING

CALGARY, ALBERTA

MARCH, 2019

Abstract

Partial Upgrading of bitumen and extra-heavy oil has gained significant relevance as an opportunity to economically satisfy pipeline specifications with reduced or no addition of diluent. Through a combination of mild hydrogenation and catalytic steam cracking processes, the Hydro-Steam technology proposed for partial upgrading of heavy oil and bitumen, produces oil with bench scale demonstrated low viscosity and high API gravity that meets the minimum standard for pipeline transportation. This process is undertaken directly on dried SAGD produced bitumen without distillation or separation of any kind.

As part of the technology development, this research conceived and carried out a set of experiments in a continuous flow isothermal trickle bed reactor using a chemically novel catalyst, disposed in a conventional fixed bed and using Athabasca bitumen as the feedstock to study the effect of operating conditions on bitumen partial upgrading. A wide set of characterization techniques was used to evaluate the performance of the hydrogenation unit in terms of liquid product quality.

The hydrogenation reactor was modeled as a trickle bed reactor and an optimization technique based on minimization of the sum of square errors (SSE) between the experimental and model predicted concentrations of sulfur and asphaltene, was developed to obtain kinetic parameters for hydrodesulfurization (HDS) and hydrodeasphaltenization (HDAs) reactions. Experiments were conducted in the temperature range of 325-350 °C and liquid Weight Hourly Space Velocities (WHSV) of 0.2-0.5 hr^{-1}, while keeping the pressure and H_2/Oil ratio constant at 1400 psig and 900 Scm^3/cm^3 respectively, in the hydrogenation reactor operating in an up-flow mode. API gravity improved substantially from 9 to slightly lower than 17 and viscosity was improved remarkably from 78750 cP to 1720 cP, both measured at 25°C. Viscosity values under 500 cP are reached once the mildly-hydrogenated bitumen is processed and further upgraded in a second catalytic steam cracking reactor. HDS up to 60% and HDA up to 55% were obtained during this hydrogenation step. The improved characteristics make the upgraded oil almost ready for export, refining and marketing.

Acknowledgements

First and foremost, I would like to express my sincere and deepest gratitude to my supervisor, Professor Pedro Pereira Almao for accepting me in the Catalysis and Adsorption for Fuels and Energy (CAFE) research group. During my tenure, he contributed to a rewarding graduate school experience by giving me invaluable insights, engaging me in new ideas, and demanding a high quality of work in all my endeavors. There are no words to describe his unconditional support.

Experimental results described in this thesis were accomplished with the help and support of fellow lab-mates and collaborates. I would like to thank Dr. Monica Bartollini, Peter Gwozdz and Josune Carbognani who helped me in the pilot plant during the reactor start-up and characterizing the collected samples. I gained a lot from Lante Carbognani's vast organic chemistry knowledge and I would like to thank Dr. Gerardo Vitale for synthesizing the catalyst without which none of my experiments in the pilot-plant could have happen. I also thank all the CAFE group members that participated somehow in this project.

I would like to acknowledge the Department of Chemical and Petroleum Engineering at the Schulich School of Engineering, University of Calgary.

I would like to express my deepest gratitude to my husband, Ali, who has been a constant source of support and encouragement during the challenges of graduate school and life and, my daughter, Eileen, who patiently watched me through all the challenging steps of my thesis.

I owe a debt of gratitude to my mother, Farideh, and my father, Vali, for their constant love and support and my sister, Saiedeh, for cheering me up constantly.

Lastly, I offer my regards and blessings to all of those who supported me in any respect during completion of this thesis.

Dedication

To my beloved daughter, Eileen

To my love, Ali

Table of Contents

List of Tables

List of Figures and Illustrations

List of Symbols, Abbreviations and Nomenclature

Symbols

A_C	Surface area (cm^2)
A_j	Pre-exponential factor for reaction j
a	Dimensionless number
a_s	Liquid-solid interfacial area (cm^{-1})
C_i^L	Molar concentration of compound i in liquid phase (mol cm^{-3})
C_i^S	Molar concentration of compound i on catalyst surface (mol cm^{-3})
$d_{15.6}$	Specific gravity @ 15.6 °C
d_P	Spherical particle diameter (cm)
D_R	Reactor diameter (cm)
D_i^L	Molecular diffusivity of component i in the liquid (cm^2 s^{-1})
De_i	Effective diffusivity of component i (cm^2 s^{-1})
EA_j	Activation energy for reaction j (J mol^{-1})
G_L	Liquid Mass velocity (g cm^{-2} s^{-1})
h_i	Henry's coefficient for component i (MPa)
H_i	Henry's coefficient for component i (MPa cm^3 mol^{-1})
i	Sul, Asph, H_2, H_2S
j	HDS, HDAs
k_i^S	Liquid-solid mass-transfer coefficient for compound i (cm s^{-1})
$k_i^L a_L$	Gas-liquid mass transfer for compound i (s^{-1})
k_j	Rate constant for reaction j
m_{cat}	Catalyst load (g)
MW	Molecular Weight (g mol^{-1})
nm	nanometer
P_i^G	Partial Pressure of component i (MPa)
P	Pressure (psig)
R	Universal constant of gases (J mol^{-1} K^{-1})
r_j	Rate of reaction j (mol g^{-1} s^{-1})
S_P	Total geometric external area of catalyst (cm^2)
T	Temperature (K)

T_{meABP}	Mean average boiling point °R
t_v	Valve cycle time (min)
u_G	Superficial gas velocity (cm s^{-1})
u_L	Superficial liquid velocity (cm s^{-1})
V_P	Total geometric volume of catalyst (cm^3)
V_g	Pore volume per unit mass of catalyst ($cm^3\ g^{-1}$)
w_i	Weight percent of component i
z	Axial reactor coordinate (cm)

Greek Letters

η_j	Catalyst effectiveness factor for reaction j
η_{CE}	Catalyst Wetting Efficiency
$\Delta\rho_T$	Temperature dependence of liquid density (lb ft^{-3})
$\Delta\rho_P$	Pressure dependence of liquid density (lb ft^{-3})
$\rho_{bitumen}$	Liquid density at pumping condition (g cm^{-3})
ρ_L	Liquid density at process condition (g cm^{-3})
ρ_0	Density of bitumen at 15.6 C and 101.3 kPa (lb ft^{-3})
ρ_B	Bulk density of catalyst particles (g cm^{-3})
ρ_P	Particle density (g cm^{-3})
λ_{H_2S}	H_2S solubility in crude oil (cm^3 MPa g)
μ_L	Liquid viscosity at process condition (mPa s)
τ	Tortuosity factor
ε	Void fraction of catalyst bed
θ	Particle porosity
φ_i	Thiele modulus for component i
υ_i	Molar volume of component i ($cm^3\ mol^{-1}$)
υ_L	Molar volume of crude oil ($cm^3\ mol^{-1}$)
υ_C^i	Critical specific volume of component i ($cm^3\ mol^{-1}$)
υ_C^L	Critical specific volume of crude oil ($cm^3\ mol^{-1}$)
$\dot{\upsilon}_{H_2}$	Volumetric flow of hydrogen ($cm^3\ min^{-1}$)
$\dot{\upsilon}_{Crude}$	Volumetric flow of crude oil ($cm^3\ min^{-1}$)

Abbreviations

API	American Petroleum Institute
ASTM	American Society for Testing and Materials
bbl/d	Barrels per day
CAFE	Catalysis and Adsorption for Fuels and Energy
CNOOC	China National Offshore Oil Company
CSC	Catalytic Steam Cracking
cSt	Centistokes
DC	Delayed Coking
EBR	Ebullated bed Reactor
FBR	Fixed Bed Reactor
HDAs	Hydrodeasphaltenization
HDM	Hydrodemetallization
HDN	Hydrodenitrogenation
HDO	Hydrodeoxygenation
HDS	Hydrodesulfurization
HDT	Hydrotreating
L-H	Langmuir Hinshelwood
MBR	Moving Bed Reactor
MCR	Micro Carbon Residue
NEB	National Energy Board
nm	Nanometer
PBR	Packed Bed Reactor
SAGD	Steam Assisted Gravity Drainage
SCO	Synthetic Crude Oil
SSE	Sum of Square Errors
SPR	Slurry Phase Reactor
TAN	Total Acid Number
TBR	Trickle Bed Reactor
USGC	US Gulf Coast
WHSV	Weight hour space velocity (hr^{-1})

Chapter One: Introduction

1.1 Overview of Partial Upgrading

The decline of conventional light and middle crude oil reserves has attracted a growing interest in heavy crude oil and bitumen exploitation to ensure secure supplies and to meet robust energy demand growth. Canada has the third largest crude oil reserves in the world, most of which in the oil sands, accounting for 10 percent of world's proven oil reserves (COR, 2017). The oil sands, the strategic resource contributing to economic opportunity and energy security for Canada, North America and the global market comprise more than 98 percent of Canada's 167.7 billion barrels of proven oil reserves as of December 2017 (COR, 2017). According to Alberta Energy Regulatory, Canadian heavier crude oil is expected to surpass medium crude oil production in 2020 and is projected to displace Mexican and Venezuelan imports to the US Gulf Coast (USGC). The Canadian heavy and extra-heavy oil production is forecasted to continue increasing to 133.3 10^3 bbl/d in 2027 (COP, 2018). In 2017, almost 43% of the raw bitumen produced in Alberta was sent for upgrading, a method of processing bitumen extracted from the oil sands to make it lighter, equivalent to synthetic crude oil (COR, 2017). Syncrude, Canadian Natural Resources, Suncor, Shell, Nexen-CNOOC and Husky are the major companies with upgrading capacity. According to Natural Resources Canada, total upgrading capacity in Canada is reported to be 1.29 million barrels per day. Most oilfields are at a considerable distance from the refineries that convert crude oil into usable products, and therefore the oil must be transported through pipelines, tankers or by rail. However, some form of treatment is required for heavy crude oil near the reservoir before it is ready to be carried considerable distances through the pipelines. The high cost of building greenfield refineries and the insufficient pipeline capacity in Canada limits heavy crude oil and

bitumen refining for either domestic use or export. The current crude oil pipeline capacity exiting Western Canada is estimated at 3.9 million barrels per day (COR, 2017), while according to Statistics Canada, in March 2018 bitumen production hit a new record of 1.81 million bbl/day, bringing the total production to 4.2 million bbl/day in Canada (Oil Sands Magazine, 2018). So far, pipelines are the most cost effective and environmentally friendly means for continuous transportation of crude oils from production fields to refineries. However, pipeline viscosity and density limits specified by pipeline companies require upgrading bitumen to a lighter crude oil to ensure a smooth and efficient operation. The pipeline companies operating extensive and complex pipelines, regulated by the NEB, include Enbridge, Kinder Morgan, Pembina, Portland-Montreal Pipe Line and TransCanada.

Over 60 percent of Alberta's oil sands production is in the form of bitumen (COP, 2018). Once produced, bitumen must be transported to refineries. The non-upgraded bitumen accounting for the majority of that is diluted with lighter viscosity products, (i.e. gas condensates, refinery naphtha or a mixture of light hydrocarbons) to make it less viscous to be transported through pipeline and a small portion is upgraded to synthetic crude oil (SCO) to be used by refineries. Generally, this alternative is too expensive and at the same time the fully upgraded oil has to compete with the expanding supply of US unconventional oil. The use of diluent to meet pipeline specifications requires plentiful supply of gas condensate or naphtha, which is usually up to 30 percent volume. This portion can reach as high as 50 percent volume in case synthetic crude oil is used as diluent. Returning the separated diluent after delivering the SCO is expensive and requires additional pipeline capacity. Producers need to find a way to reduce or eliminate diluent that would free up as much as 600,000 bbl/day of Canada's export pipeline (Oil Sand Magazine, 2018). This is equivalent to the volume of either Trans Mountain or Keystone expansion line. Diluted Bitumen

is a combination of heavy oil extracted from the oil sands, bitumen and diluent. The diluted mixture allows the crude oil, usually referred to as "dilbit" in the industry, to meet pipeline specifications in line with federal regulations.

In March 2012, Suncor cancelled the Voyageur upgrader and in July 2016, the upgrader at the Long Lake in situ project was suspended by CNOOC, and having the Northwest Sturgeon Upgrader as the only constructed upgrader which required substantial public investment by the province of Alberta, indicates that without public subsidies there is no strong business case for full upgraders (Alberta Oil, 2014). In addition, as per Alberta's Royalty Review Advisory Panel, not being able to compete with the expanding supply of U.S. light unconventional oil, makes marketing of Alberta's synthetic crude oil (SCO), difficult or infeasible due to its high capital costs (ARRAPR,2016). This has led "**Partial Upgrading**" to gain significant relevance in the industry as an opportunity to process bitumen into a transportable product having the potential to reshape the oil sands industry. In contrast to full upgrading, partial upgrading produces a crude oil with the characteristics of a medium or heavy crude oil at a lower cost per barrel. A new approach is required for developing processes that upgrade bitumen just enough to meet pipeline specifications and to reduce the cost of downstream processing units.

The principal objective for partial upgrading of bitumen is to economically satisfy pipeline specifications, also known as Enbridge Mainline Specifications meeting both density of 940 kg/m^3 at 15 °C and viscosity of 350 cSt at the published Enbridge Reference Temperature, with reduced or no addition of diluent. Table 1.1 shows the current specifications for pipeline transportation, and the corresponding properties for bitumen. Viscosities higher than the defined specification in Table 1.1 result in a high pressure-drop in pipeline making the transportation costly and energy intensive. Apart from the desired viscosity and API gravity which affects the transportation cost,

the higher sulfur, nitrogen, metals and high proportions of asphaltene contents add more challenges and limitations when processing heavy and extra-heavy oil in refineries.

Table 1.1 Pipeline specifications and representative Alberta bitumen products (NEB Tariff No. 282).

Property	Pipeline Specification	Athabasca Bitumen	Diluted Bitumen	Synthetic Crude
Viscosity	max 350 cSt at 15°C	~1,000,000 cSt at 25 °C	209 cSt at 15°C	7 cSt at 15°C
Density , kg/m^3	< 940	1015	922	860
Gravity, °API	> 19	8	22	33

1.2 Incentives for Partial Upgrading

The significant benefits associated with partial upgrading of bitumen can be classified into three major groups. The first is the value uplift gained as a result of converting hard to process bitumen to easier to process partially upgraded bitumen. The second benefit is associated with the considerably easier shipment of partially upgraded bitumen with no need or substantially less need of diluent owing to its lower viscosity, which also has an overall effect on transportation costs. As a sequence of the second benefit, eliminating or reducing the need of dilution, frees up the existing pipeline capacity for additional crude oil export representing potential economic benefits.

As discussed earlier, on average 30 volume percent or more of diluent is required to transport bitumen to refineries which takes up pipeline capacity. In addition, owing to the high vapor pressure of the light condensate, it could not be easily returned to Alberta and is used as a gasoline blendstock in the US, especially in summer time. Reports from second quarter of 2017 indicate that approximately US $14 diluent per barrel of bitumen is the cost to reduce the viscosity of

bitumen and to make it transportable by pipeline. On the other hand, the capital cost for a full upgrader per flowing barrel of approximately 60,000 bbl/day was estimated at $11.5 billion in 2013 and ever since, the costs to install new upgraders to produce synthetic crude oil have been escalated. Figure 1.1 illustrates the financial benefits that could be obtained from partially upgrading the bitumen and the overall cost reduction associated with less amount of dilbit.

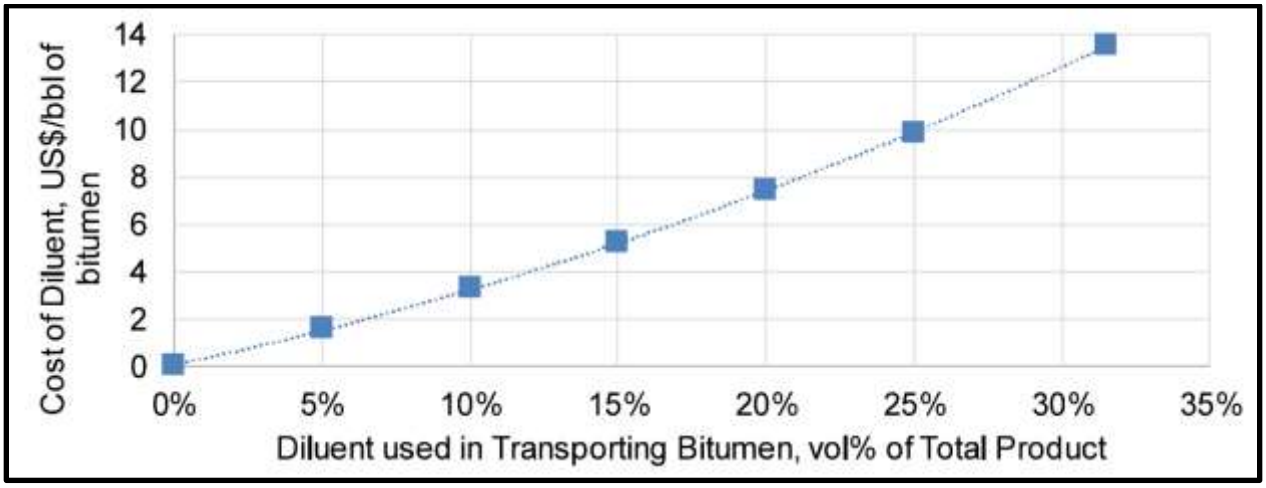

Figure 1.1 Cost of diluent in transporting bitumen (Alberta Innovates, 2018).

An exchange rate of 1.3 CAD/USD, US $35.8 dil-bit price at USGC, US $9.2/bbl pipeline tariff from production site to USGC via Enbridge pipeline with no benefits taken from any bitumen improvements is used as the basis of developing Figure 1.1. It is also assumed that the product meets pipeline specification.

Based on the discussion above, the search for new partial upgrading methods has significant incentives. The CAFE group at the university of Calgary has been focused on developing original catalysts for this purpose and their studies resulted in original and novel manufacturing methods for pelletized fixed bed catalysts applicable for hydrogenation and steam cracking purpose. It has advanced a proposition combining a hydrogenation step that significantly reduces asphalthenes in

the feed and a steam cracking step that increases the light fractions and achieve final quality in the synthetic oil that makes it fully transportable through pipelines, eliminating the diluent fraction, and that generates the hydrogen needed for the first step.

1.3 Objectives

The objective in the experimental studies during this M.Sc. program aims to propose an evaluation of a new partial upgrading technology from the perspective of the province of Alberta. A technology with a focus on consuming full range bitumen as feedstock to meet overarching objectives such as, reduction or elimination the requirement of diluent for transportation purpose, diversification of the bitumen product range, increasing the refining value of the produced product, increasing market accessibility and adding value to Alberta's bitumen resources and increasing investment and creating more jobs within Alberta province. The proposed Hydro-Steam technology aimed to partially upgrade bitumen through a combination of two major processes including mild hydrogenation followed by catalytic steam cracking (CSC) of the hydrogenated feedstock. Bitumen is mildly hydrogenated in the first reactor to prevent rapid catalyst deactivation in the CSC reactor. High quality hydrotreated product from mild hydrogenation unit is directed to CSC for further processing in order to reach the desired viscosity and API gravity. Water molecules are dissociated on a dual function catalyst and the hydrogen radicals are used for promoting cracking. The unconsumed hydrogen produced in CSC unit is recycled back to hydrogenation unit, reducing the hydrogen make-up required for the first step. The proposed scheme for partial upgrading of full range bitumen is shown in Figure 1.2.

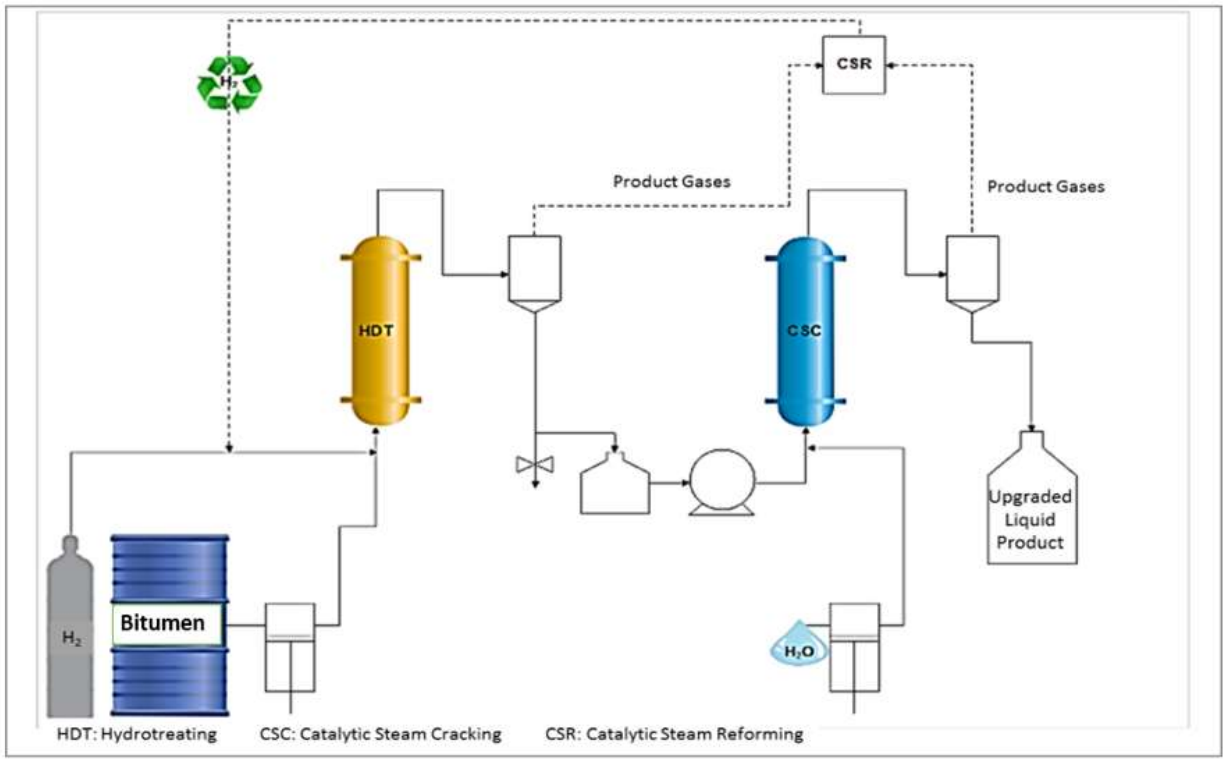

Figure 1.2 Proposed scheme for partial upgrading of full range bitumen (adapted from Truijillo, 2018).

The scope of this thesis is focused on the fixed bed reactor in the hydrogenation step and its major applications can be grouped into the following categories:

1) Bitumen pretreatment, aiming to reduce the contents of sulfur, nitrogen, metals and asphaltene for the catalytic cracking step. In fact, its primary objective is to provide upgraded feedstock in terms of catalyst deactivating agents (Dahl et al., 1996). It is essential to remove sulfur in order to prevent poisoning metallic catalysts in the downstream unit.

2) Partial upgrading of bitumen. In this application, bitumen is hydrotreated in order to upgrade the API gravity and viscosity for transportation purposes, to convert heavy fractions to reduce

impurities for commercialization purposes and to produce better quality oil to be able to be handled by refineries that are not capable to process heavy petroleum.

1.4 Thesis Outline

This thesis is organized in six chapters.

- Chapter 1 introduces the relevance of the research topic and the main objectives proposed for this study.
- Chapter 2 presents a literature review related to main topics related to the thesis including: physical and chemical composition of bitumen and heavy oil, general classification of heavy oil upgrading processes, hydrotreating catalysts and reactors and the main reactions occurring during the catalytic hydrotreating of heavy oil.
- Chapter 3 describes the experimental procedure and the characterization methodology used in this thesis.
- Chapter 4 includes the formulation for the trickle bed reactor model and a description on the numerical and optimization methods used to solve the equations.
- Chapter 5 presents the upgraded liquid product characterization results to evaluate the performance of the unit. In addition, the determined kinetic parameters for hydrodesulfurization and hydrodeasphaltenization reactions along their reaction orders with respect to sulfur, asphaltene and hydrogen and the reactor behavior is studied.
- Chapter 6 summarizes the major conclusions of this thesis and presents recommendations for future research.

Chapter Two: Literature Review

2.1 Physical Composition of Bitumen and Heavy Oil

Heavy oil and has a much higher viscosity and lower API gravity compared to conventional petroleum. Usually in Canada, thermal stimulation of the reservoir is required for the recovery of heavy oil. Petroleum and heavy oils are generally defined in terms of physical properties. Typically heavy oils are considered to have a gravity falling in the API range of 10° to 15°. Cold Lake heavy crude oil for example, has an API gravity equal to 12°. Extra heavy oils are generally incapable of free flow under reservoir conditions and usually have an API gravity in the range of 5° to 10° and a viscosity lower than 10,000 cP (@ reservoir T) whereas Athabasca bitumen for example has an API gravity equal to 8° and its viscosity is above 10,000 cP (@ reservoir T). Depending on the temperature at which the distillation is terminated, residua API gravity would vary but typical values are in the range of 2° to 8° (Speight, 2000). The term bitumen, also on occasion referred to as extra heavy oil, includes a wide variety of reddish brown to black materials of semisolid and viscous character and is frequently found filling the pores of sandstone, limestone or argillaceous sediments. The recovery of bitumen largely depends on the composition and construction of the sands. In general, the bitumen found in tar sand deposits is an extremely viscous material that is immobile under reservoir conditions. Although viscosity is the most important physical property involving the movement of fluids, the use of a single physical parameter is not enough to define bitumen, heavy oil and conventional petroleum. As it is shown in Table 2.1, the properties of two Canadian oil sands derived bitumen are considerably higher than those of a typical bench-mark light crude oil, making it challenging to process these bitumens.

Table 2.1 Selected Properties from two Canadian oilsands-derived bitumens in comparison with West Texas Intermediate (WTI) as a benchmark light crude oil (adapted with permission from Rashad et al., 2012).

Property	Cold Lake bitumen	Athabasca bitumen	Light crude oil (WTI)
Sulfur Content [wt.%]	4.4	4.9	0.3
Metals Content [wt.%]	220	280	3
Gravity, °API	10	9	40.8
Density [kg m^{-3}]	1,000	1,007	821
Viscosity at 40 °C [$mm^2 s^{-1}$]	5,000	7,000	4
Vacuum Residue, > 524 °C	52	52	12.9

2.2 Chemical Composition of Bitumen and Heavy Oil

Crude oil varies in composition from one oil field to another, from one well to another in the same field, and even from one level to another in the same well. This variation can be in both molecular weight and the types of molecules present in crude oil. By definition, a hydrocarbon contains hydrogen and carbon only and if an organic compound contains nitrogen, or sulfur, or oxygen, or metals, it is not anymore a hydrocarbon and instead, it is a heteroatomic compound. It is the location of hetero-elements in the molecule which determines the organic compound. In fact, the chemical and physical reactivity of heteroatomic compounds depend to a large extent, on the heteroatomic function (Fessenden, 1995). It should be noted that the chemical and physical reactivity of the heteroatomic compounds is quite different from those of the hydrocarbons. The primary factors that determine the nature of product that can be obtained from the upgrading of bitumen are the chemical composition and colloidal structure of bitumen which also set the requirements necessary to achieve an economically feasible process.

2.2.1 Elemental Composition

In general, any petroleum including bitumen are composed of five elements to the extent of about 99.4%, comprising carbon, hydrogen, nitrogen, oxygen and sulfur. The rest (up to about 0.6%) is made up of metals in the form of organometallics such as vanadium and nickel. After carbon and hydrogen, sulfur is the most abundant element in petroleum ranging from 0.03 to 7.89 weight percent (Mehran et al., 2007). The main sulfur species found in crude oil are organic and in the form of thiols, sulfides and thiophenic compounds. Figure 2.1 represents the important forms of organic sulfur compounds. More complex sulfur compounds are found in heavy oils with high viscosity and density. During a hydrodesulfurization reaction the cyclic sulfides such as thiolanes and aliphatic acyclic sulfides such as thioethers are much easier to remove when compared to the more resistant to remove sulfur compounds found in aromatic rings, such as thiophene, benzothiophene, dibenzothiphene, benzonaphthothiphene, etc. (Gray et al., 1995). Bitumen contains less aliphatic sulfur and more aromatic sulfur. 62 percent of sulfur in bitumen derived from the oilsands is reported to be in the form of aromatics and the rest are aliphatics (Brons et al., 1995).

Because of the complex nature of petroleum, it is almost impossible to perform an accurate elemental characterization. Hence, a fractional characterization based on polarity and solubility is satisfactory. SARA analysis is the most widely used method for separation of crude oil into four fractions known as: saturates, aromatics, resins, and asphaltenes on the basis of their solubility properties. Asphaltenes being the highest molecular weight fraction in the oil and well known to be coke precursors leading to catalyst deactivation are reviewed in more detail in the next section.

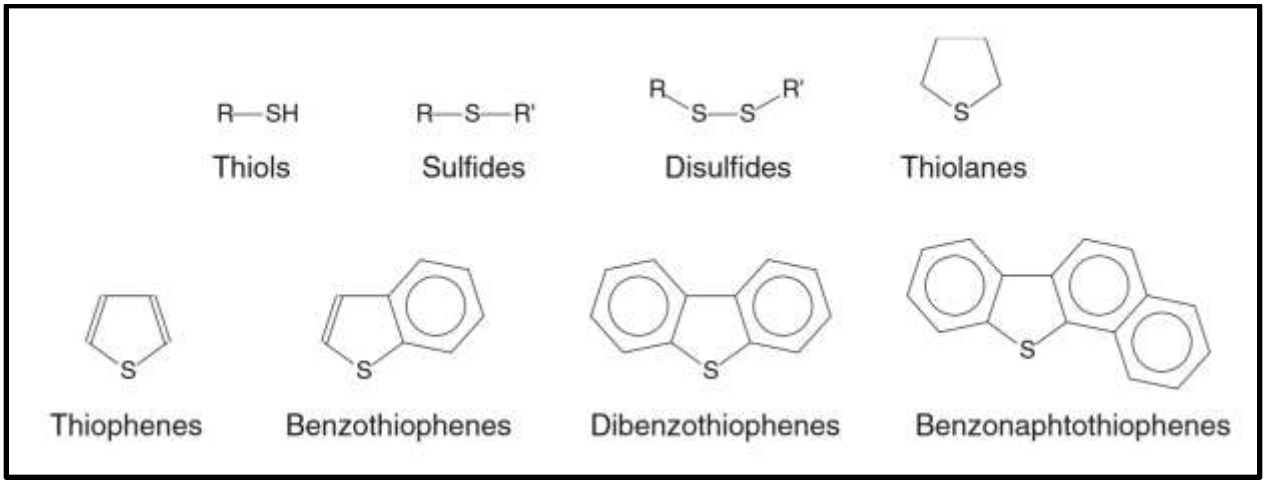

Figure 2.1 Different classes of sulfur containing compounds in crude oil (R=alkyl).

2.2.2 Asphaltenes

Treatment of heavy oil or bitumen with a low-boiling liquid hydrocarbon results in the separation of the most complex fraction known as asphaltenes, which is a brownish to black material and is commonly used in roofing and road paving. The solid to semisolid material has a great tenacity, resistance to break or deforming, will leave little ash when ignited and melts when is heated. The reagents for effecting this separation are commonly n-pentane and n-heptane. Asphaltenes separated from residua, heavy oil and petroleum dissolve readily in benzene, carbon disulfide and chloroform solvents. However, the n-pentane or n-heptane insoluble fraction may not dissolve completely in the aforementioned solvents. Therefore, the definition of asphaltene is restricted to n-pentane or n-heptane insoluble material that dissolves in such solvents as benzene. The portion which is soluble in pentane or heptane is often referred to as maltenes and is further subdivided by percolation through any surface-active material such as alumina to yield an oil fraction. A more strongly adsorbed, red to brown semisolid material known as resins remains on the adsorbent until

desorbed by a solvent such as benzene/methanol mixed solvent. The oil fraction can be further subdivided into aromatics and a saturates fraction. The major parts of heavy feeds contain aggregates of resins and asphaltenes dissolved in oil fraction held together by weak physical interactions. Asphaltenes are a solubility class of compounds mostly found in the residual fractions of petroleum. They are complex polar structures with a poly-aromatic character containing metals, mostly nickel and vanadium, and are usually defined according to their solubility properties. The exact structure of asphaltenes is difficult to obtain. Speight has found alkylic chains of up to 30 carbon atoms (Speight, 1999). Asphaltenes from different sources are characterized by decreased H/C atomic ratios and elevated concentration of heteroatoms, nitrogen, oxygen and sulfur as well as of trace metals and reservoir fines relative to their source material. The sulfur content of asphaltenes is always higher than that of its source material and in the case of oil sands and bitumens, the ratio may be as high as two. Trace metals and heteroelements, N, O, S in petroleum tend to accumulate in the resin and especially the asphaltene fraction. Asphaltenes are known to be composed of sheets of condensed polynuclear and heterocyclic systems with naphtenic rings and alkyl side chains including sulfur, nitrogen, and metal (mainly V and Ni) compounds. Asphaltenes are surrounded by resins when they are in a colloidal state in crude oil and stable in those forming micelles. Aromatics and resins catalytically react easily when compared to asphaltenes owing to their less complex structures. Under hydrogenation conditions, the structure of resins is modified while at the same time cracking of alkyl chains in asphaltene happens leaving the aromatic core with minimum number of branched chains. Metals and other contaminants such as sulfur and nitrogen are present as organo-compounds in the asphaltene aggregates resulting in a heavier structure than its original one. Figure 2.2 represents a schematic representation of an asphaltene aggregate.

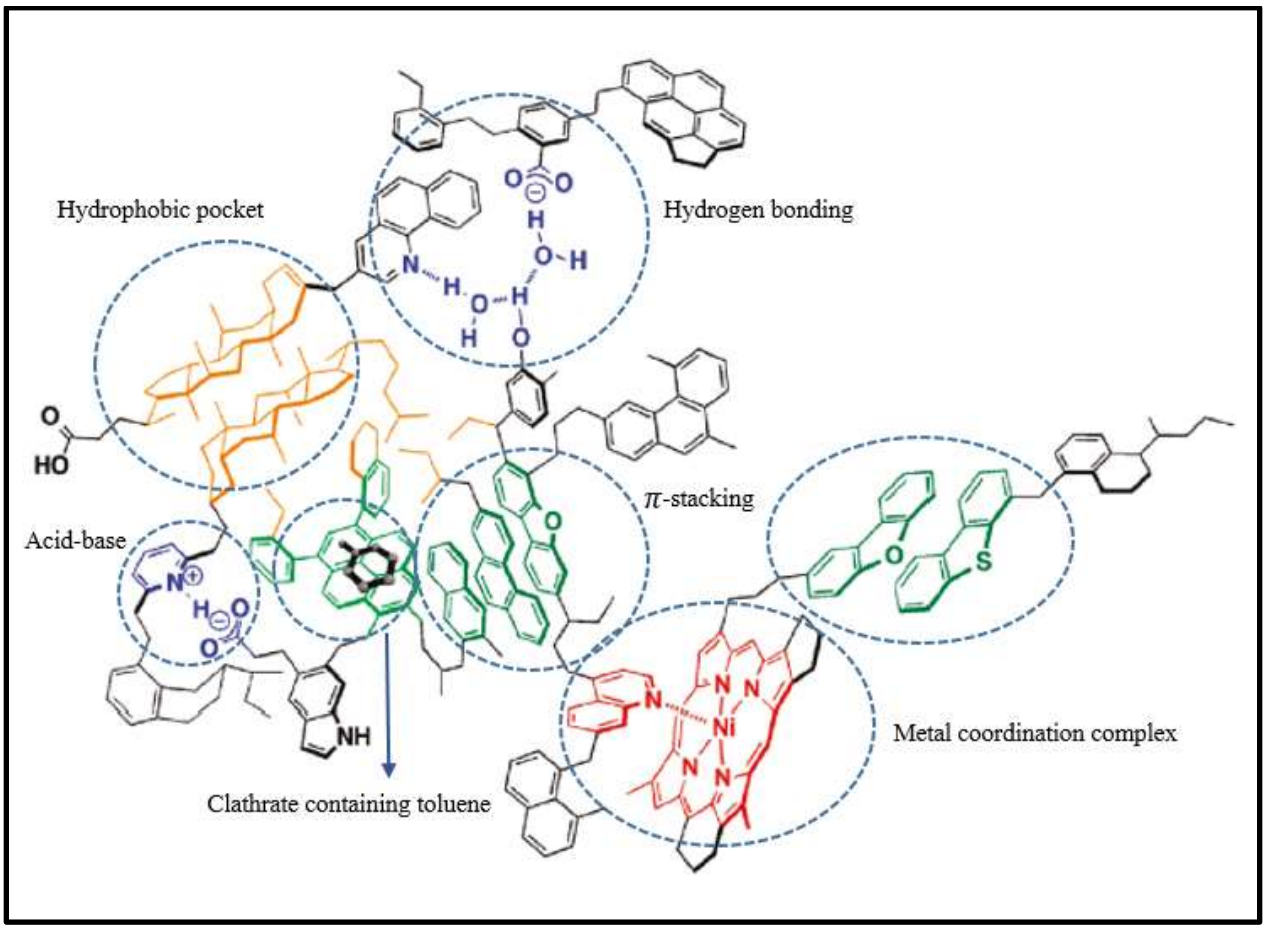

Figure 2.2 Schematic representation of an asphaltene aggregate (adapted with permission from Gray et al., 2011).

2.3 General Classification for Heavy Oil Upgrading Processes

Developing advanced technologies for heavy oil hydro-processing is deemed necessary in order to meet changes in petroleum demand and particularly the reduced demand for heavy oil. A number of technologies have been developed over the years for heavy oil upgrading which have employed two fundamental processes based on hydrogen addition and/or carbon rejection (Le Page et al., 1992) to increase its H/C ratio. In general, the upgrading technologies are either catalytic or non-

catalytic. The non-catalytic carbon-rejection technologies comprise of solvent deasphalting, gasification, coking and visbreaking. Thermal cracking of residue belongs to carbon rejection classification. Hydrotreating and hydrocracking are hydrogen addition technologies, while hydrovisbreaking is a non-catalytic hydrogen addition process. The classification of various technologies used for processing heavy oils is tabulated in Table 2.2.

Table 2.2 Classification of Heavy Oil upgrading processes.

	Non-Catalytic Processes		Catalytic Processes
Carbon Rejection	Solvent Deasphalting	**Hydrogen Addition**	Residue Fluid Catalytic Cracking (RFCC) [1]
	Thermal		Hydro-Visbreaking [2]
	Gasification		Hydroprocessing
	Delayed Coking		Fixed Bed Hydrotreating
	Fluid-Coking		Moving Bed Hydrocracking
	Flexi-Coking		Slurry-Phase Hydrocracking
	Visbreaking		Ebullated Bed Hydrocracking

1. RFCC is a carbon rejection process.
2. Hydro-Visbreaking is a non-catalytic process.

The primary aim of the above upgrading technologies is to obtain synthetic crude oils from heavy oils which contain relatively large amounts of contaminants such as S, O, N, metals and other impurities.

In general, it is not an easy task to decide which upgrading technology is more suitable for certain crude oil. The price of crude oil, level of impurities of the feed, target of upgraded oil quality and process scheme of the refinery at destination must be taken into account while choosing the technology (Ancheyta et al., 2007). A recent review has provided an overview of the emerging technologies having the potential to be used for partial upgrading of heavy oil. Details of some of the key attributes of the technologies are listed in Table 2.3.

Table 2.3 Summary of various partial-upgrading technologies (adapted from ROI., 2015).

Base Technology	Partial Upgrading Technology		Company	API	Diluent Required
Delayed Coking				>27	No
Carbon Reduction	Heavy Improved Quality	HI-Q	MEG Energy	19	No
Carbon Reduction	Heavy to Light	HTL	Fluid Oil Ltd.	19	No
Carbon Reduction	Western Research Institute Thermal Expansion	WRITE PROCESS	Wyoming University	19	Yes
Carbon Reduction	TriStar Project	VCI ADC	Value Creation Inc.	19	No
Hydrogen Addition-Carbon Rejection	Super Critical Water Cracking	SCW	JGC Corporation	19	No
Hydrogen Addition-Carbon Rejection	De-Sulphurization & Upgrading	DSU	Field Upgrading	19	Yes
Hydrogen Addition-Carbon Rejection	ETX IYQ	ETX IYQ	ETX Systems Inc.	23	No
Hydrogen Addition	Fischer-Tropsch Crude	FT-Crude	Expander Energy	22-24	No
Hydrogen Addition	HCAT	HCAT	Headwaters Inc.	22	No
Hydrogen Addition	Eni Slurry Technology	ENI EST	Eni	25-27	No

The technologies are principally different based on the characteristics of the partially upgraded product, the uplift value compared to diluted bitumen, and the cost associated with the complexity of the technology and its development. It should be noted that none of the potential technologies are currently commercially viable. It must be said that Delayed Coking (DC) is not a partial upgrading technology due to the need for distillation, hydrotreating of produced light fractions and coke and gases handling, all considerably increasing the complexity of the upgrading plant. If a

criteria based on complexity and investment per barrel throughput were established, not only DC, but also the ENI slurry process and many others in table 2.3. would not be considered as a partial upgrading methodology.

2.4 Hydroprocessing Catalysts

Although the field of catalysis development for middle distillate hydrotreating and in particular deep-hydrodesulfurization is mature and has advanced to a good extent during the last 50 years (Topsoe et al., 1996), yet challenges remain for heavy oil hydroprocessing. Hydroprocessing of heavy oil is in principle affected by the catalyst properties and its preparation method. Properties such as textural properties of support, acidic or basic nature of catalyst, its catalytic sites and their interaction with support affects to a greater extent the catalyst development. The limitations due to asphaltene precipitation and sediment formation when upgrading heavy crude oil using fixed bed reactors has forced the researchers towards catalysts with large pore size which are able to retain a high quantity of metals and an optimum quantity of nitrogen and sulfur removal. As a result of catalyst improvements during the last years, longer run lengths and lower operating temperatures have been obtained. Knowing that the existing catalysts are still not working as efficient as required, some researchers believe that catalysts need to be improved in the direction of better selectivity for hydrogenation and hydrocracking purposes turning the acid base nature of catalysts aiming to reduce the gas production (Leyva et al., 2007). In general, the hydrotreating catalysts are composed of a support to provide the textural nature along with the acid-base properties and active metals to give the desired catalytic activity. Al_2O_3 and its mixed oxides supports such as Al_2O_3-TiO_2, Al_2O_3-TiO_2, Al_2O_3-MgO_2, etc. are commonly synthesized in the laboratory using the homogeneous precipitation method. Owing to the appropriate acidic nature,

mixed oxides such as Al_2O_2-TiO_2 (Jaffe, 1968) and SiO_2-ZrO_2-TiO_2 (Hansford, 1964) were initially developed for hydrocracking purposes. Using an incipient wetness method, Molybdenum was impregnated and with a sequential impregnation procedure on Molybdenum loaded catalyst, Ni or Co promoted catalysts were prepared. In hydroprocessing applications in order to promote hydrogenolysis and hydrogenation functions of the catalysts and to some extent diminish support acidity, active metals (mostly Mo, W, Ni and Co) are deposited on the amorphous and crystalline supports. Depending on the application, one catalyst type would be preferred over another. In general, CoMo catalyst are better for hydrogenolysis whereas, those based on NiCo are more hydrogenating (Topsoe et al., 1996). In order to remove the most refractory sulfur compounds, NiMo catalysts are more efficient and they are used when extreme hydrogenation is required whereas, CoMo catalysts are applied for sulfur removal from unsaturated hydrocarbons (Betaille et al., 2000). CoMo catalysts are preferred in batch reactors while NiMo catalysts are more efficient in flow reactors and when the contact time between crude and hydrogen is limited (Lecrenay et al., 1997). Ni/Mo catalyst supported on γ-alumina is widely used for hydrotreating process. The active metals are in their sulfide forms in the presence of hydrogen sulfide or any organic sulfur compounds, with NiS acting as a catalytic promoter of crystalline MoS_2 (Prins et al., 2008). Typically 10-14 wt% of the catalyst (on a metals basis) contains molybdenum while the nickel promoter is added up in the range of 2-4wt%. Metal sulfides supported on γ-alumina are known to be bifunctional catalysts where the metal crystallites provide hydrogenation activity and the alumina surface promotes cracking. In summary, in the case of hydrogenating bitumen and heavy oil, large molecules of asphaltene consisting of highly condensed heterocyclic and aromatic rings containing nickel and vanadium are expected to deposit coke on the catalyst surface near the pore mouth. In addition, since most of the heteroatoms are concentrated in the asphaltene fraction, the

deposited metal sulfides such as V_xS_y and Ni_xS_y during hydrodemetallization reactions decrease the number of active sites and prevent the transport of reacting molecules to the internal surface of catalyst and cause a complete plug of the catalyst pore. Thus, characterization of catalyst textural properties is of great importance when dealing with asphaltene and heteroatoms. Observations from studies on the catalytic sites during hydrotreating reactions, particularly when dealing with heavy oils containing heteroatoms, show that it is not only the acidic/basic and metal catalytic sites affecting the reaction mechanism but also the physical processes such as reactants diffusion into the pores, adsorption, reactions occurring on the catalytic sites and products desorption and diffusion influence the mechanism to a great extent.

2.4.1 Pore Size

Removing metals and asphaltene is known to be the main objective of the heavy oil processing catalyst. Owing to their large molecular size, both hydrodemetallization and hydrodeasphaltenization reactions are known to be diffusion limited. For example an asphaltene molecule may be 4 to 20 nm in diameter which is too large to pass through micropores or even mesopores of a catalyst. Therefore, in addition to other aspects, pore diameter of the catalyst becomes an important factor in selecting catalysts for hydrotreating purposes. In addition, in order to define the catalyst stability, substantial penetration of metals from the nearest surface to the core of the particle and their retention on the surface is required. The smaller pores contribute to higher surface area whereas larger pores allow easier access for large reactant molecules. The relationship between the surface area and pore diameter is presented in Figure 2.3. In general, the higher active metal dispersion is associated with the higher surface area and the easy diffusion of large reactant molecules is provided with larger pores. Thus, considering the nature of bitumen, bimodal pore

size distribution with an emphasis on keeping a balance between the active metal dispersion and pore diameter must be incorporated into the catalyst. Literature studies reveal that asphaltene conversion is more affected by the pore diameter of catalyst compared to the metallic function such as Mo-Co active sites (Rana et al., 2007). In addition, investigations show that metal removal requires a catalyst which is macroporous in nature (Ancheyta et al., 2005). Catalysts with an average pore diameter of 6.5 nm have shown greater activities towards hydrodesulfurization reactions in comparison to metal and asphaltene removal. In summary, an appropriate catalyst for bitumen hydrogenation should account for diffusion limitations of complex molecules and pore diameter limitations for asphaltene molecules.

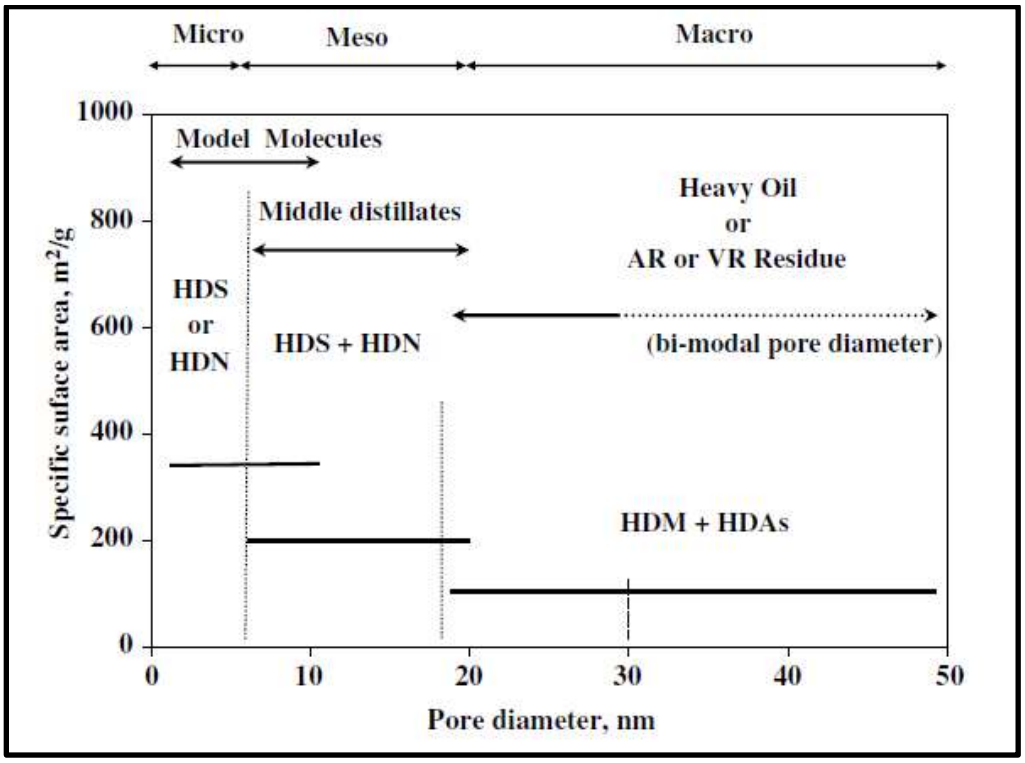

Figure 2.3 Effect of pore diameter and specific surface area on hydrotreating catalyst activities (adapted with permission from Ancheyta et al., 2005).

2.5 Hydrotreating Reactors

Several types of reactors exist for hydrotreating reactions. These include fixed bed reactors (FBR), co-current and counter-current moving bed reactors (MBR), fluidized ebullated bed reactors (EBR) and slurry phase reactors (SPR). In the multiphase catalytic reactions of hydroprocessing, packed bed reactors (PBR) operating with a continuous gas, composed majorly of hydrogen, liquid hydrocarbon feed and solid catalyst phase, so called trickle-bed reactors (TBR) are regularly used as a model reactor. Because of the simplicity, flexibility and ease of TBRs operation, they are widely used in the petroleum and petrochemical industry, especially when dealing with heavy petroleum fraction processing, such as hydrocracking, hydrogenation, hydrodesulfurization, hydrodenitrogenation, etc. Depending on the physical properties of the gas and liquid phases, the flow rates, and the nature and size of the catalyst packing, different flow regimes can exist in a TBR (Lemcoff et al., 2007). A thin liquid film tends to form over the catalyst particle in the TBR reactor and the remaining empty spaces of the catalysts are filled with the gas. In general, at relatively low liquid and gas velocities and at low interaction between these two phases, trickle flow is achieved. The tubular reactors permit a vigorous heat exchange in the reaction zone and ensure a uniform residence time for all particles in the flow. In order to accelerate the mass transfer between phases and to reduce the variation in residence time of the reactants, these reactors are filled with the solid catalysts. Due to the motionless catalyst bed a plug flow is achieved in TBRs which makes them preferable to other reactors where the catalyst is fluidized or slurried. In addition, the low energy dissipation rate and the high catalyst loading per unit volume of the liquid make the TBRs superior to slurry reactors. Several drawbacks are associated with TBRs including the diffusional limitations inside the catalyst as a result of the large particle size. In order to avoid

excessive pressure drop, the reactor must be loaded with large catalyst particles in commercial scales. However, rapid catalyst deactivation caused by metal deposition and coking and therefore reduced length of run is reported to be their main disadvantage when dealing with heavy oil [Sie, 2001]. The presence of any solid particles in the feedstock (iron scale, salts, etc.) and in the reaction products (coke plugs and metal deposits) increase the fouling related problems in TBRs [Chou,2004]. Another main disadvantage of TBRs is related to maldistribution of reactants flow as a result of the reactor's internal hardware poor performance (Alvarez et al., 2007 b). This is leading to an overuse of some parts of the catalyst bed while the rest remains underused. This may induce hot spot formation and as a result, shorter cycle lengths and an overall underperformance of the reactor. The best options to overcome the problems related to catalyst life cycle associated with high metal and asphaltenes content feedstocks is known to be MBRs and EBRs. MBRs are specifically applied in demetallization in front-end of hydrodesulfurization and hydrocracking reactions [Sie, 2001]. The most advanced hydroprocessing reactors applied for upgrading heavy feeds without any pre-treatment requirement are the EBR reactors [Rana et al., 2007]. Van Hasselt et al. reported that applying a counter current reactor results in deeper sulfur conversion of vacuum gas oil (Van Hasselt et al., 1999). Up-flow reactors are preferred when dealing with high gas reactant flux and low liquid reactant flux to catalyst surface (liquid limited reactions) as they provide better catalyst wetting and faster liquid reactant transport to the catalyst surface. In addition, in up-flow reactors the more reactive low boiling point components, are swept out more rapidly when passing into the vapor phase compared to the high boiling material progressing relatively low through the bed. Hence, providing more residence time for the heavy liquid fractions. This results in a better liquid-solid contact and therefore a more accurate kinetic data could be obtained.

2.5.1 Effect of Pressure

In fixed bed reactors pressure affects the transport phenomena and the fluid dynamics through the influence on the properties of gases and liquids. In general, gas solubility, Henry's constant, density, molecular diffusivity, dynamic viscosity, thermal conductivity, heat capacity and surface tension are the most sensitive properties to pressure. However, in the pressure range of trickle bed reactors, above atmospheric conditions and less than 30 MPa, it is expected that the gas phase properties are affected by pressure while the liquid phase is more sensitive to temperature. Among the properties of gas-phase, gas density and diffusivity, gas solubility in the liquid and Henry's constant are reported to be most affected by pressure (Reis et al., 1987). High pressures prevent vaporization of lighter material ensuring it remains in liquid phase and as a result a more efficient contact between hydrocarbon and the catalyst is expected. High pressure is also required in hydrogenation reactions to ensure keeping the hydrogen partial pressure high and increasing the available hydrogen in contact with catalyst and bitumen molecules. This is necessary to avoid undesired loss of catalytic activity due to possible coke deposition on the catalytic surface.

2.5.2 Effect of Liquid Holdup and Wetting Efficiency

Changes in parameters such as wetting efficiency, gas-liquid interfacial area and liquid holdup have been investigated to interpret the effect of pressure and gas density on the hydrodynamics in trickle bed reactors (Al Dahhan and Dudukovic, 1995). The resisting frictional forces at the catalyst surface and driving forces on liquid flow assist the energy dissipation in the reactor. Beside the catalyst bed characteristics, velocities of both gas and liquid phases and the physiochemical properties of flows influence the pressure drop across the reactor. Gas density is the

physicochemical property most affected by pressure and a higher gas density leads to higher pressure gradient across the reactor. In general, the gas phase affects the pressure drop through the superficial gas velocity and gas density whereas the increased gas density may arise from either the use of high molecular weight gases or from higher operating pressures in the reactor. In any of these cases the increased gas density enhances the gas liquid interaction and leads to an increase in the pressure drop. The retention of liquid in the packed-bed or liquid holdup, which is a fractional bed volume and is defined as the volume of liquid per volume of empty reactor, is an important parameter which plays an important role in the performance of heat and mass transfer in a TBR and its hydrodynamics. Liquid holdup is an approximate measure of the liquid and solid catalyst contacting effectiveness. It is essential to have knowledge of liquid holdup to avoid hot spots as a result of poor hydrogen accessibility and poor wetting efficiency leading coke and thus preventing reactor run-aways in highly exothermic reactions such as hydrotreating. Two-phase pressure drop studies show that for given gas and liquid superficial velocities, liquid hold up decreases as a result of an increase in the pressure (Wammes et al., 1990).

The primary design variables affecting holdup are the liquid flowrate, shape and size of catalyst particles, catalyst bed height, gas flowrate and wetting characteristics of packing and fluid (Satterfield, 1975). The partial catalyst wetting is found to be a common phenomenon in TBRs (Sakornwimon, 1982). This may result from a poor liquid distribution caused by an inappropriate design of the liquid distributor or from an inadequate ratio between reactor and particle diameter. The external wetting efficiency or the fraction of the external surface of particle wetted by the liquid has an important effect on the rate of reaction in a TBR.

2.6 Chemistry and Reaction Mechanisms of Hydroprocessing

The simplified chemistry of hydrotreating (HDT) reactions can be generalized as a hydrogen transfer process where the heteroatoms are replaced with hydrogen supplied from an external source and as a result of various hydrogenation and hydrogenolysis mechanism to reduce the molecular weight of the hydrocarbon mixture. Heteroatoms are any atoms present in the petroleum other than hydrogen or carbon. Depending on the objective of the process the reactions taking place during catalytic HDT are classified based on the removed impurity from crude oil. Kinetic studies for hydrotreating of heavy oil focus on the overall rate of several classes of reactions simultaneously occurring: hydrodesulfurization (HDS), hydrodenitrogenation (HDN), hydrodeoxygenation (HDO), hydrodemetallization (HDM), hydrodeasphaltenization (HDAs) and hydrodearomatization (HDAr). Hydrogenolysis and hydrogenation are known to be the two parallel mechanisms occurring in catalytic HDT reactions. By the action of hydrogen, the reaction path of hydrogenolysis involves the direct scission of a carbon-heteroatom single bond whereas in hydrogenation, without cleaving bonds, hydrogen is added to the molecule. In most cases, hydrogenation is necessary prior to hydrogenolysis. The main reactions occurring during catalytic hydrotreating of heavy oil are reviewed in the following section:

2.6.1 Hydrodemetallization

Nickel and Vanadium concentrated in the heaviest fraction of heavy oil, specially the asphaltenic fraction are in the form of metalloporphyrins. A reaction mechanism proposed for metalloporphyrins HDM involves hydrogenation of pyrrole subunits, followed by the hydrogenolysis path involving bond cleavage of Ni-N and N-V (Janessens et at., 1996). During

the irreversible reaction of hydrodemetallization (HDM), Ni and V are converted to their respective metal sulfides and deposit onto the catalyst surface. Asphaltenes disintegration is a prerequisite to allow HDM reactions to proceed as most of V and Ni is associated with asphaltenic fractions.

2.6.2 Saturation Reactions

Hydrogenation reactions comprise of saturation of olefins and aromatics. Aromatics in petroleum fractions are divided into mono-, di-, tri-, and polynuclear aromatics. Due to the stability of benzene and its homologues, saturation of mono-aromatics is the most difficult step. Hydrogen addition on multi-aromatics proceeds sequentially ring by ring and equilibrium favors the saturation of the first ring (Ali, 2017). Hydrogenation of olefins are found to be irreversible while saturation of aromatics to produce naphthenes are reversible.

2.6.3 Hydrodesulfurization

Hydrodesulfurization (HDS) is aimed to extract sulfur from S-heterocycles and as a result H_2S is produced. Both the structure of sulfur components and the hydrocarbon type greatly affect the HDS reaction. Alkyl Sulfides are the most reactive hydrocarbons followed by naphtenes and aromatics. In terms of structure, the most reactive species are sulfides and mercaptans followed by naphthenic aromatic structures. The least reactive compounds are pure aromatic S-compounds like benzothiophenes, di-benzothiophenes and alkyl-substituted dibenzothiophenes whereas the most refractory species are the five-membered aromatic structures (Mochida et al., 2006). Direct hydrogenolysis mechanism or indirect hydrogenation as the two possible pathways for HDS reactions are shown in Figure 2.4. Saturation of the aromatic ring is required prior to sulfur removal

in the indirect route while the other mechanism requires elimination of sulfur atom and replacing it with hydrogen. As a result of further hydrogenation, a complete saturation of the S-free product is possible. With respect to hydrogen consumption and efficiency, direct route is the preferred pathway. However, it is strongly influenced by the structural effect of the molecules. The substitution of alkyl groups close to the sulfur atom in the ring or the aromatic ring condensation leads respectively to steric hinderance of the molecule and additional stability and, as a consequence, makes it less reactive. On the other hand, the indirect route is less affected by molecular structure. The S-C energy bond is reduced as a result of aromatic ring hydrogenation allowing easier bond cleavage. Saturated structures are believed to reduce the barrier for sulfur atoms to access the catalyst active sites (Mochida et al., 2006). It has been reported that the hydrodesulfurization of resins and aromatics are limited as a result of the presence of asphaltene in the HDM section during hydroprocessing in fixed bed reactors (Guibard et al., 2005). Proceeding from the HDM section the asphaltene aggregates exposed to HDS section are still large and could not easily access the pores and as a result the HDS reaction is limited. The experiments carried out by a group of researchers (Le Lannic et al., 2007) reveal that sulfur is removed almost 100% from resins and aromatics during HDS of demetallized and deasphatled feedstock. Due to the presence of asphaltenes which block and ultimately retard the access to active sites, HDS is reported to undergo a slower reaction when dealing with asphaltenic feedstocks.

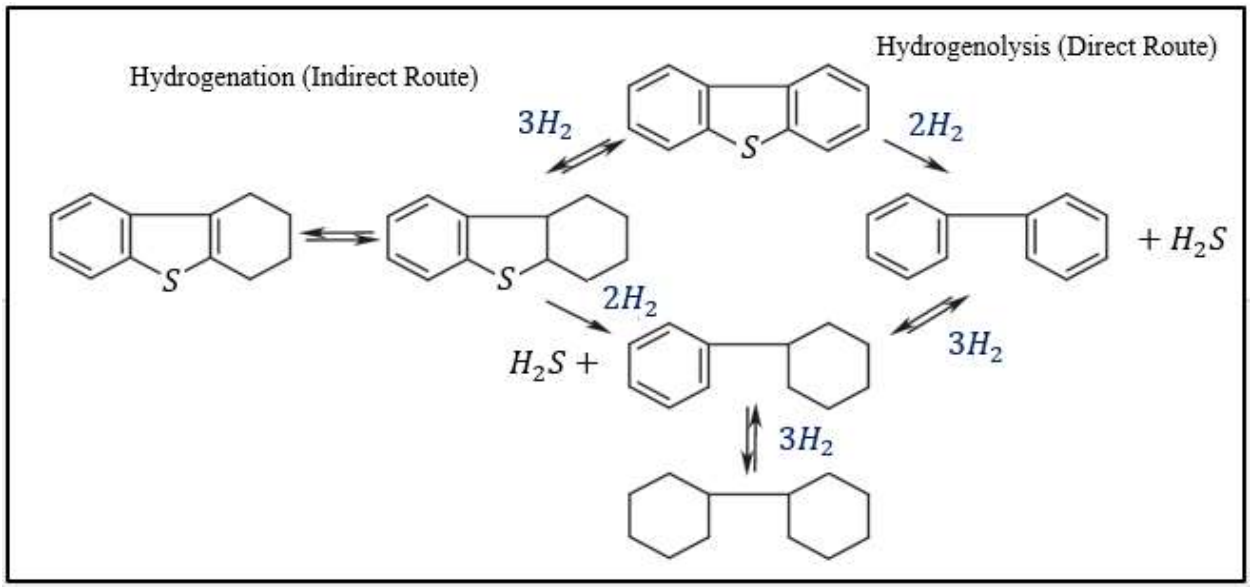

Figure 2.4 Hydrogenation and hydrogenolysis reaction pathways for hydrodesulfurization of dibenzothiophenes (Whitehurst et al., 1998).

Depending on the required degree for desulfurization and sulfur structure, conditions in the hydrotreating reactor are set up. The most reactive aliphatic sulfurs are completely removed during HDS as presented by Equations 2.1 – 2.3 (Rashad et al., 2012).

$$Thiols: R - SH + H_2 \rightarrow R - H + H_2S \quad 2.1$$

$$Sulfides: R_1 - S - R_2 + 2H_2 \rightarrow R_1 - H + R_2 - H + H_2S \quad 2.2$$

$$Disulfides: R_1 - S - S - R_2 + 3H_2 \rightarrow R_1 - H + R_2 - H + 2H_2S \quad 2.3$$

The resonance stabilization of the sulfur lone pair electrons participating in the π structure of C=C bonds is less than that of benzene in thiophenic rings and makes the indirect pathway which is saturation of aromatics prior to HDS the desirable route. However, due to the strong driving force for aromatization followed by dehydrogenation, the equilibrium concentration of the intermediate product is low. In general, the effectiveness of desulfurization is strongly influenced by properties

of heavy oil such as high metal content, coking and fouling propensity and steric protection of the thiophenic sulfur. The latter makes the adsorption of sulfur compounds difficult on the catalyst surface while the first two lead to a catalyst deactivation. Also, high molecular size of sulfur compounds limit access to smaller pores in the catalyst. Literature reviews also show a change in reaction selectivity being hydrogenation dominant at lower temperatures and hydrocracking dominant at high temperatures (Ancheyta et al., 2003).

2.6.4 Hydrodenitrogenation

Nitrogen species in petroleum are categorized as basic (quinoline, acridine, pyridine, etc.) and nonbasic N-compounds (indole, carbazole, pyrrole, etc.) and are mostly found in aromatic rings. Non-basic nitrogen compounds rapidly react with hydrogen and convert to basic compounds (Furimsky et al., 2005). Basic N-compounds are known as site inhibitors for hydrogenation and all hydrotreating reactions following this reaction route. For the HDN reaction to occur, a complete hydrogenation of aromatic rings is required to weaken the strong C-N bond prior to hydrogenolysis (Girgis et al., 1991). As it is presented in Figure 2.5, the fast and preferred reaction route proceeds by first saturating both rings of quinoline followed by the C-N bond cleavage. The other route is known to be very slow and is neglected while studying the reaction mechanism of HDN reaction (Dolbear, 1998). It is widely accepted that HDN is more difficult compared to other hydrotreating reactions such as HDS and even HDM and HDAs specially when dealing with heavy oil and residue.

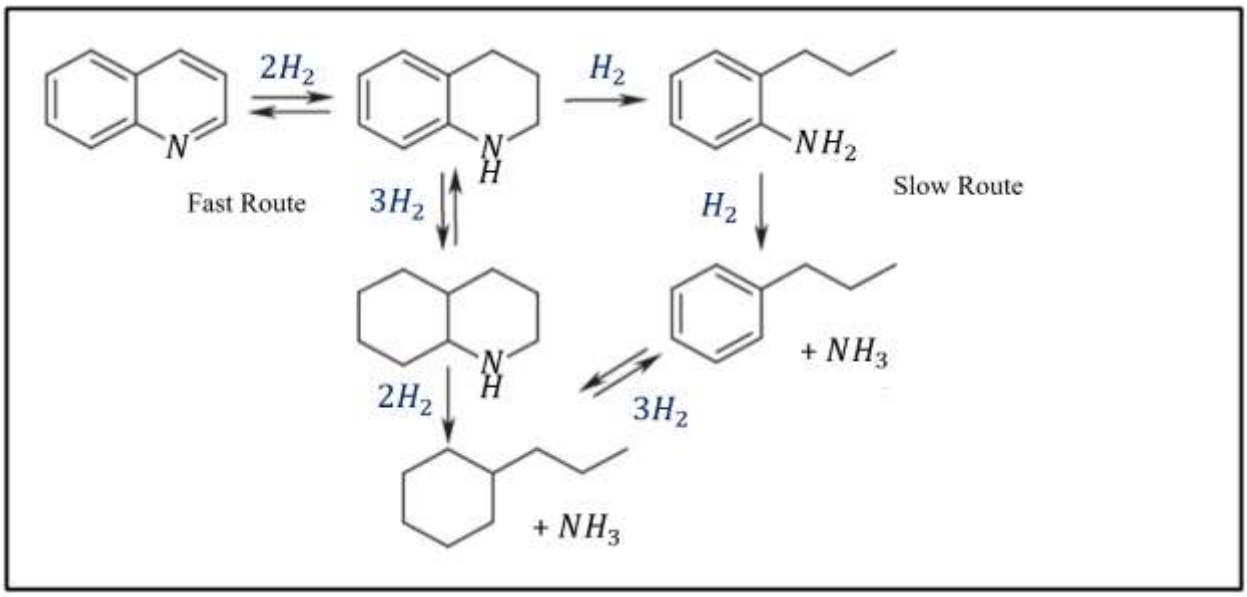

Figure 2.5 Proposed reaction mechanism for hydrodenitrogenation of quinoline (Giola et al., 1986).

2.6.5 Hydrodeoxygenation

Oxygen containing compounds in crude oil are mostly found in the form of furan, naphthol, organic phenols and carboxylic acids. During the hydrodeoxygenation reaction, the O-atom is removed and is converted to water (Furimsky, 1983). Proceeding through partial saturation of aromatic rings is reported to be the preferred reaction mechanism for HDO rather than direct hydrogenolysis (Girgis and Gates, 1991). However, because of the low concentration of oxygen compounds in crude oil, this type of reaction has received less attention when compared to HDS and HDM.

2.6.6 Hydrodeasphaltenization

Asphaltenes undergo a series of complex chemical transformations when subjected to hydroprocessing conditions. Operating conditions and molecular structure strongly affect the reaction mechanism. During upgrading reactions, asphaltenes like other compounds experience changes in their structure. Studies on structural modification from Athabasca Bitumen conclude that as a consequence of the reaction, asphaltene aggregates in crude were broken even when the content of vanadium in asphaltene is high (Asaoka et al., 1983). HDAs reaction is found to be very sensitive to temperature where at low temperatures, hydrogenation is dominant whereas at higher temperatures hydrocracking is dominated (Ancheyta et al, 2003). Depending on hydroprocessing reactions severity, the asphaltene conversion involves different steps starting with evolution of large asphaltene aggregates into smaller ones, followed by dealkylation of small side chains and ending with cracking of alkyl bridges (Gauthier et al., 2008). As stated earlier, most heteroatom molecules are fused into the asphaltenic structure. Therefore the asphaltene conversion is closely linked to the elimination of sulfur, nitrogen, and metals.

It is notorious from the review that no partial catalytic upgrading has been proposed for heavy oil thus far, perhaps due to the lack of sufficient catalytic science development and original ideas for that purpose. This thesis contributes to increase the options in that direction and after having revised the essential literature knowledge that supports and enables this work, the experimental chapter will introduce the experimental plan and procedure employed to obtain all the data and information obtained for this thesis.

Chapter Three: Experimental Procedure

3.1 Description of Experimental Resources and Procedures

3.1.1 Feedstock and Catalyst

Athabasca bitumen provided by Japan Canada Oil Sands Limited was used as the feedstock for the pilot-plant scale hydrogenation process presented in this research work. The main physicochemical properties of the feedstock are reported in table 3.1.

Table 3.1 Characterization of feedstock (Athabasca Bitumen).

Analysis		Athabasca Bitumen
API Gravity		9.0
Microcarbon Residue		13.83
Viscosity @ 25°C [mPa.s]		78752
Metals	Sulfur Content [ppmwt.]	40673
	Ni+V [ppmwt.]	248
SARA	Saturates [%wt.]	15
	Aromatics [%wt.]	48
	Resins [%wt.]	25
	Asphaltenes [%wt.]	12
Distillation Cuts	Naphtha (28 – 190 °C) [%wt.]	2.18
	Kerosene (190 – 260 °C) [%wt.]	4.88
	Diesel (260 – 343 °C) [%wt.]	10.8
	VGO (343 – 550 °C) [%wt.]	31.95
	Vacuum Residue (550°C+)	50.19

The so-called M3 novel catalyst examined during the experiments was prepared by the research fellow Dr. Gerardo Vitale. The information related to the composition of catalyst M3 cannot be

disclosed in this report but the properties necessary to calculate the catalyst effectiveness factor applied in modeling of the reactor are listed in Table 3.2.

Table 3.2 Properties of M3 catalyst.

Catalyst Parameter	Value
Particles bulk density (g cm^{-3})	1.124
Particle diameter (cm)	0.1
Specific area (m^2g^{-1})	151
Pore Volume (cm^3g^{-1})	0.295

3.1.2 Process Variables

Two set of experiments were carried out through test runs 1 (RXN-1) and 2 (RXN-2) in the reactivity test unit 1 (RTU-1) illustrated in Figure 3.3. Table 3.3 presents the various operating conditions studied for bitumen hydrogenation experiments.

Table 3.3 Run conditions for temperature and WHSV effect studies.

Process Parameter	Run 1 (RXN-1)	Run 2 (RXN-2)
Temperature (°C)	325, 335, 345	330, 340, 345, 350
Pressure (psig)	1400	1400
WHSV (hr^{-1})	0.2,0.25,0.3	0.2, 0.4, 0.5
H2/Oil (Scm^3/cm^3)	900	900
Time on Stream (hr)	397	336.5

The details of the whole experimental plan and procedure implemented during RXN-1 and RXN-2 are shown in Figures 3.1.

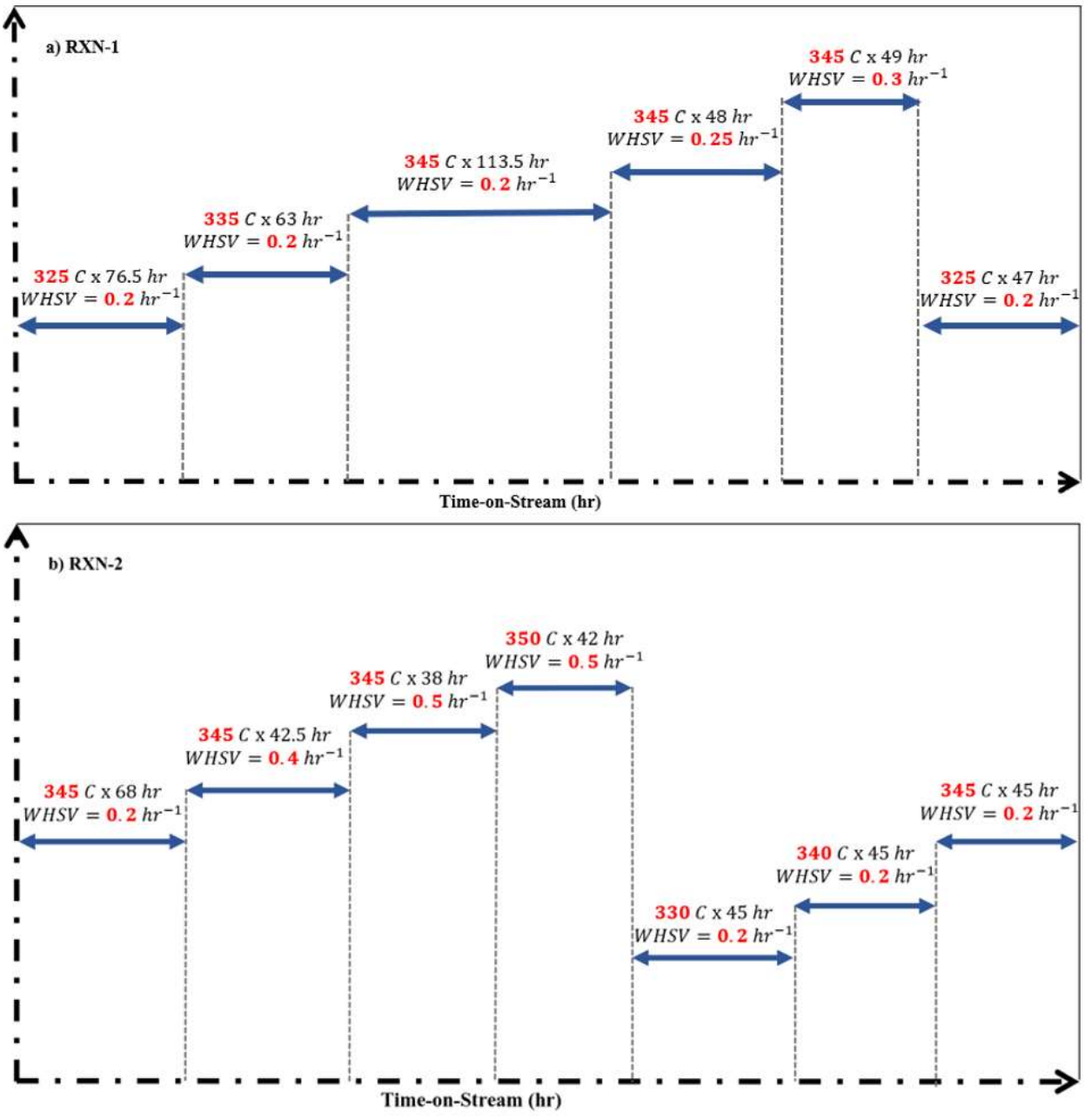

Figure 3.1 Experimental plan for studying the effect of temperature and WHSV during a) RXN-1 and b) RXN-2.

During the 397 hours of operation for RXN-1, the samples were collected and analyzed at three values of temperature and three values of WHSV, which gives a set of 5 experiments. For RXN-2, a set of 6 experiments were carried out at four values of temperature and three values of WHSV during 336.5 hours of operation. At the end of each test run, a check-back test was performed to study the catalyst activity for the time on stream.

In order to be able to enhance the quality and quantity of liquid yield from heavy oil and bitumen conversion and to have the most beneficial effect of catalytic processes, catalyst type, feedstock composition, reactor and reactor conditions need to be properly selected. Space velocity is an indication of the number of reactor volumes occupied by catalyst processed in a unit time with the feedstock and is used to determine the amount of catalyst and the reactor capacity for desired production rate. It is a ratio of the liquid hydrocarbon feed over the amount of catalyst loaded into the reactor and can be described either on a volume basis or on a weight basis. In the present work tests were conducted at various weight hourly space velocities (WHSV) defined by the following equation:

$$WHSV = \frac{Total\ Liquid\ Hydrocarbon\ Mass\ Flowrate,(\frac{g}{h})}{Total\ Catalyst\ Weight,(g)}\ [=]\ h^{-1} \qquad 3.1$$

The severity of process is inversely proportional to WHSV. The lower WHSV is an indication of the less amount of feedstock being processed per hour and the more contact time with the catalyst. Usually heavy oil hydrotreating is carried out at lower WHSV (<1) compared to hydrotreating of lighter feedstock such as distillates (WHSV>1).

Hydrogen to oil ratio is used to measure the volumetric rate of hydrogen flowing into the reactor with respect to the feedstock volume and is described by the following relationship:

$$H_2/Oil = \frac{Total\ Hydrogen\ to\ Reactor, (\frac{Scm^3}{min})}{Total\ Liquid\ Feed\ to\ the\ Reactor\ , (\frac{cm^3}{min})}\ [=]\ \frac{Scm^3}{cm^3} \quad 3.2$$

The H_2 to bitumen ratio should be sufficiently high to ensure keeping the hydrogen partial pressure high and increasing the available hydrogen in contact with bitumen molecules and the catalyst. It is common in most HDT reactors that a small portion of feedstock is vaporized and as a result the gas composition and reaction rates are altered. High H_2 to bitumen ratio concentrates the heaviest and most refractory components in the liquid phase and provides more contact time with the catalyst.

3.1.3 Reaction Unit 1 (RTU-1)

Two Teledyne ISCO series 500 D dual-pumps are connected to the main 10 L feed tank. Nitrogen is used as a blanket gas to pressurize the tank to ensure the feedstock is not oxidized and in addition, to provide the required head pressure to fill the ISCO pump cylinders with no bubbles. The tank is also equipped with a spring type depressurization valve at the outlet which pops at pressures above 100 psig. The outlet line of pumps directing to the inlet of reactor is equipped with another spring type relief valve as an ultimate protector in case of any plug upstream of the reactor. The set point of this safety valve is adjustable based on different operating condition and is set at 1600 psig for the purpose of our experiments. Hydrogen is injected through a Brooks Instrument 5850EM mass flow controller. The lines connecting feed tank to the pump and consequently to the reactor are made of ¼" O.D. 316 stainless steel tubing from Swagelok and are kept warm with heating tapes plus insulating fibers to avoid any heat loss. An up-flow trickle bed reactor, as illustrated in Figure 3.2, is utilized at the core of the pilot-plant Reactivity Test Unit 1 (RTU-1), constructed from a stainless steel tube equipped with a thermocouple at the central axis of the

reactor to monitor the reaction temperature. The internal diameter and length of reactor are 1.092 cm (0.5" O.D. and 0.049" wall thickness) and 35 cm respectively. The reactor is heated and controlled by means of seven electric resistances to ensure isothermal operation. Five sensing points are distributed inside the reaction zone (TI-802 to TI-806) and the other two indicate the temperature at the reactor inlet (T-801) and outlet (T-807).

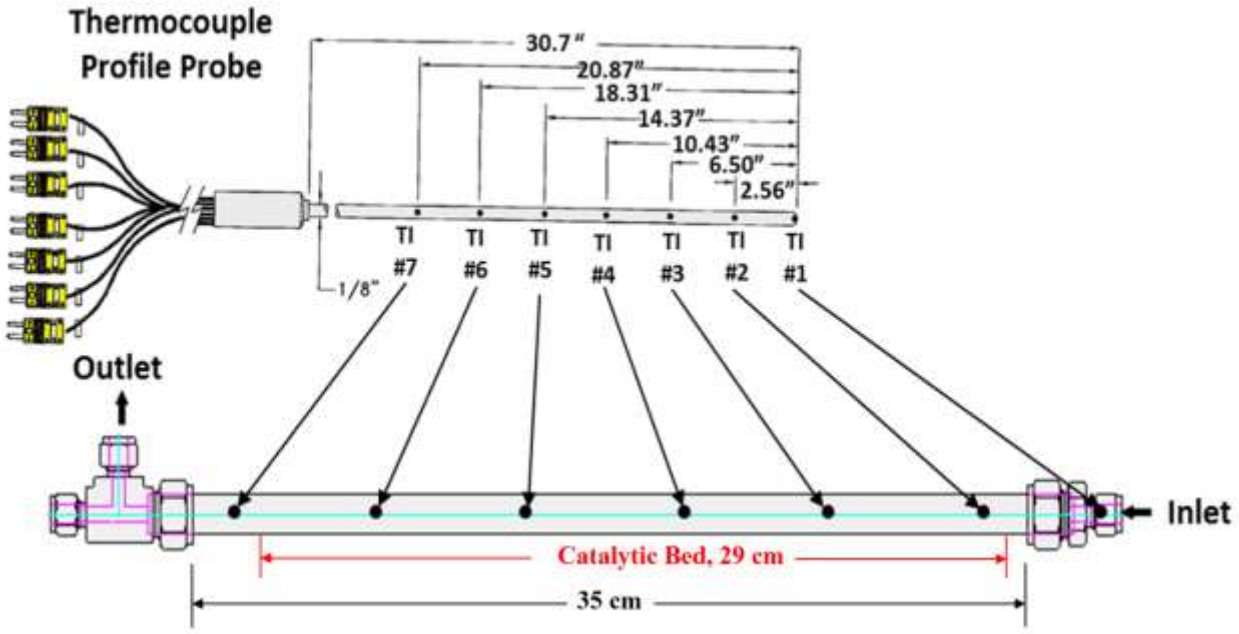

Figure 3.2 Reactor and thermocouple schematic (adapted from Cabrales-Navarro, 2016).

Figure 3.3 illustrates the schematic diagram of the experimental setup of the hydrogenation unit (RTU-1). More details of the equipment and instruments incorporated in the unit are presented in the P&ID diagram (Appendix. A). In order to maintain an isothermal temperature profile, three heating tapes (TC-204, 205 & 206) are installed around the reactor to be able to control the temperature at each section individually. The mixture of gas and liquid products from the reaction zone are directed to a 1 L 304 stainless steel hot separator. The temperature of the hot separator should not be set too low to avoid the presence of any water in oil emulsions and that no water

condensation is occurred. Because of the high operating pressure (1400 psig) the liquid products are transferred to an atmospheric tank to ensure a safe sample collection procedure. This transition occurs through a 40 mL Swagelok vessel in between of two computer-controlled pneumatic valves. The opening time of the lower valve is set up on the basis of a 67% occupation of the vessel. The upper valve is left open for 300 s and then it closes. In 10 seconds, the valve at the bottom opens for 300 seconds and the product is released to the atmospheric collector. Each time the upper valve opens, a small pressure drop (less than 3%) is implemented in the system which does not cause any instability on the reactor. Equation 3.3 was used to calculate the valves cycle time:

$$t_v = \frac{\frac{2}{3}\times 40\ (mL)}{Oil\ Flowrate\left(\frac{mL}{\min}\right)}[=]\ min \qquad 3.3$$

The gases from hot separator are directed into a KOH trap to neutralize the H_2S product and sweeten the gas and either flow to a Gas Chromatograph (GC) for gas composition analysis or to a wet gas meter (WTM) for gas flow measurement and consequently to the vent.

A computer software programmed with the LabView code was adopted to set, control, and to monitor the desired temperatures and pressure in the system. The program is subdivided in 7 interactive sections: feed section, reaction section, heavy products, light products, heaters and pump control, alarm control, alarm settings and heater tuning. The operating data is measured every 5 seconds and it is recorded in an excel spreadsheet.

3.1.4 Reactor Set-up and Catalyst Loading

The reactors used in the set of experiments were sealed at the bottom with a Swagelok 60 micron stainless steel filter and then packed with quartz wool, carborundum, catalyst, carborundum and quartz wool in sequence from bottom to top. For both experiments the reactor was loaded with 29

grams of a special catalyst built by researchers in the lab, the so-called M3 Catalyst. Following successful mounting of the assembled reactor and performing the leak test, prior to the process start-up, hydrogenating catalysts were activated in order to reach an optimum level of catalytic sites to remain active in the presence of H_2 and H_2S pressures during the reaction. In order to activate the catalyst, a reduction under nitrogen and hydrogen was required to reach the desired oxidation state of metals. Previous studies reveal that the metals are reduced at 500 °C (Vitale et al., 2011). At this temperature and atmospheric pressure, nitrogen was introduced to the system for 6 hours at a rate of 60 mL/min followed by hydrogen flowing into the reactor for 8 hours.

3.1.5 Operation Procedure

Following pilot plant leak test and the catalyst treatment, the start up procedure for hydrotreating begins with increasing the temperature in the feed, separation and sampling section to 100 °C. Pressure was increased gradually and was set at 1400 psig and hydrogen flowrate was set at desired reaction condition. The reactor temperature was set at tested condition by increasing this variable at a rate of 10 °C/min. Then, oil was pumped into the system at a flowrate of 2 mL/min for approximately 1 hour and once the lines and reactor are filled, the oil flowrate was determined knowing the WHSV and using Equation 3.1. Ultimately, the operation cycle of the previous described computer-controlled pneumatic valves was activated, and the experiments were started. The oil had to pass three reactor volumes in order to reach stability after changing the reaction conditions during the set of experiments.

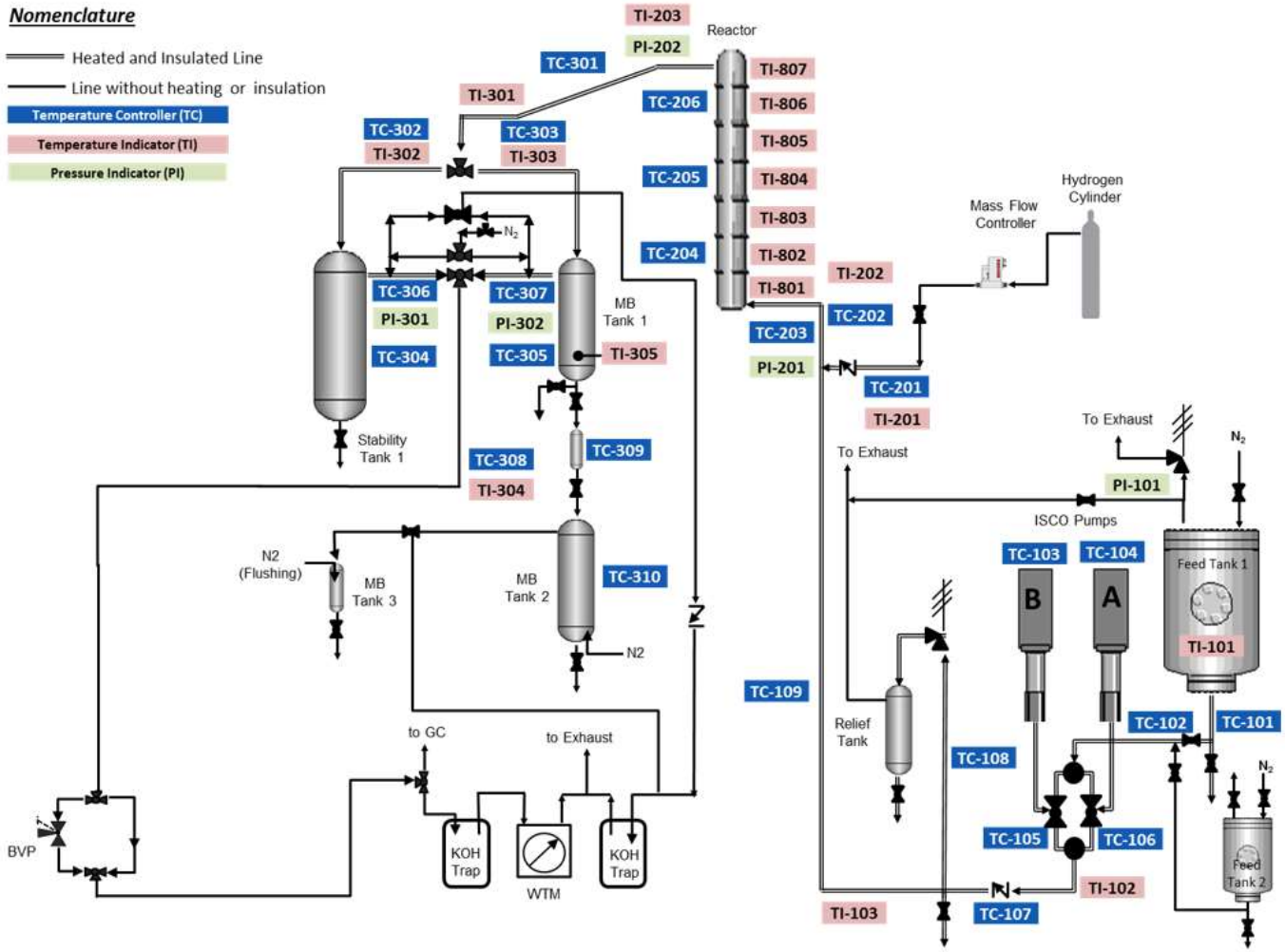

Figure 3.3 Schematic of experimental setup for reactivity test unit 1 (RTU-1) (Scheele, 2018).

3.2 Feedstock and Liquid Product Characterization

3.2.1 Liquid Product Distribution (SimDist)

SimDist is a laboratory scale technique used to determine the boiling point profile of an oil sample and calculate its oil fraction percentage. Due to the large number of compounds present in crude oil, liquid products are classified into lumps and pseudo components based on their boiling point range. The following classification were used in this research work: naphtha (28-190 °C), kerosene (190-260 °C), diesel (260-343 °C), vacuum gas oil (345-550 °C) and vacuum residue (550+ °C). The methodology and conditions follow ASTM norm D-7169. In this technique, 1µl of a filtered solution is prepared consisting of 0.15 g of oil sample and 20 ml carbon disulfide (CS_2) and is injected into a temperature programmed chromatograph column (Agilent 7890A). The procedure is based on a steady increase in temperature that gradually vaporizes and elutes part of the hydrocarbons, depending on their boiling point. Those molecules are flown into a detector that measures the amounts of sample eluted in a given time and each temperature (Banerjee, 2012). The gas chromatograph is calibrated using a range of different molecular weight alkanes at given concentrations. It has been found that High Temperature Simulated Distillation (HTSD) is able to determine fraction boiling points up to 3 °C errors and is able to reproduce fraction yields with standard deviations around 0.5% (Raia et al., 2000). Alternatively, it has also been reported errors of 1% for samples with boiling point below 550 °C and of 4% for heavier fractions (Rodriguez-DeVecchis et al., 2015). The distillation curve profile is obtained from SimDist Expert software v.8 after analyzing signals and vacuum residue conversion (X_{VR}) in this thesis was calculated based on SimDist data following equation 3.4:

$$X_{VR} = \frac{(\%\ wt.\ Vacuum\ Residue\ 550°C+)_{Feed} - (\%\ wt.\ Vacuum\ Residue\ 550°C+)_{Product}}{(\%\ wt.\ Vacuum\ Residue\ 550°C+)_{Feed}} \times 100 \quad 3.4$$

3.2.2 Viscosity

Viscosity is one of the most important parameters characterizing a crude oil and is a measure of the resistance to flow of a fluid and directly related to its transportability. As explained in the introduction of this work, bitumen is not transportable and has to be either blended with diluents or upgraded into a synthetic crude oil in order to reach pipeline specifications, among which viscosity is one of the main factors. In this work, a Brookfield viscometer model DV-II+ Pro equipped with a glycol recirculation system model TC-502 was used to measure viscosity. The measurement starts by setting up the temperature controlling system at the required value, in this work at 25 °C. The spindle was screwed to the bottom of the rotatory shaft and the viscometer was closed with the sample cell, adjusting the distance between the spindle and the bottom of the cell to 0.1 mm. Once the required amount of sample enough to cover the whole surface of the spindle was placed in the sample cell, the rotation engine was started, and the velocity was adjusted in such a way that the shear generated by the cohesive forces between the fluid and the metal plates measured by the equipment's dynamometer was within the 50-70% range. At least 5 full rotations of the spindle were required to guarantee proper formation of the fluid film and any variation in the temperature set point should be avoided to not affect the measurement accuracy.

3.2.3 API Gravity

API gravity is the most commonly used parameter to present the specific gravity (sg) of the fluid in a more sensitive scale and is defined by Eq. 3.5 from the ASTM D287-92 norm.

$$API\ gravity = \frac{141.5}{sg^{60^\circ F}_{60^\circ F}} - 131.5 \quad (3.5)$$

Along with viscosity, API gravity is a very important parameter assessing the transportability of a crude oil. Moreover, it is an indication of the nature of the chemical compounds present in the crude oil as heavier compounds such as asphaltenes have considerably lower API. In this work, specific gravity was determined using a digital densitometer, Rudolph Research Analytical model DDM2911, as described by (Carbognani et al., 2015). It is not possible to inject heavy viscous samples directly in the equipment cell and as a result two diluted sample solutions at concentrations close to 0.5 % v/v and 1% v/v were analyzed. The density of the pure sample was extrapolated by assuming an ideal mixture for diluted solutions of components with similar polarity and additive volumes as represented in the following equation.

$$\rho_{sample} = \frac{m_{sample}}{(m_{sample}+m_{toluene})(1/\rho_{toluene}) - m_{toluene}(1/\rho_{toluene})} \quad (3.6)$$

3.2.4 Sulfur and Nitrogen

The sulfur content of Athabasca Bitumen was measured following the ASTM 5463 procedure and using the technique of combustion/fluorescence. Similarly, the ASTM D4629 procedure was used to determine the total nitrogen content of bitumen. Nitrogen and sulfur contents in the liquid sample was quantified with an Antek 9000NS analyzer. A solution of about 0.4 g of sample in 2.6 g of toluene was prepared and weighted to the nearest 0.1 mg. Pyrolysis of a sample is conducted at 1100°C to guarantee a complete conversion of sulfur and nitrogen to their corresponding oxides, SO_2 and NO_2. Hydrocarbons are converted into CO_2 and water, while nitrogen and sulfur oxides are detected through the pyro-chemiluminescent technology and pyro-fluorescent technology,

found respectively in the equipment. Each sample was automatically injected several times in order to assure good precision of less than 5% error.

3.2.5 Asphaltene Stability Index (P-value)

The asphaltenes in oil can show the tendency to flocculate and precipitate causing several problems. The P-value method, developed by Shell, does asses the peptization capacity of the sample that keeps the asphaltenes in suspension; it can be used to calculate and predict the stability of crude oils (Van Den Berg, et al., 2010). The P-value of an oil sample was obtained using Eq 3.7. By titrating the same amount of sample, placed in different vials, using different volumes of hexadecane, the P-value can be determined. After digestion at 100°C for 30 min, each final solution was analyzed in an optical microscope with a magnification of 40X to observe formation of particles. The known volume of hexadecane and mass of sample used gives the P-value of the sample. The higher the amount of solvent required to observe precipitation, the more stable the product is. If the sample with no solvent added shows the presence of asphaltenes, a P-value equals to one is reported. For the purpose of analysis of products, a P-value of 1.15 can be considered as the limit of stability (Higuerey et al., 2002).

$$P - value = 1 + \left(\frac{volume\ of\ hexadecane\ (ml)}{mass\ of\ samples\ (g)}\right) \quad 3.7$$

3.2.6 Microcarbon Residue (MCR)

The MCR content of bitumen was measured following ASTM D4530 procedure. This characteristic was measured by pyrolyzing the sample in the absence of oxygen under controlled conditions. The amount of solid residue, determined as a fraction of initial sample weight, indicates

the tendency to form coke in a coking process. The three methods of measurement that are commonly used are the Conradson carbon residue (CCR), Ramsbottom carbon residue (RCR) and micro-carbon residue (MCR) determinations. The concept is same in each case and the differences are related to the details of the apparatus and the heating conditions. All measure the mass of carbon-rich solid residue as the weight percent of solid material remaining after thermal cracking or pyrolysis of a sample in an inert atmosphere, thereby providing indications of coke yield in large-scale processing. Since MCR requires only small amounts of samples, its has become the standard technique. This method uses a semi-automatic analyzer and the numerical results are equivalent to those of the CCR method. For residual oil samples, 150 mg of oil is weighed in a glass tube. The tube is placed in an oven in a nitrogen atmosphere, heated at a rate of 10 °C/min to 520 °C, held at that temperature for 20 minutes and then cooled and weighed. The amount of solid residue gives an indication of coke yield. The set-up used in our laboratory, is a miniaturized version of MCR described elsewhere (Hassan et al., 2008).

3.2.7 Saturates, Aromatics, Resins and Asphaltenes (SARA)

Following the procedure described elsewhere (Carbognani et al., 2007), the SARA group hydrocarbon separation method was carried out to analyze the asphaltenes, resins, aromatics and saturates fractions. This method is divided into two sections. First, the content of pentane (nC5) insoluble asphaltenes is determined by microdeasphalting of the sample. Then, by using thin layer chromatography with flame ionization detection (TLC-FID) the Saturates, Aromatic & Resins group types for the maltene phase (deasphalted oil) is analyzed. For the first section,, microdeasphalting, 0.4 g of sample weighted to the nearest 0.1 mg was placed in a 100 mL beaker along with 20 mL of n-pentane (ratio of 50/1 vol. nC5/wt. sample). In order to minimize

evaporation of the paraffinic solvent, the beaker was covered with a Petri dish and subsequently placed over a heating plate maintained at a temperature of 50 °C for 30 min and in order to promote the formation of solid asphaltene particles, the content was gently mixed several times with a metallic spatula. To maintain a constant solvent content Pentane was added as required. Following that, the mixture was cooled down to ambient temperature and the precipitate was filtered out by vacuum filtration in a 47 mm millipore unit provided with 0.45 µm nylon membranes from Pall Corporation. To dry out any remaining amount of solvent, membrane containing the precipitated solids was placed in a Petri dish inside an oven operating at 80 °C, for 5 min. At the end, the membrane was cooled down to ambient temperature and weighted to quantify the amount of nC5 asphaltenes in the sample. In the next section of the analysis in order to remove nC5, the maltene (SAR) plus solvent fraction is rotoevaporated in a round bottom 100 mL flask. An inert environment was provided with nitrogen stripping to avoid the oxidation of resins. Then, the collected maltene was diluted with toluene (99.9 % Aldrich) to get a concentration of 10 mg of maltenes per mL of toluene. SAR distribution for the maltene fraction was subsequently conducted in an Iatroscan model MK-6 chromatograph controlled with a Peak Simple chromatographic data system. S-III silica chromarods activated by burning at least 5 times were used for the analysis. One microliter of the diluted maltene solution was spotted at the bottom of at least three rods per sample (triplicate analysis). Next, the chromarods were placed in a TLC chamber filled with 100 mL of heptane (Aldrich) and the Saturates fraction was eluted up to 10 cm in the chromarods during approximately 30 min. Subsequently, chromarods were placed in a different TLC chamber filled with 100 mL of toluene (Aldrich) for elution up to 6 cm to separate the Aromatics fraction for approximately 15 min. The Resins fraction remains at the bottom of the rods. The next step was to scan the chromarods in the Iatroscan chromatograph FID operated with a mixture of air and

hydrogen at flowrates of 2 mL/min and 160 mL/min respectively, with a scanning speed of 30 s/rod. The contents of SAR HC group types were estimated in the Peak Simple software applying a pre-established response factor to the Resins fraction and renormalizing.

3.2.8 Total Acid Number (TAN)

Total Acid Number (TAN) is an indication of the naphthenic acid content of a crude oil and a measure of its corrosivity. TAN is defined by the milligrams of potassium hydroxide (KOH) required to neutralize one gram of crude oil. The acidity of collected samples were measured following the ASTM D644 norm (ASTM-D664, 2011). A titrant solution of 0.05 M potassium hydroxide in 2-propanol and water was used to measure the acidity by means of a Mettler Toledo T70 Titration Excellence apparatus. In this method, 60 ml solvent solution composed of 50% v/v toluene, 49.5% v/v 2-propanol and 0.5% v/v water, is used to dilute masses of samples varying between 0.5 to 0.7 g. The analysis is performed following the placement of vessel containing the solution on an auto-sampler tray with the electrode, titrant dispenser and mixer placed inside the vessel. Once the titrant solution is pumped, the neutralization reaction is monitored by potentiometry and the solution acidity is determined by the inflection point. Depending on the amount and concentration of titrant and the amount of sample used, TAN number is determined by the equipment and TAN conversion is calculated by Equation 3.8:

$$X_{TAN} = 1 - \frac{TAN_{Sample,}[mgKOH/g]}{TAN_{Feed,}[mgKOH/g]} \quad 3.8$$

The relative error for TAN measurement is 20% for TAN <1 mgKOH/g, 10% for values ranging from 1 to 5 mgKOH/g and 3% for values as high as 50 mgKOH/g.

Chapter Four: Reactor Modeling

Several studies have been published on hydrotreating reactions in trickle bed reactors however, most of them are applied to specific feedstocks with reduced range of boiling points or they are focused only on the heavy fraction of oil. To a lesser extent, some light whole crude oils with API gravities higher than 30 have been studied. The primary focus of this work is on developing kinetic models for whole range bitumen hydrogenation, containing a wide variety of sulfur, organometallic species and high molecular weight asphaltenes, which has not been the focus of attention so far. Most kinetic models reported in literature are based on lumping approach, where the feedstock and products are classified into pseudo components depending on their boiling point range. The main drawback of lumping approach is the dependency of rate parameters on the composition of the feedstock which extrapolation capability. The effect of grouping a broad distribution of chemical species, is reflected in the reaction order. Common observations for lumped kinetics reaction orders are between 0.5 and 2. In spite of these limitations, since hydrogenation process was undertaken directly on a very complex feedstock, dried SAGD produced bitumen without distillation or separation of any kind, lumping approach was selected for the modeling purpose.

4.1 Modeling Approach

The aim of this chapter is to develop a model for the trickle bed reactor used in the set of experiments and to validate the model for describing hydrotreating reactions and to provide relevant information about optimal operating conditions, reactor design and catalyst formulation. In this study a three phase plug-flow reactor model is proposed based on Hoffmann mathematical

model (Hoffmann, 1997). Correlations to estimate mass-transfer coefficients, gas solubility and properties of fluid at process conditions which have been used in the model are described in further details in section 4.2.3. Among the several reactions occurring in hydroprocessing, the kinetic data on HDAs and HDs are of particular interest in this study because they are known to be crucial in downstream catalytic reactors. The model describes the conversion of two chemical lumps (sulfur [Sul] and asphaltenes [Asph]). Thus, the following reactions: hydrodesulfurization (HDS) and hydrodeasphaltenization (HDAs) are taken into account in the model.

In this work, the following assumptions were considered in developing the mathematical model for three phase reactor:

1. Reactor operates in plug-flow mode and concentration gradients along the radial direction are not considered.
2. Liquid expansion under moderate hydrotreating condition is negligible, therefore liquid and gas linear velocities are constant along the reactor.
3. Vaporization of light cuts in reactants or products is negligible.
4. Due to the reactor's small dimensions, pressure is assumed to be constant across the reactor section and no heat transfer resistance is considered to exist between the three phases and the reactor operates in an isothermal and isobaric mode.
5. Catalyst activity does not change with time.
6. Chemical reactions take place at the catalyst surface, and not in the gas or liquid phase.
7. The resistances to mass transfer in the gas-liquid interface is expressed through the gas-liquid thermodynamic equilibrium calculation based on Henry's law.
8. The driving force between liquid and solid phase is described by the chemical reaction rate.

9. The internal diffusion (mass transfer inside the catalyst particle) is described by the catalyst effectiveness factor and varies with conversion along the reactor.
10. Reactor operates at steady state condition.

It should be noted that these assumptions are valid and adequate to represent the reactor studied in the pilot plant. Other models proposed by several authors have taken in consideration different assumptions. For example to adjust the reaction order a packed bed reactor is modeled without considering the resistance to mass transfer in gas-liquid and liquid-solid interface (Marafi et al., 2003) or, in another work the resistance to mass-transfer in the liquid-solid interface is not included but the heat transfer is considered in the reactor model (Botchwey et al., 2006). The reactor size incorporated in the experiments is small and therefore the one-dimensional model is justified. All mass balances were collected at steady-state conditions of the reactor and a back-pressure valve maintains the pressure of the system at a constant and high pressure of 1400 psig and the negligible phase change of light cuts is justified.

4.2 Model Equations

As shown in Figure 4.1, based on the two film theory for the reactions to occur, hydrogen forming the bulk of gas phase, transfers from the gas phase to the liquid phase. Dissolved hydrogen and reactants in liquid phase, namely, sulfur and asphaltene transport to the catalyst particle and then adsorb onto the catalyst surface to react with other reactants. The gaseous reaction products such as H_2S, are released to the gas phase passing through the liquid phase, whereas hydrocarbon products will be transported to the liquid bulk.

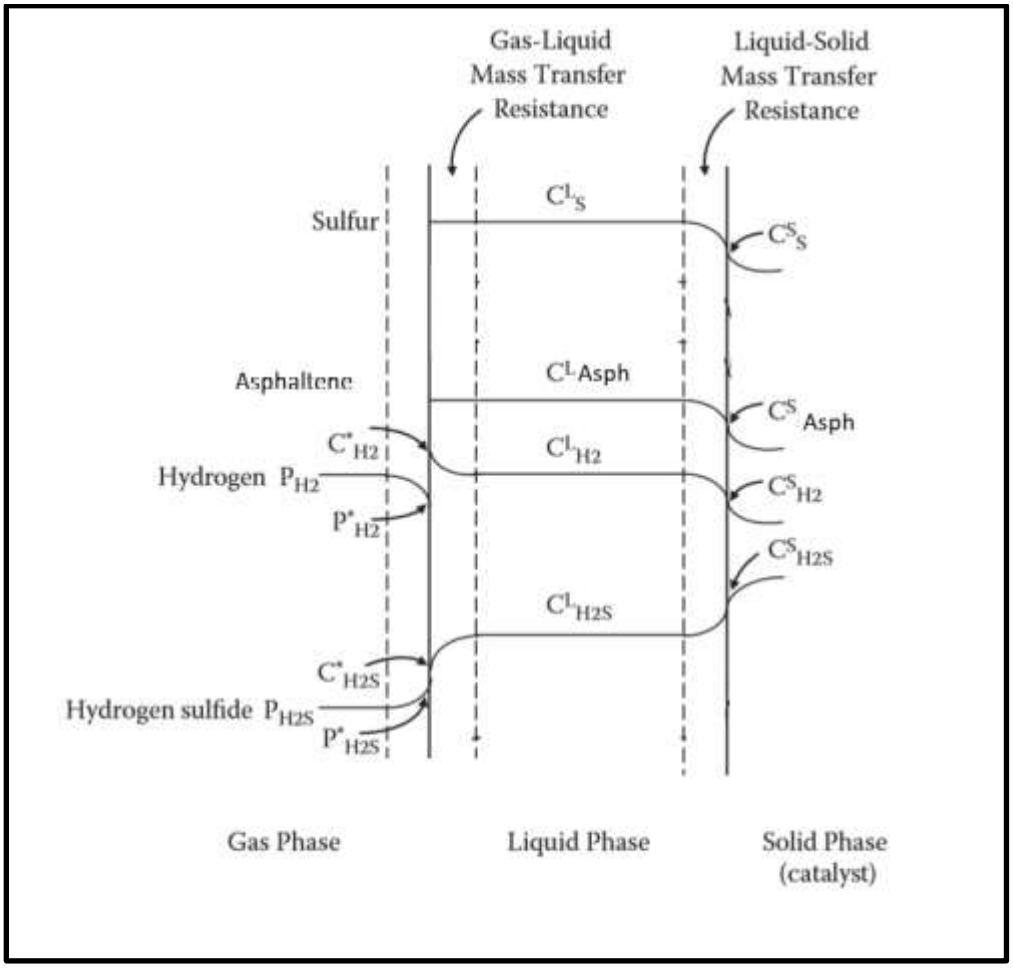

Figure 4.1 Representation of concentration profiles in a trickle bed reactor (Adapted from Bhaskar et al., 2004).

4.2.1 Steady-State Mass Balance Equations

4.2.1.1 Gas Phase Mass Balances

As mentioned before, no reaction occurs in the gas phase. Therefore, at steady state condition, equating the mass transfer rate of gas component across the gas-liquid interface to its pressure gradient in the gas phase results in the ordinary differential mass balance equation for gaseous compounds along the reactor:

Hydrogen: $$\frac{dP^G_{H_2}}{dz} = -\frac{RT}{u_G} k^L_{H_2} a_L \left(\frac{P^G_{H_2}}{H_{H_2}} - C^L_{H_2} \right) \quad 4.1$$

where u_G is the superficial velocity of the gas, R is the universal gas constant, T represents the reactor temperature, $P^G_{H_2}$ is the partial pressure of H_2 and $k^L_{H_2} a_L$ describes the mass transfer between the gas and liquid phases. It is assumed that gas-liquid equilibrium can be described by Henry's law and that the liquid-phase concentration of hydrogen in equilibrium with the bulk partial pressure is expressed by the term $C^G_{H_2} RT / H_{H_2}$, where H_{H_2} is Henry's coefficient for hydrogen. The solubility of hydrogen in the Athabasca bitumen were determined from experimental data and are presented in Appendix B (Lal et al., 1999). At a given pressure, the solubility increases with increasing temperature, an effect typical for hydrogen systems.

Similarly, we can write equations for the other gas phase component, H_2S, as follows:

Hydrogen Sulfide: $$\frac{dP^G_{H_2S}}{dz} = -\frac{RT}{u_G} k^L_{H_2S} a_L \left(\frac{P^G_{H_2S}}{H_{H_2S}} - C^L_{H_2S} \right) \quad 4.2$$

It should be noted that the gas phase is considered to be constituted mainly by hydrogen (almost 98%).

4.2.1.2 Liquid Phase Mass Balances

Equating the concentration gradient to the mass transfer of hydrogen across the gas-liquid and liquid-solid interfaces results in the following differential mass balance equation for the liquid-phase concentration of hydrogen in the liquid phase:

$$\frac{dC^L_{H_2}}{dz} = \frac{1}{u_L} \left(k^L_{H_2} a_L \left(\frac{P^G_{H_2}}{H_{H_2}} - C^L_{H_2} \right) - k^S_{H_2} a_S \left(C^L_{H_2} - C^S_{H_2} \right) \right) \quad 4.3$$

where u_L is the superficial velocity of the liquid and $k^S_{H_2} a_S$ accounts for the mass transfer between liquid and solid phase. Similarly, the mass balance equations for H_2S can be written as follows:

$$\frac{dC^L_{H_2S}}{dz} = \frac{1}{u_L}\left(k^L_{H_2S} a_L \left(\frac{P^G_{H_2S}}{H_{H_2S}} - C^L_{H_2S} \right) - k^S_{H_2S} a_S \left(C^L_{H_2S} - C^S_{H_2S} \right) \right) \quad 4.4$$

Equations (4.3) and (4.4) represent the mass balance equations for the gaseous compounds, but since the sulfur compound is assumed to be nonvolatile and bitumen vaporization is negligible under hydrotreating condition, the mass balance equations for sulfur and asphaltene lumps can written by equating their liquid phase concentration gradients to their mass transfer between the liquid and solid phase.

$$\frac{dC^L_{Sul}}{dz} = -\frac{1}{u_L} k^S_{Sul} a_S \left(C^L_{Sul} - C^S_{Sul} \right) \quad 4.5$$

$$\frac{dC^L_{Asph}}{dz} = -\frac{1}{u_L} k^S_{Asph} a_S \left(C^L_{Asph} - C^S_{Asph} \right) \quad 4.6$$

Equations (4.5) and (4.6) can be integrated along the length of the catalyst bed to obtain concentration profiles of sulfur and asphaltene. The concentrations of these components on the catalyst surface change as the reactions proceed along the length of the catalyst bed.

4.2.1.3 Solid Phase Mass Balances

Surface concentrations of hydrogen, hydrogen sulfide, sulfur and asphaltene are required to solve equations 4.1 to 4.6. At steady-state the hydrogen, sulfur and asphaltene compounds transferred across the liquid-solid interface are consumed and hydrogen sulfide is produced through the chemical reactions.

$$k_{H_2}^S a_S \left(C_{H_2}^L - C_{H_2}^S \right) = \rho_B \eta_{CE} \left(\eta_{HDS} * r_{HDS} + \eta_{HDAs} * r_{HDAs} \right) \quad 4.7$$

$$k_{H_2S}^S a_S \left(C_{H_2S}^L - C_{H_2S}^S \right) = -\rho_B \eta_{CE} \eta_{HDS} \left(r_{HDS} \right) \quad 4.8$$

$$k_{Sul}^S a_S \left(C_{Sul}^L - C_{Sul}^S \right) = \rho_B \eta_{CE} \eta_{HDS} \left(r_{HDS} \right) \quad 4.9$$

$$k_{Asph}^S a_S \left(C_{Asph}^L - C_{Asph}^S \right) = \rho_B \eta_{CE} \eta_{HDAs} \left(r_{HDAs} \right) \quad 4.10$$

where ρ_B represents the bulk density of catalyst pellets in the bed, η_{CE} represent the wetting efficiency, and η_{HDS} and η_{HDAs} represent the catalyst effectiveness factors for HDS and HDAs reactions. The algebraic equations 4.7 to 4.10 represent the extent of chemical reactions at the catalyst surface where r represents the intrinsic rate of reaction per unit mass of catalyst. The following boundary conditions are required at $z = 0$ to solve equations 4.1 – 4.6:

$$C_{H_2}^G (z = 0) = C_{H_2}^G (initial) \quad 4.11$$

$$C_{H_2S}^G (z = 0) = 0 \quad 4.12$$

$$C_{H_2}^L (z = 0) = C_{H_2}^L (initial) = P_{H_2}^G (initial) / \mathrm{H}_{H_2} \quad 4.13$$

$$C_{H_2S}^L (z = 0) = 0 \quad 4.14$$

$$C_{Asph}^L (z = 0) = C_{Asph}^L (initial) \quad 4.15$$

$$C_{Sul}^L (z = 0) = C_{Sul}^L (initial) \quad 4.16$$

When dealing with high purity hydrogen the values of H_2S molar concentration in the liquid phase and gas phase (partial pressure) at the entrance of the reactor (z = 0) are very close to zero. The concentration of sulfur compounds at the reactor inlet is calculated based on the assumption that

this components has the same molecular weight as the whole crude oil. The molecular weight for the sulfur and asphaltene lump is considered to be 600 and 900 g/mol respectively. The following equation is used to determine the liquid concentration of these compounds at the inlet and outlet of reactor:

$$C_i^L(initial) = \left(\frac{\rho_L}{MW}\right) w_i \ , \ \ i = Sul, Asph \qquad 4.17$$

4.2.2 Reaction Kinetics

As it was described in the literature review, the number of different reacting species of sulfur and asphaltene in bitumen are so high that determining the exact number of each of them is a difficult task. Therefore, the aggregation or grouping of compounds is inevitable when performing a kinetic analysis of hydrogenation of such a feedstock. The hydrodesulfurization reactions are reported to be irreversible under general process condition according to researchers (Girgis et al., 1991). Hydrogen sulfide adsorbs on the active sites of the catalyst. Therefore, the hydrodesulfurization reaction is described by a Langmuir-Hinshelwood (L-H) kinetic model accounting for the inhibitory effects of H_2S (Bhaskar et al., 2004):

$$r_{HDS} = k_{HDS} \frac{\left(C_{Sul}^S\right)^n \left(C_{H_2}^S\right)^m}{\left(1 + K_{H_2S} C_{H_2S}^S\right)^2} \qquad 4.18$$

Exponent 2 in the denominator is a result of the assumption that the adsorption of sulfur compounds and H_2 occurs on two different sites over the catalyst surface, but H_2S adsorbs on both. Like sulfur, it is a challenging task to account for the different types of the reactivity of asphaltenes in modeling the kinetics of hydrodeasphaltenization reaction. Therefore, for simplification, the rate

of chemical reaction for such a complex feed is lumped into a single power law reaction as follows (Mederos et al., 2007):

$$r_{HDAs} = k_{HDAs}\left(C^{S}_{Asph}\right)^{e}\left(C^{S}_{H_2}\right)^{f} \quad 4.19$$

While most researchers have applied the single power law model to describe the HDAs reaction, the rate of reaction has been modified in this work to a L-H model in order to account for inhibitory factors of H_2S which is competing with hydrogen to adsorb on the same catalytic sites:

$$r_{HDAs} = k_{HDAs}\frac{\left(C^{S}_{Asph}\right)^{e}\left(C^{S}_{H_2}\right)^{f}}{\left(1+K_{H_2S}C^{S}_{H_2S}\right)^{2}} \quad 4.19^{1}$$

The temperature dependencies of reaction rate constants for hydsrodesulfurization and hydrodeasphaltenization reactions are evaluated by employing the Arrhenius equation as follows:

$$k_{HDS} = A_{HDS}\exp(-\frac{EA_{HDS}}{RT}) \quad 4.20$$

$$k_{HDAs} = A_{HDAs}\exp(-\frac{EA_{HDAs}}{RT}) \quad 4.21$$

And the adsorption equilibrium constant for hydrogen sulfide is described by Van't Hoff equation (Mederos et al., 2006):

$$K_{H_2S}(T) = 41769.8411\exp(\frac{2761}{RT}) \quad 4.22$$

4.2.3 Correlations to Predict Product Properties

The importance of proper estimation of mass transfer and thermodynamic properties lies on the fact of their influence on the reactor performance. Since the experimental pilot plant reactor operates under a trickle bed regime, the possible liquid maldistribution phenomena could be taken into account by using the liquid hold up and catalyst wetting efficiency factor. These factors are

interrelated through the bed void factor. As mentioned earlier, because of the lack of information on the transport phenomena and thermodynamic properties of whole range Athabasca bitumen at tested condition, the published correlations in the literature have been used to estimate these parameters. The correlations used for estimating the gas-liquid mass transfer coefficients (Rodriguez and Ancheyta, 2004), the liquid-solid mass transfer coefficients calculated by Van Krevelen-Krekels equation (Froment and Bischoff, 1990), the molecular diffusivity of components H_2, H_2S, Sulfur and the asphaltene in the liquid described by Tyn-Calus correlation (Raid et al., 1987), molar volumes of H_2, H_2S and crude oil (Dudukovic et al., 2002), the critical specific volume of bitumen obtained by a Riazi-Daubert correlation (Macias et al., 2004), Henry coefficient of H_2 (Lal et al., 1999) and H_2S (Mederos et al., 2007), bitumen density as a function of temperature and pressure based on the Standing-Katz equation (Macias et al., 2004) and bitumen viscosity (Korsten et al., 1996) are all presented in detail in Appendix B. The developed correlation for a packed bed of spheres used to estimate the bed void fraction and the correlation to determine the surface area of catalyst particles (Froment and Bischoff, 1990) can be found in the same section. Catalyst effectiveness factor which had been widely used to express the internal diffusion phenomena, have been estimated as a function of Thiele Modulus. Diffusion limitations are negligible for slow reactions and Thiele Modulus values less than 0.5 whereas values greater than 1.0 indicate a fast reaction and strong diffusion limitation. The following generalized form of Thiele Modulus for "n" th order of irreversible reactions is employed for the values of φ_{HDS} and φ_{HDAs} (Froment and Bischoff, 1990):

$$\Phi_j = \frac{V_P}{S_P}\left[\left(\frac{n+1}{2}\right)\left(\frac{k_j C_i^{S(n-1)}\rho_P}{De_i}\right)\right]^{0.5}, j = HDS\ and\ HDAs, i = Sul\ and\ Asph \qquad 4.23$$

The phenomenon occurring inside the catalyst particle when hydroprocessing heavy oil is described very well with this form of Thiele modulus by including the effective diffusion which mainly depends on the porosity, tortuosity and the size of molecules being diffused into the pores. Commonly, the pores are not oriented along the normal direction from the catalyst surface to the center of the particle. As a result, the tortuosity factor of the catalyst pore network, τ, is used in the calculation of effective diffusion to account for the hard accessibility of reactants into the pores. According to literature reports, tortuosity factor is assumed to be 4 (Macias et al., 2004). Considering a fast reaction, the total catalyst effectiveness factor is strongly influenced by external wetting efficiency because if the wetting efficiency is small, the reactants cannot get into the catalyst rapidly enough and the reaction occurs in a thin layer near the catalyst surface. In the case of slow reactions, the problem of reactants diffusion is less important and therefore the catalyst effectiveness is less affected by the wetting efficiency. Ideally, mass transfer effects need to be eliminated during the experiments to obtain the intrinsic rate parameters but for the industrial scale up those are of a lesser value and instead apparent rate constants are utilized. The following equation can be used to correlate the intrinsic and apparent rate parameters:

$$k_{apparent} = \eta_j * \eta_{CE} * k_{intrinsic}, j = HDS\ and\ HDAs \qquad 4.24$$

4.3 Parameter Estimation Technique and Numerical Solution

In order to obtain a useful reactor model that can be confidently applied for predicting the reactor behavior under different process conditions, an accurate estimation of kinetic parameters is required. The sulfur order “n”, asphaltene order “e”, hydrogen order in HDS and HDAs reactions “m” & “f”, reaction rate constants, k_{HDS} and k_{HDAs}, activation energies, EA_{HDS} and EA_{HDAs}, and

pre-exponential factors, A_{HDS} and A_{HDAs}, are unknown and the focus of this section is to accurately estimate these parameters. In the present work, the very popular and widely used method of optimization technique is used to estimate the unknown parameters where the sum of square errors (SSE) between the experimental and calculated values are minimized. While both linear (LN) and non-linear (NLN) regressions have been widely utilized in process model optimizations, estimation of activation energy and pre-exponential factor with simultaneous calculation of kinetic parameters by NLN regression is preferred as linearizing the Arrhenius equation gives a greater error compared with NLN regression. Therefore, the non-linear approach is utilized to describe the pilot plant TBR behavior. Among several NLN optimization approaches available for estimating the best values of kinetic parameters, such as Successive Quadratic Programming, Levenberg-Marquardt, Genetic Algorithm and Bees algorithm, the latter algorithm was found to be an appropriate approach due to the high number of parameters. The following objective function based on minimization of SSE between the experimental concentrations of sulfur and asphaltene and their calculated concentrations in the hydrotreated products at the reactor outlet, is used:

$$SSE = \sum_{i=1}^{N_{Data}} \left[C_{Sul,i}^{exp} - C_{Sul,i}^{cal}\right]^2 + \left[C_{asph,i}^{exp} - C_{asph,i}^{cal}\right]^2 \qquad 4.24$$

The set of equations 4.1 through 4.10 was solved in MATLAB by evaluating all the transport and thermodynamic properties at the specific operating conditions. The forward finite difference method with a numerical optimization solution nested inside was used to solve the system of differential equations and estimate the unknown kinetic parameters associate with the equations. The length of reactor was divided into 100 increments in order to improve accuracy. To achieve the convergence, initial values of sulfur and asphaltene concentrations at the catalyst surface were assumed to be same as their initial liquid concentrations.

Chapter Five: Results and Discussion

5.1 Estimation of Kinetic Parameters

The kinetic parameters for hydrodesulfurization and hydrodeasphaltenization reactions for Athabasca bitumen were determined based on the experimental data and the TBR process model explained in Chapter 4. In the optimization approach implemented, all parameters have been calculated simultaneously. The kinetic parameters obtained for HDS and HDAs reactions are presented in Table 5.1.

Table 5.1 Kinetic parameter values estimated with non-linear approach (Catalyst M3).

	n	**m**	**EA_{HDS} (kJ/mol)**	**A_{HDS}**
Hydrodesulfurization	1.64	0.39	153.7	2.67e13
	e	**f**	**EA_{HDAs}(kJ/mol)**	**A_{HDAs}**
Hydrodeasphatenization	1.71	0.45	119.2	6.25e10

The results of kinetic parameters were derived by using three levels of temperature (325, 335 and 345°C), and two levels of WHSV (0.2 and 0.3 hr^{-1}) at a total initial pressure of 1400 psig and a hydrogen to oil ratio of 900 sccm/cc. The reaction order for sulfur at catalyst surface "n" was found to be 1.64 which is typical for single lumped kinetics and is in good agreement with previous literature reports (Kam et al., 2008 and Rodriguez et al., 2004). Although the reaction order for some sulfur species undergoing HDS reactions follow first-order kinetics, grouping different species into a lump result in an increase of the overall reaction order. Reaction orders between 0.5 and 2 are widely observed for kinetics based on lumped models. The wide disparity of molecular reactivities of individual sulfur containing species in the single lump is attributed to any reaction order higher than unity. Second order kinetics were obtained for HDS reaction of Maya feed while

1.5 order kinetics were observed for bitumen-derived gas oils (Yui et al., 1989). Reaction orders in the range of 1.4 – 2 were reported during the HDS of conventional distillates (Shiflett, 2002). It has also been observed the reaction order increased from 1.7 to 2 with an increase in the molecular weight and sulfur content of feedstock (Ancheyta et al., 2005). Most activation energies in the literature review are in the range of 105 to 146 kJ/mol with some exceptions, i.e. 287 kJ/mol. The activation energy for HDS in this work was found to be 153.7 kJ/mol. Studies have confirmed that at higher temperatures, the overall reaction order for HDS would decrease.

For the HDAs reaction, the order for asphaltene "e" and the activation energy was found to be 1.71 and 119.2 (kJ/mol) respectively. The low activation energy is attributed to the strong influence of intraparticle diffusion of large asphaltene molecules on its reaction rate. Values in literature are reported for asphaltene hydrocracking and scarce information is available for hydrogenation of these compounds. Summary of studies on kinetics of asphaltene conversion, reveals the activation energy to be catalyst dependent, varying from 59 kJ/mole for one catalyst to 116 kJ/mol for another catalyst (Shimura et al.,1986). In a similar study for asphaltenes hydroconversion over Mo/Al_2O_3 in a continuous packed bed reactor, an activation energy of 99 kJ/mol was observed (Stanislaus et al., 1999). Reaction orders reported in literature for asphaltenes in residual oil hydrocracking varies considerably from 0.5 to 2. A second-order kinetics has been reported for asphaltenes conversion in the hydrotreating of Boscan and Greek residues while for the Maya residue the reaction order is found to be 1.5 (Callejas et al., 2000). The reaction orders are found to be less affected by catalyst and more influenced by refractory fractions of the feedstock. The overall orders of "n" and "e" can be described as parameters reflecting the catalyst ability to attack refractory species of sulfur and asphaltene. The lower the activity, the higher the orders of reaction. In general, when using the

grouping or lumping approach for kinetic studies, reaction orders up to second order are expected when a fraction of feedstock remained unreactive.

The values obtained for order of reaction for hydrogen, “m” = 0.39 and “f “= 0.45 reveals that a dissociation of hydrogen on the catalyst site is happening. The theoretical value for hydrogen dissociation is reported to be 0.5. The mechanism utilized to describe the HDAs and HDS reaction, resulted in the order of hydrogen concentrations less than 1.0 at the catalyst surface. Hence the model predicts increased conversion of sulfur and asphaltene with an increase in pressure. In order to validate the model and obtain the reaction order for hydrogen, the effect of total pressure needs to be studied in the pilot-plant while keeping the other variables constant.

The non-linear approach resulted in a sum of square errors (SSE) equal to 6.9×10^{-10} indicating an accurate calculation.

5.1.1 Factors effecting Kinetic Data

Several factors have an impact on the reliability of kinetic data. First, cumulative error in measuring and analyzing experimental parameters incorporated in equations may affect the accuracy of obtained kinetic data. Besides the usual operating conditions employed during the set of experiments, such as temperature, total pressure, hydrogen pressure and contact time (space velocity), the reaction order and activation energy variations observed in different studies reported in the literature can be attributed to differences in configuration and type of reactor (e.g. batch versus continuous), catalyst type and particle size, the nature of feedstock and time on stream at which the measurement is taken. The latter needs to be considered because of a gradual catalyst deactivation. In addition, different mathematical models employed to treat kinetic data may result in different kinetic values.

5.1.1.1 Effect of Kinetic Model

Two different kinetic models, including the simple power law model (Eq. 4.19) and the Langmuir-Hinshelwood model (Eq. 4.19[1]) were used to study the kinetics of HDAs reaction. It was demonstrated by the results shown in Table 5.2 that the type of mathematical model used, affects the kinetic parameters. The different results in activation energy were attributed to the competitive H_2S adsorption on catalyst sites considered in the L-H model whereas, the power law model does not account for this effect.

Table 5.2 Kinetic parameter values estimated for HDAs reaction considering different models (Catalyst M3).

	EA_{HDAs} (kJ/mol)	A_{HDS}
Power Law	102.6	5.95e8
Langmuir Hinshelwood	119.2	6.25e10

5.2 Reactor Simulation under Steady State Catalyst Activity

A comparison between model predictions and experimental data for sulfur and asphaltene conversion is provided in Figure 5.1. The following equation is used to calculate the theoretical conversions of sulfur and asphaltene at the reactor outlet:

$$X_j = \frac{(C_i)_{Reactor\ Inlet} - (C_i)_{Reactor\ Outlet}}{(C_i)_{Reactor\ Inlet}} \times 100,\ j = HDS\ and\ HDAs, i = Sulfur\ and\ Asphaltene \qquad 5.1$$

Figure 5.1 illustrates the parity plot of the proposed model for HDAs and HDS reactions. The distribution of points on the lower side of the straight line indicates that the model slightly underpredicts the experimental data. As it is illustrated in Figures 5.2 and 5.3 asphaltene and sulfur conversion is increased with increasing temperature and decreasing WHSV, as it is expected. This

is attributed to the fact that both HDAs and HDS kinetic parameters used in previous chapter are affected by process parameters. The correlations used to describe the diffusivity of components, solubility and Henry's coefficients of hydrogen, mass velocity of the gas and liquid phase, mass transfer coefficients at both gas-liquid and liquid-solid interfaces, viscosity and density shown in Appendix B, show the effect of reaction temperature on each of these parameters. The reaction rate constants described by the Arrhenius equation increase as a result of increasing the reactor temperature leading to an increase in the reaction rate of HDAs and HDS. This supports the fact that reaction temperature is very crucial to enhance the degree of asphaltene and sulfur removal. WHSV is another important operating condition affecting the efficiency of hydrotreating reactions. A decrease in WHSV translates into an increase in the residence time leading to an increase in the effectiveness of the catalyst.

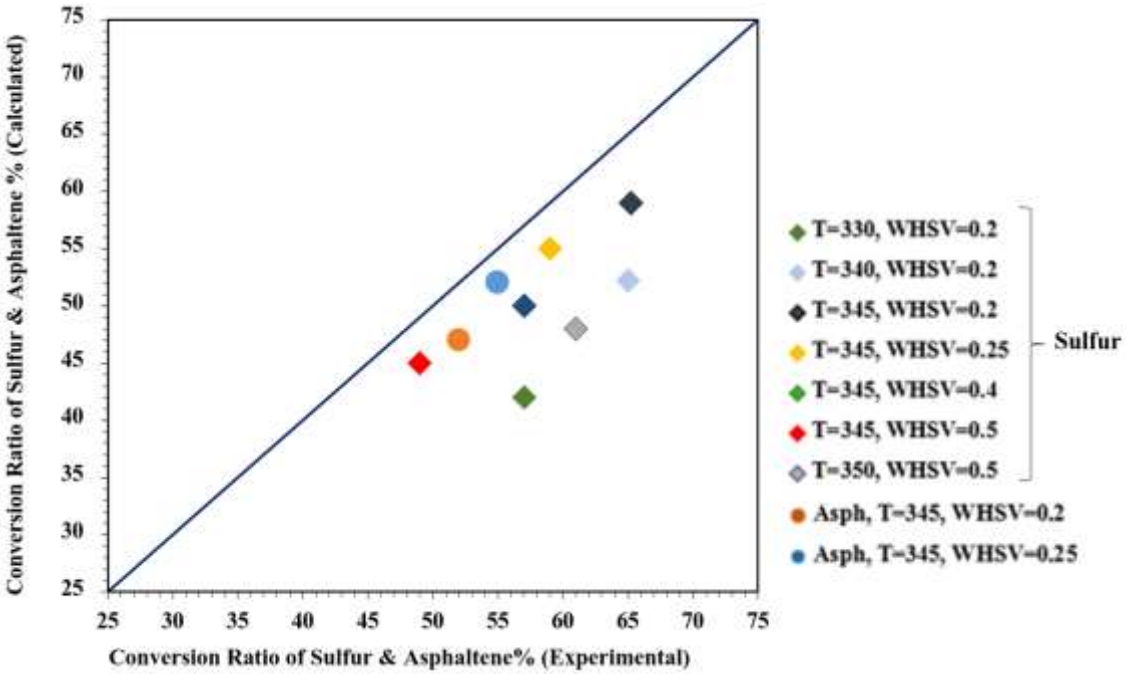

Figure 5.1 Comparison between experimental and model predicted conversion of sulfur and asphaltene

Several reasons can attribute to the lower HDS and HDAs conversion rates calculated by the mathematical model. First, as a result of hydrogenation reactions happening in the reactor the feed becomes lighter and mass transfer, which mainly depends on the physical properties of the liquid (viscosity and density), improves notoriously along the catalytic bed the concentration gradients. As a result, the concentration gradient existing between the liquid and solid phase should disappear progressively along the reactor. The mathematical model developed does not account for density changes along the reactor length. Thus, the increase in mass transfer coefficient along the catalytic bed is not reflected. Also, the deviations observed between measured and calculated sulfur and asphaltene concentrations may be due to an underestimate of the wetting efficiency which results in lower sulfur and asphaltene conversion by the proposed mathematical model.

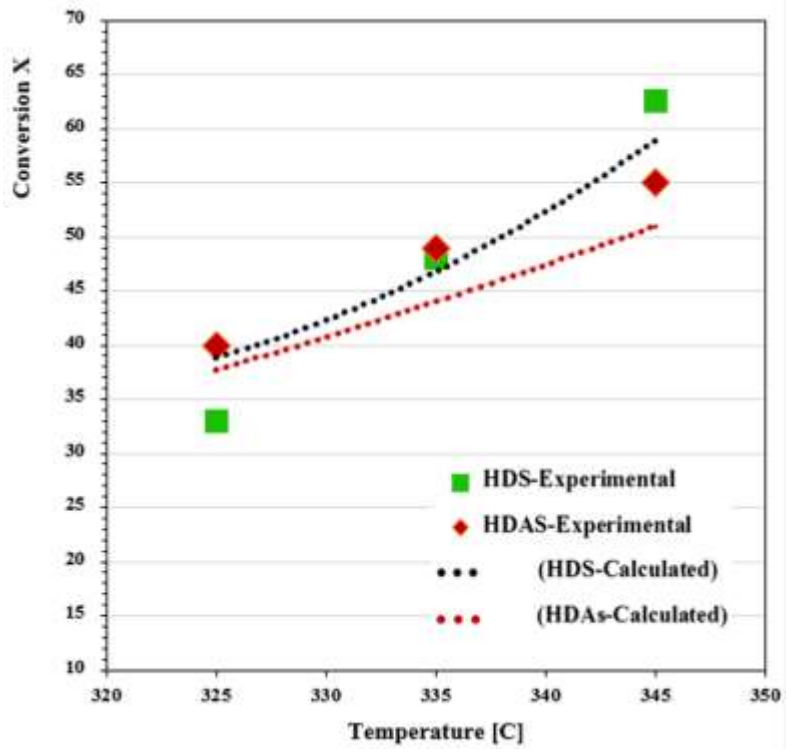

Figure 5.2 Model predicted and experimental performance of HDS and HDAs as a function of temperature.

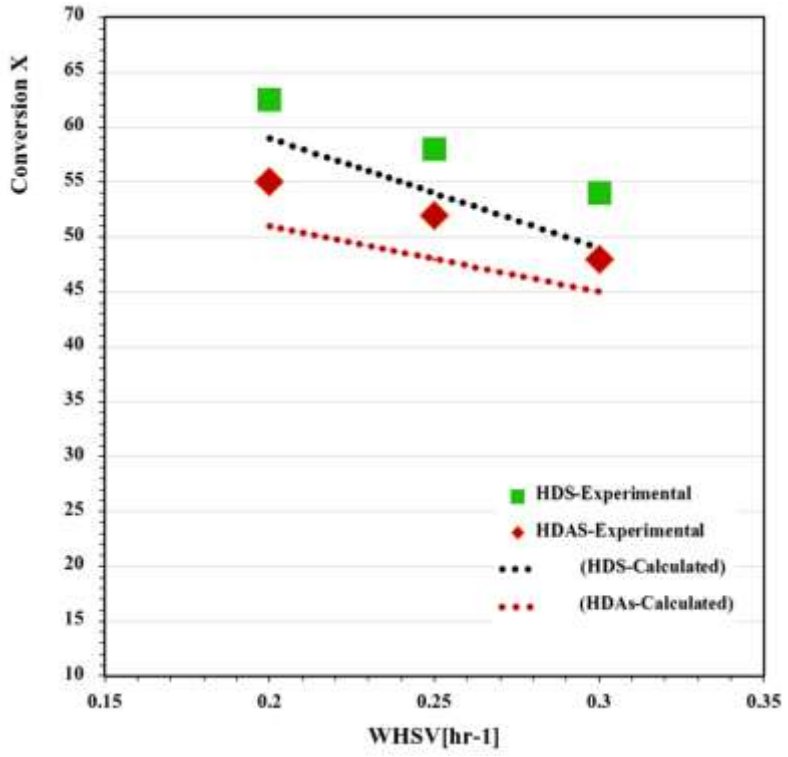

Figure 5.314 Model predicted and experimental performance of HDS and HDAs as a function of weight hour space velocity.

As it is shown in Figure 5.4 the effectiveness factor for tested catalyst (M3) is in the range of 0.52 to 0.73 for HDS reaction and 0.41 to 0.61 for HDAs reaction, all translating in a Thiele modulus greater than unity which imply that both reactions may consider to be within strong internal diffusion limitations. Very small catalyst effectiveness factors observed is also an indication of the reactions taking place only on the outer surface of the catalyst. In this case, the conversion in TBRs are greatly affected by the wetting efficiency. It is evident from the results shown in Figure 5.2 and 5.3 conversion is more affected by small changes in temperature when compared to space velocity. Similar behavior is observed in the effectiveness factor values obtained from the model. Effectiveness factor decreases more as the reactor temperature decreases and an increase in WHSV provokes only a marginal reduction in this value which suggests that internal diffusion does not

depend largely on flowrates. As the reactor temperature increases, effectiveness factor is incremented and the reaction approaches towards surface-reaction limitations. The lower effectiveness factor values obtained for HDAs reaction is an indication of the stronger influence of intraparticle diffusion of large asphaltene molecules on its reaction rate when compared to HDS reaction.

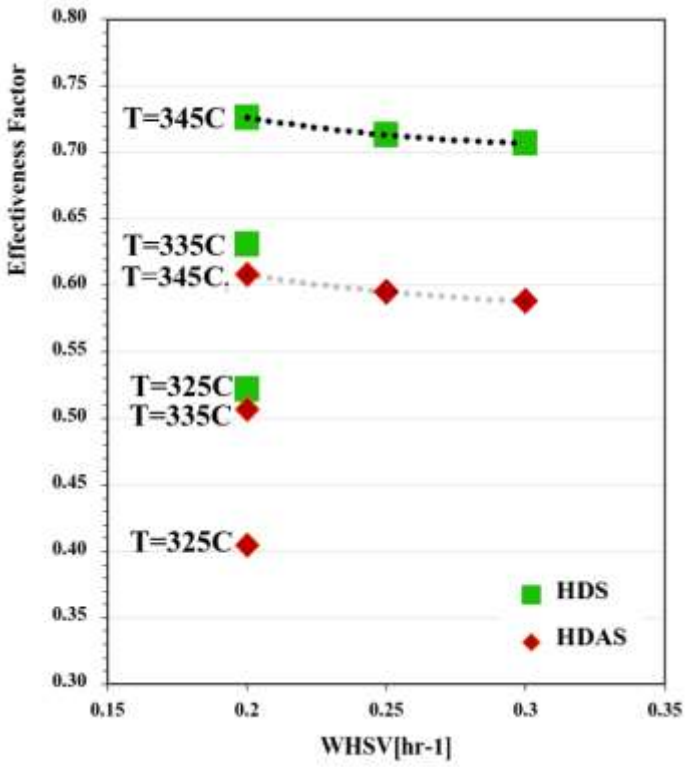

Figure 5.4 Catalyst (M3) effectiveness for HDS and HDAs vs. weight hourly space velocity at different reactor temperatures.

In general, it can be concluded that the trend of HDS and HDAs conversion predicted by the mathematical model is in good agreement with experimental observations. The model can be employed to predict the sulfur and asphaltene contents under various operating hydrogenation conditions for which experimental data is not available.

5.3 Concentration Profiles along the Reactor

The model developed is employed to describe the behavior of the pilot plant reactor used for bitumen hydrogenation. The evolution of H_2 and H_2S concentration in the gas phase is plotted in Figure 5.5 as function of reactor length. Partial pressures of H_2S increases as a result of its production during HDS and HDAs reactions whereas the diminution of H_2 is related to its consumption by same chemical reaction.

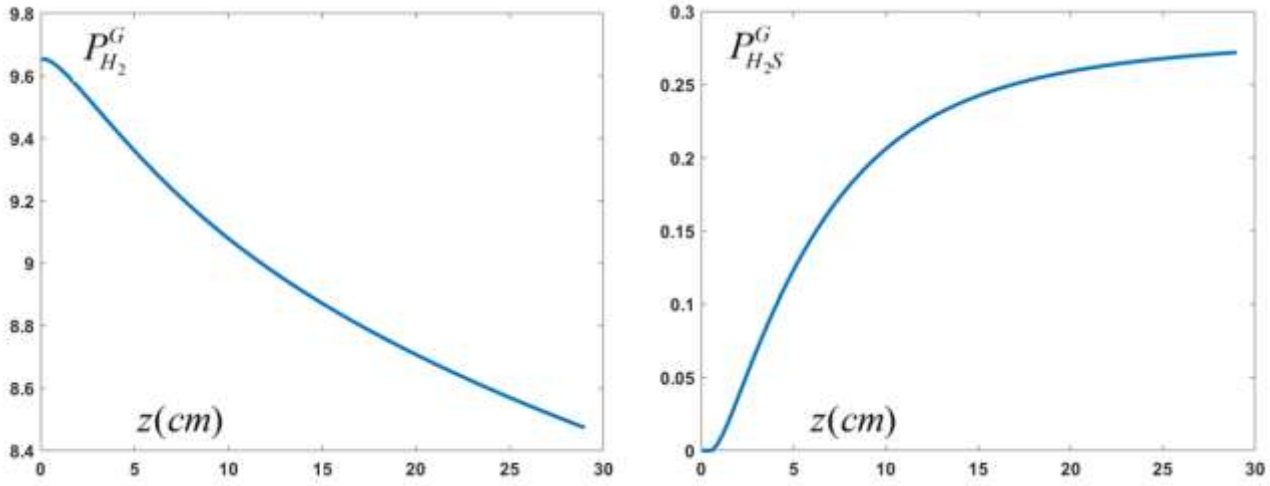

Figure 5.5 H_2 and H_2S partial pressures (MPa) as function of reactor length at 345°C, WHSV=0.2 hr^{-1} and 1400 psig.

Figures 5.6 presents the molar concentration profiles of H_2 and H_2S in the liquid phase at the reactor temperature of 345°C. Highest concentration of H_2S and the lowest concentration of H_2 is observed near the entrance of the reactor. It is observed that H_2 concentration drops substantially from the reactor entrance to the first 3 cm of reactor length (accounting for 10 percent of total length), whereas H_2S increases quickly in the same section. The negative gradient can be explained by high reaction rates in this section of reactor. This means that the term related to chemical

reaction is greater than the term related to mass transfer at this section. At the entrance of the reactor the mass transfer rate between liquid and solid interface predominates over the liquid and gas interface. As a result, hydrogen is rapidly consumed in the liquid phase. On the other hand, produced hydrogen sulfide remains in the liquid phase. Gradual and progressive concentrations of H_2 in the liquid phase along with the release of H_2S from liquid to gas phase in the remaining length of reactor is an indication of gas-liquid governed equilibrium. As a result of equilibrium, constant concentrations of H_2 and H_2S are expected at the end of the reactor, which has not occurred in the tested reactor. The trend of hydrogen concentration in liquid phase shows that the initial part of the reactor is far from being saturated with hydrogen.

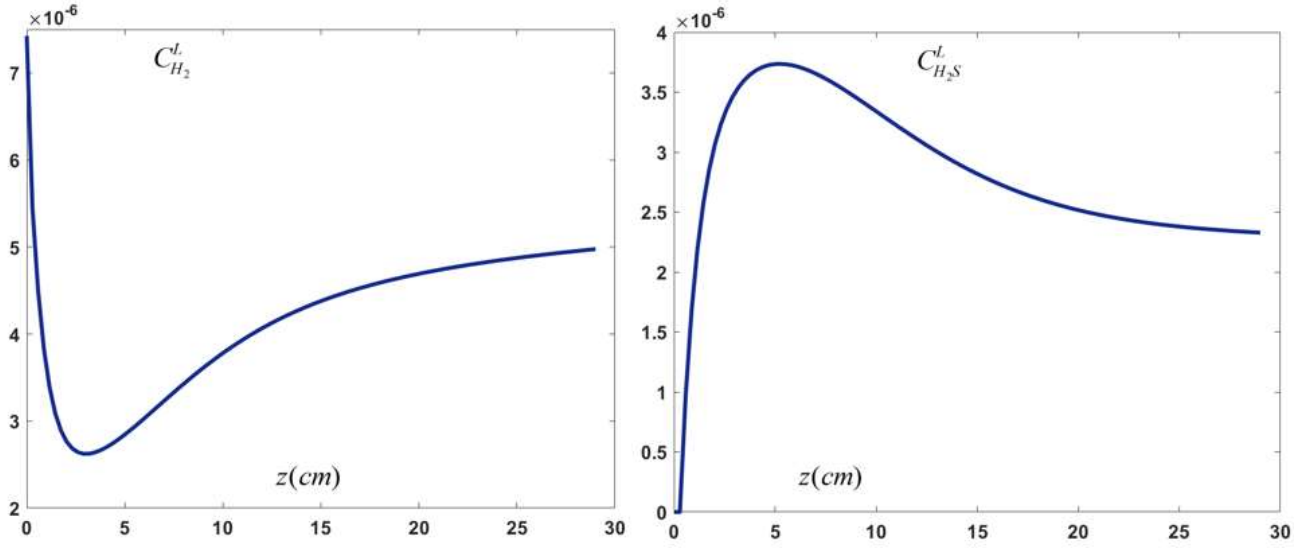

Figure 5.6 H_2 and H_2S concentration (mol cm^{-3}) profiles in liquid phase as function of reactor length at 345 °C, WHSV=0.2 hr^{-1} and 1400 psig.

As it is shown in Figure 5.7, typical behavior for the concentration of sulfur and asphaltene is observed in the liquid phase. As the mixture passes through the reactor a diminution of asphaltene and sulfur concentration is observed in the liquid phase. As expected, conversion for HDS is higher

than for HDAs. The concentration differences between the liquid bulk phase and the catalyst surface were found to be negligible.

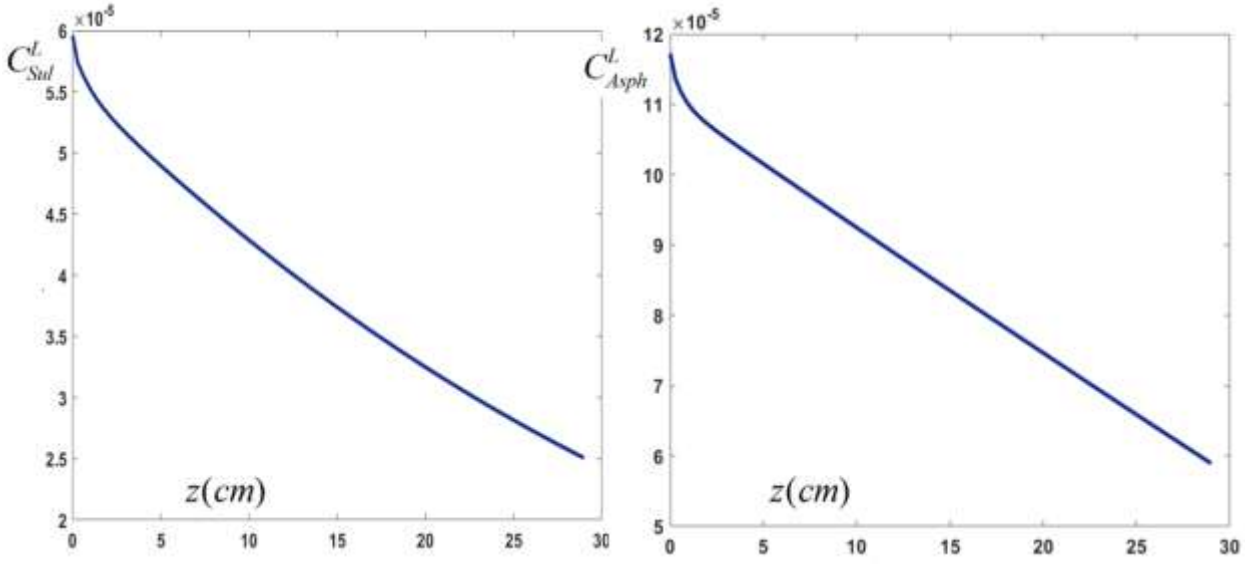

Figure 5.7 Sulfur and asphaltene concentration (mol cm^{-3}) profiles in liquid phase as function of reactor length at 345°C, WHSV=0.2 hr^{-1} and 1400 psig.

5.4 Liquid Product Characterization Results

5.4.1 Effect of Operating Variables on Whole Liquid Product Properties

As an example of the performance of the implemented technology at RTU-1, the distillation curves of various upgraded oils and their respective original bitumen are plotted in Figure 5.8. The yields follow the typical cascade where vacuum residue is converted to vacuum gasoil followed by distillates and kerosene. At the most severe condition, 345°C and 0.2 hr^{-1} space velocity the yields of middle distillates (kerosene and light gas oil) is slightly increased by about 4.47 wt.% whereas naphtha yield remains almost unchanged. At the same condition the yield of heavy vacuum gas oil increased by about 2.64 wt.% while vacuum residue was converted 12.64 wt.%, approximately.

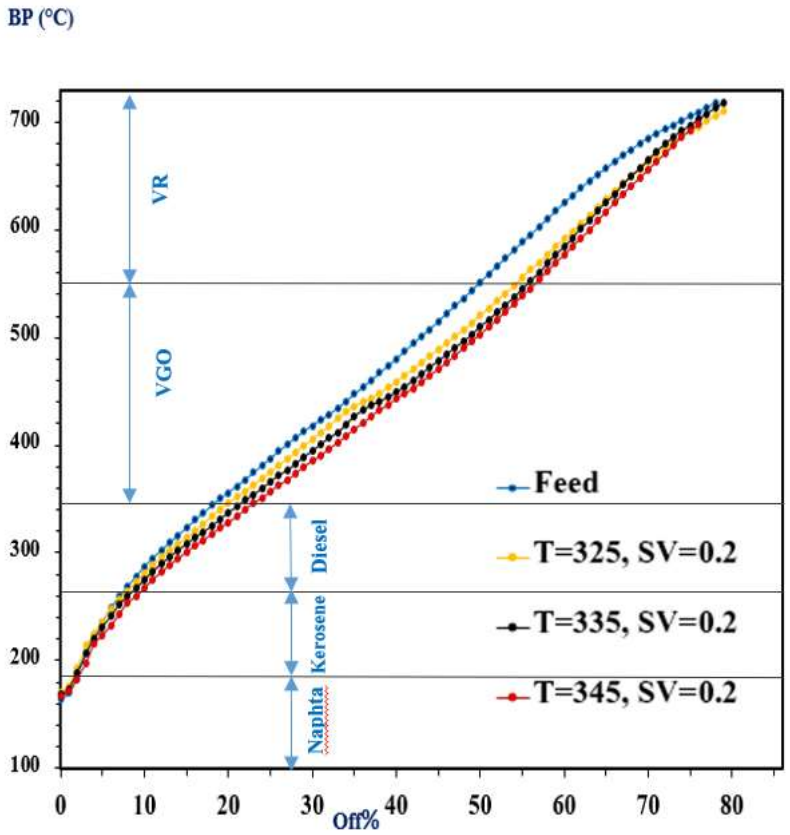

Figure 5.8 Distillation Curves of feedstock and upgraded products.

The high viscosity of bitumen is associated with the high boiling point components in the vacuum residue, aggregated asphaltene species and the strong interactions of large molecules. As it is observed in Table 5.3 and Figure 5.9, the viscosity and API gravity of bitumen have improved substantially as the temperature was increased and space velocity was decreased. The minimum viscosity values during RXN-1 and RXN-2 were obtained at T=345 °C and WHSV=0.2. Unlike viscosity changes in the absence of chemical reactions, the reduction in the viscosity during hydrogenation reactions, is not reversible.

API gravity follows a linear dependency with respect to temperature and WHSV. However, as it is indicated by the correlation factor, R=0.97, temperature has shown a stronger effect on density improvement when compared to WHSV.

Table 5.3 Effect of operating condition on upgraded product viscosity.

Avg. Reaction Temperature (°C)	Liquid WHSV (hr^{-1})	Whole Product Viscosity (cP at 25°C)	
		RXN-1	RXN-2
Bitumen		78,750	64,470
325	0.2	9,369 ∓ 114	
330	0.2		3,073 ∓ 113
335	0.2	3,987 ∓ 271	
340	0.2		1,752 ∓ 27
345	0.2	1,727 ∓ 25	1,424 ∓ 56
345	0.25	2,046 ∓ 30	
345	0.3	2,358 ∓ 118	
345	0.4		2,665 ∓ 39
345	0.5		2,906 ∓ 72
350	0.5		2,230 ∓ 13
325 [a]	0.2	4,721 ∓ 302	
345 [b]	0.2		1,236 ∓ 13

a. Check back condition for RXN-1 to monitor catalyst activity.
b. Check back condition for RXN-2 to monitor catalyst activity.

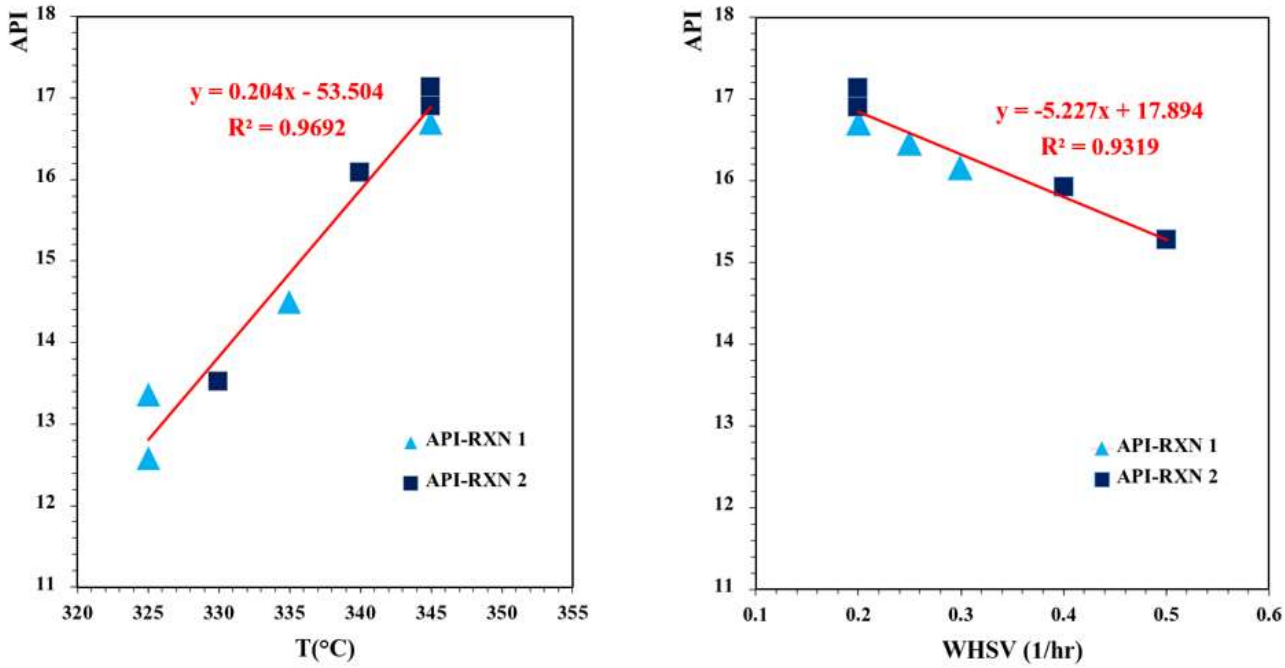

Figure 5.9 API gravity of whole upgraded products as a function of temperature at WHSV=0.2 hr^{-1} and weight hour space velocity at T=345 °C.

An important parameter for upgrading is the coke-forming tendency. A typical value for MCR in whole Athabasca bitumen is 13.6% MCR by weight. The effect of WHSV and temperature on the removal of MCR during hydrogenation of Athabasca bitumen is shown in Table 5.4. It is observed from the table that during RXN-2 as the WHSV is decreased from 0.5 to 0.2 hr^{-1} at a constant temperature of T=345 °C, the removal of MCR is improved by almost 22 wt. percent and in a same manner during RXN-1 as the temperature is increased from 325 °C to 345 °C at a constant liquid WHSV of 0.2 hr^{-1}, microcarbon content in improved by 25 wt. percent. The total microcarbon conversion during RXN-1 and RXN-2 was calculated to be 41 wt.% and 48 wt.% respectively.

Table 5.4 Effect of temperature at WHSV=0.2 hr^{-1} and weight hour space velocity at T=345°C on the Microcarbon Residue.

Avg. Reaction Temperature (°C)	Liquid WHSV (hr^{-1})	Whole Product MCR	
		RXN-1	RXN-2
Bitumen		13.83	12.95
325	0.2	10.73 ∓ 0.16	
330	0.2		8.76 ∓ 0.05
335	0.2	9.58 ∓ 0.23	
340	0.2		7.37 ∓ 0.01
345	0.2	8.08 ∓ 0.18	6.71 ∓ 0.025
345	0.25	8.22 ∓ 0.24	
345	0.3	8.33 ∓ 0.09	
345	0.4		8.09 ∓ 0.035
345	0.5		8.59 ∓ 0.01
350	0.5		8.02
325 [a]	0.2	9.29 ∓ 0.06	
345 [b]	0.2		7.34 ∓ 0.01

c. Check back condition for RXN-1 to monitor catalyst activity.
d. Check back condition for RXN-2 to monitor catalyst activity.

The optical microphotographs shown in Figure 5.10 includes hydrogenated products at 3 different temperatures during RXN-1. No solid precipitations were observed at tested temperatures even at the highest severity condition. It can be concluded that these images along with the data obtained from MCR analysis, confirm the effectiveness of the M3 catalyst in incorporating hydrogen in an effective way and decreasing coke formation in downstream process. The unreacted bitumen is reported to have a P-value of 2.4 and is stable in a mixture with up to 80% oil. The stability of the whole hydrotreated product increases at highest severity hydrotreating condition and reaches a P-value of 2.2 at 345 °C and WHSV=0.2 hr^{-1} and unlike thermal cracked products which would start to precipitate when mixed with only 25% diluent, is stable. The result is that the hydrogenated product is compatible with diluent and refinery streams.

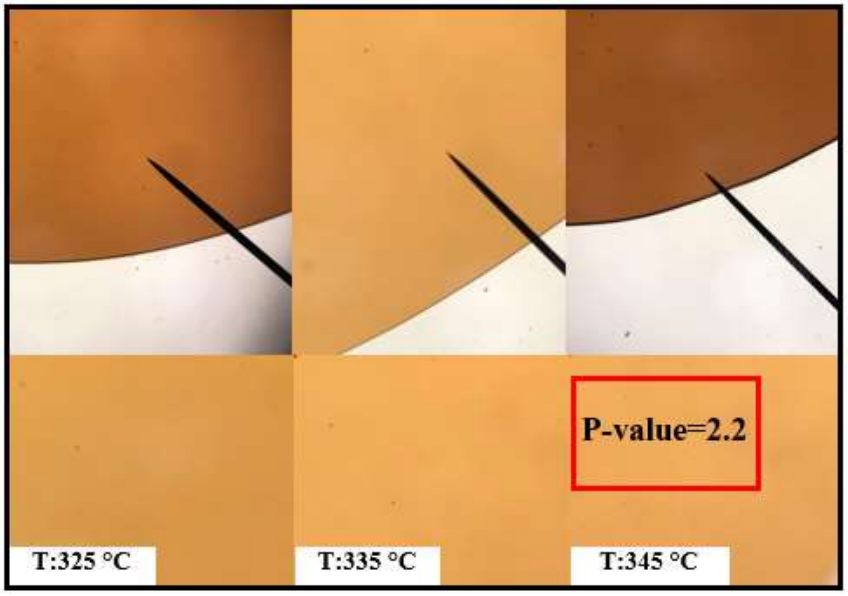

Figure 5.10 Optical microphotographs for bitumen and hydrogenated products at different temperatures (WHSV=0.2 hr^{-1}).

Asphaltenes, the largest molecular weight fraction in oil have high amounts of heteroatoms and a high aromaticity. Studies show production of lower molecular weight asphaltenes; however, higher aromatic species remain in the produced oil while some asphaltenes moieties convert into distillates with almost same molecular weight when processing asphaltene-rich oils (Ali et al., 2006). It is evident from Figure 5.11 that the total amount of asphaltenes in all hydrogenated products diminished as well as resins. However, the aromatic components were found to increase suggesting that heteroatomic moieties from resins and asphaltenes were catalytically removed. Normal production of α-olefins was not observed, probably because thermal cracking reactions were not activated at the low temperature range followed during the present study. Based on reports available for asphaltene changes during hydroprocessing at different conditions, a reduction of alkyl chain length occurs with the increase of the severity of reaction (Merdrignac et al., 2006).

The CH_2/CH_3 ratio can be used to determine the dealkylation mechanism. Our present results did not agree with these reported trends, believed to occur because the lower temperatures set up for the experiments did not lead to the type of reactions described by others studying severe hydroprocessing schematics.

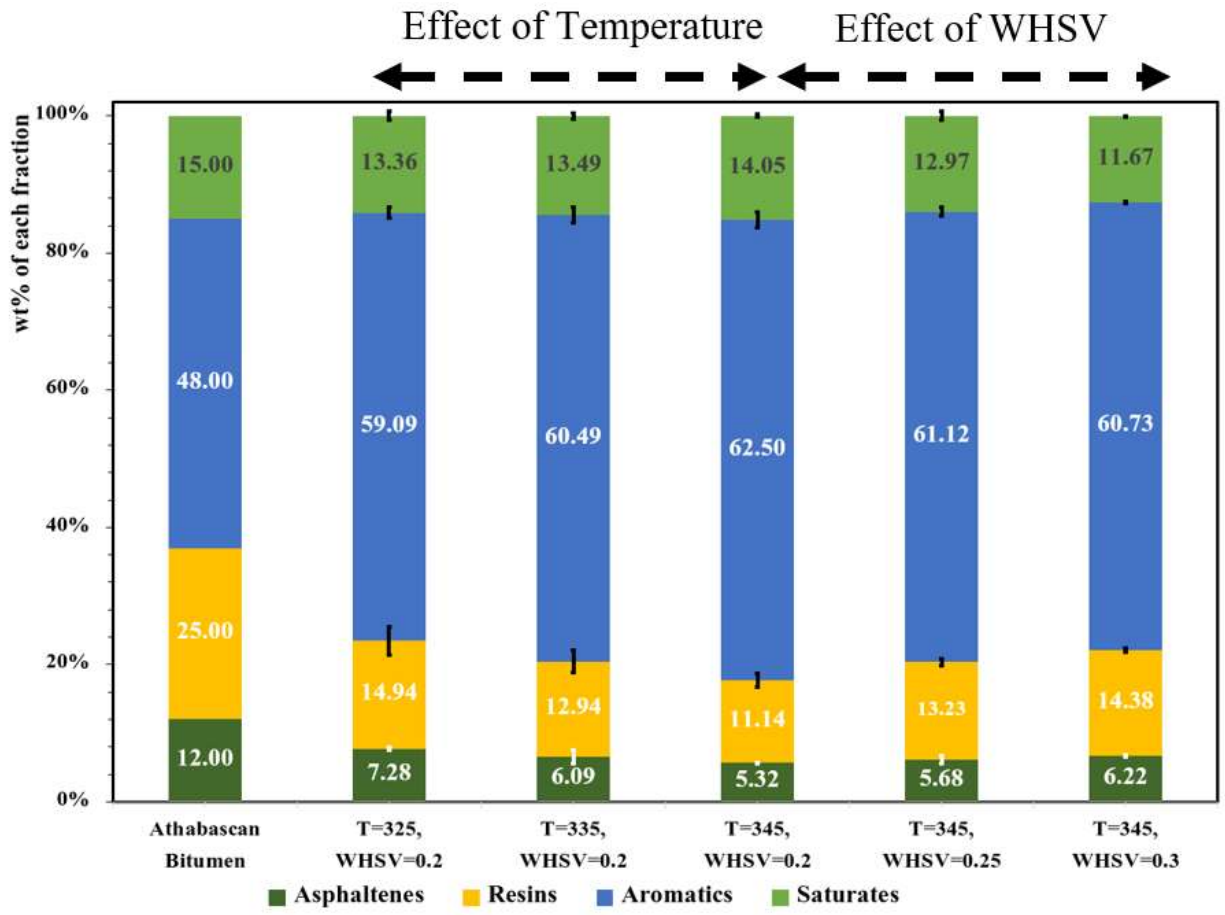

Figure 5.11 SARA analysis of feedstock and whole hydrogenated products.

The conversion of asphaltenes fraction to aromatics can also described by totally removing the polar oxygen from its structure. 100% TAN conversion was observed for all hydrogenated products during both set of experiments.

The effect of temperature and WHSV on sulfur removal in hydrotreated products during the experimental runs is presented in Figure 5.12. It has been observed that the sulfur compounds tend to decrease when reaction conditions are more severe, i.e. higher temperatures and lower space velocities. When space velocity is reduced the higher conversion of sulfur is attributed to the increased residence time in the catalytic bed. However, temperature effect is greater compared to WHSV. This is clearly demonstrated while increasing the temperature from 345 to 350°C and WHSV from 0.4 to 0.5. Despite the lower residence time, the 5°C temperature difference has led to a 12 %wt. increase in the sulfur conversion.

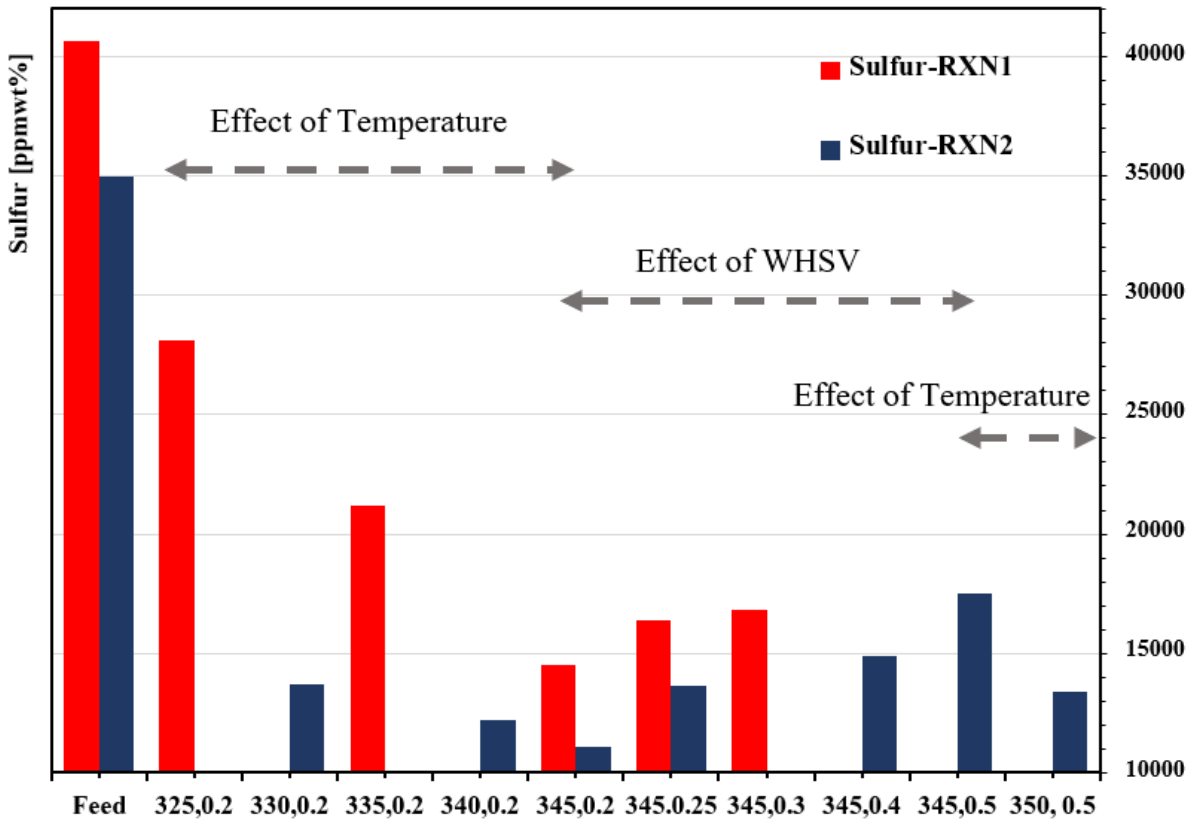

Figure 5.12 Effect of temperature and WHSV on sulfur content of whole hydrogenated products.

An increase of osmosis rate in the catalyst pores on the active sites where the HDS reaction occurs associated with low viscosity of oil at high temperatures may be one reason of the increased sulfur removal (Isoda et al.,1998). Up to 64% sulfur conversion was obtained during RXN-1 as the temperature was increased from 325 °C to 345 °C at a constant space velocity of 0.2 hr^{-1}, whereas the conversion during RXN-2 is slightly higher. The difference in conversion level can either be attributed to the catalyst preparation as two different batches have been implemented, non-uniform reactor packing or to the small variations in operating condition for each set of experiment. Although prior to start-up of the process, the same catalyst activation procedures were followed for both RXN-1 and RXN-2 but achieving different oxidation states of catalysts along the reactor may be another possibility contributing to the different level of sulfur removal during each experiment. As expected, the extent of sulfur removal is inversely proportional to WHSV. HDS conversion was studied at 4 different space velocities varying from 0.2 to 0.5 hr^{-1} at 345 °C and the least conversion was obtained at 0.5 hr^{-1}.

Table 5.5 shows the effect of temperature and WHSV on metals contents. In general, it is observed that the extent of HDM reaction increases at higher temperatures and lower WHSV. The overall HDM kinetic parameters are influenced by origin of feedstock and process conditions. However, studies on CoMo based catalysts reveal that the extent of metal removal may be influenced by the type of support. In this study, almost 56% uptake capacity for Ni and up to 65% removal for V at most severe condition, T=345 °C and WHSV = 0.2 hr^{-1}, is observed. The results of metal conversion are in good agreement with previous experimental observations indicating that V is easier to remove when compared to Nickel. The reactivity difference between Ni and V is attributed to the fact that Ni porphyrins are hidden in the core of asphaltene and for the reaction to take place a previous molecule disaggregation and hydrocracking is required, whereas V

porphyrins are found to be concentrated on the surface of asphaltene (Beuther and Schmid, 1963). Another study also relates the difference to the protruding oxygen atom linked to V porphyrin providing enhanced adsorption surface on the catalyst, whereas in Nickel such a linkage is not observed (Kobayashi et al., 1987).

Table 5.5 Tendency of heteroatoms removal of whole product as a function of process variables.

Avg. Reaction Temperature	Liquid WHSV	Ni [ppmwt.]	V [ppmwt.]
Bitumen		64.2	188.6
325	0.2	34.1	90.5
330	0.2	32.7	87.1
335	0.2	31.8	85.4
340	0.2	30.1	82
345	0.2	27.9	66.3
345	0.25	28.3	70.6
345	0.3	32.1	86.3
345	0.4	32.7	88.3
345	0.5	38.1	105.3
350	0.5	35	76.2

5.4.2 Effect of HDAs on Physical and Chemical Properties of Upgraded Oil

Most of the physical and chemical properties of the upgraded oil present a functional dependency on the asphaltene content. As it is presented in Table 5.6 by decreasing the asphaltene content, viscosity of the product decreases and inversely, API increases which is an indication of asphaltenes being mostly responsible for the high density and viscosity of crude oils. The MCR content strongly depends on the coke forming precursors in the feed. Therefore, both polyaromatic and asphaltenes play an important role in this regard. That is why the kinetics of asphaltenes conversion not necessarily reflect the conversion of MCR and no linear dependency is observed between MCR content and those of asphaltenes. When asphaltenes conversion approaches 55%,

the reduction in MCR reaches almost 41%. The results in table 5.5 confirm that V and Ni in bitumen are associated with asphaltene content. When the HDAs approaches 55% level, about 63% HDM on the basis of total metal (ppmwt. Ni+V) and 64% HDS is achieved. Metals are present in asphaltenes in the form of porphyrins. Therefore the higher removal of asphaltenes correlates with higher metal removal. Asphaltenic metals are known to be the least reactive of all metals present in the feedstock. The available data for crude oils and bitumens show that Ni and V are present in highest concentration and that these elements exhibit a weak negative correlation with API and a positive correlation with the asphaltene content (Curiale, 1984).

Table 5.6 API gravity, viscosity, MCR, sulfur and metal variation in upgraded product as a function of asphaltene contents.

Asphaltene [%wt.]	12	7.28	6.09	5.68	5.32
API Gravity	9	12.59	14.5	16.45	16.9
Viscosity 25°C [mPa.s]	78,752	9,369	3,987	2,046	1,727
Microcarbon Residue	13.83	8.22	9.58	8.22	8.08
Sulfur [ppmwt.]	40,672	28,139	21,187	16,380	14,517
Ni+V [ppmwt.]	253.1	124.6	117.2	98.9	94.2

Figure 5.13 shows that viscosity reduction follows a linearized logharithmic dependence with asphaltene removal with a correlation factor of 0.98. Thus, the higher asphaltene conversion, the lower viscosity of bitumen. Similar dependency is observed for viscosity as a function of resins plus asphaltene content.

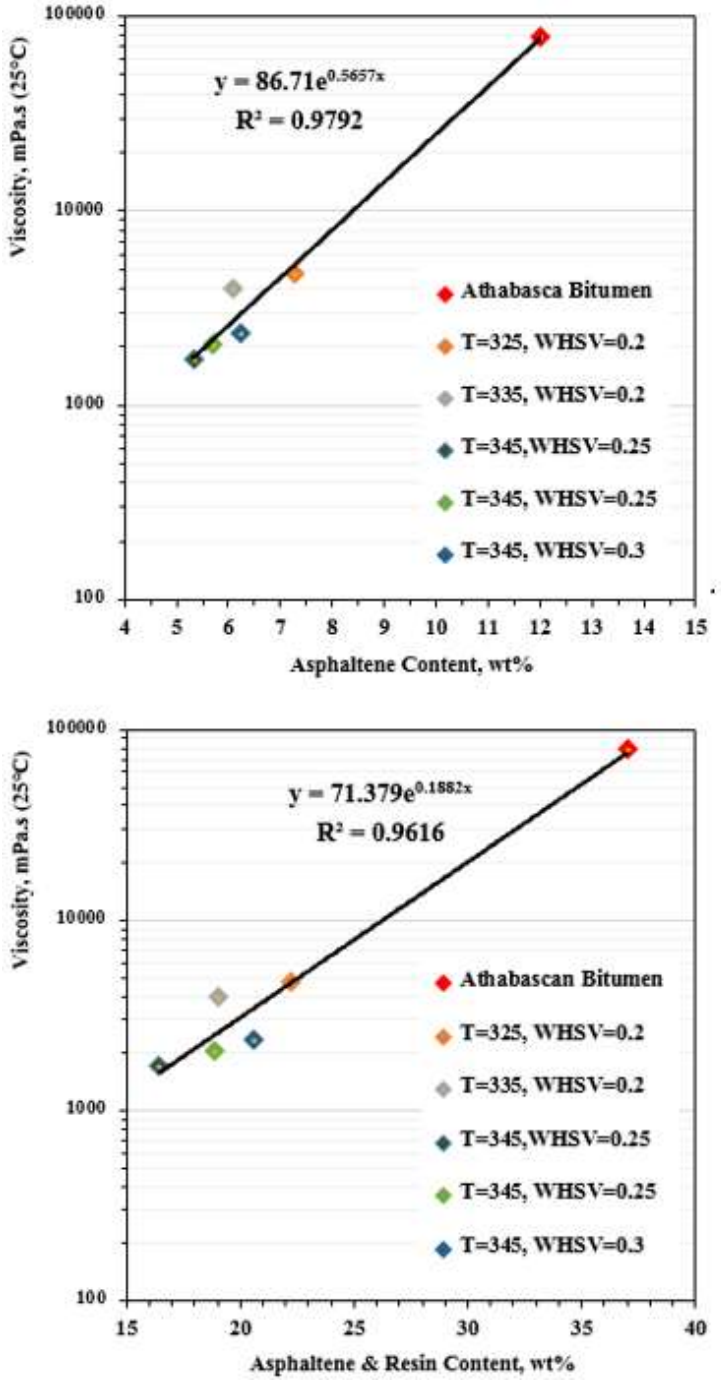

Figure 5.13 Viscosity variation in whole upgraded product as a function of asphaltene and asphaltene+resins contents during RXN-1.

5.5 Catalyst Lifecycle

Catalyst deactivation during hydrogenation of heavy oil and bitumen is driven either by the amount of metals (Ni + V) deposition on catalyst during the whole experimental cycle at axial position or coking. Catalyst M3 activity test has been performed for the both set of experiments, RXN-1 & RXN-2 by repeating the initial condition at the end of length of run. As it is observed in Figure 5.14, the first 350 hours of operation corresponds to temperature and WHSV screening and during the final 47 hours the initial condition (T=325°C, WHSV=0.2 hr^{-1}) was repeated to check the catalyst activity for RXN-1.

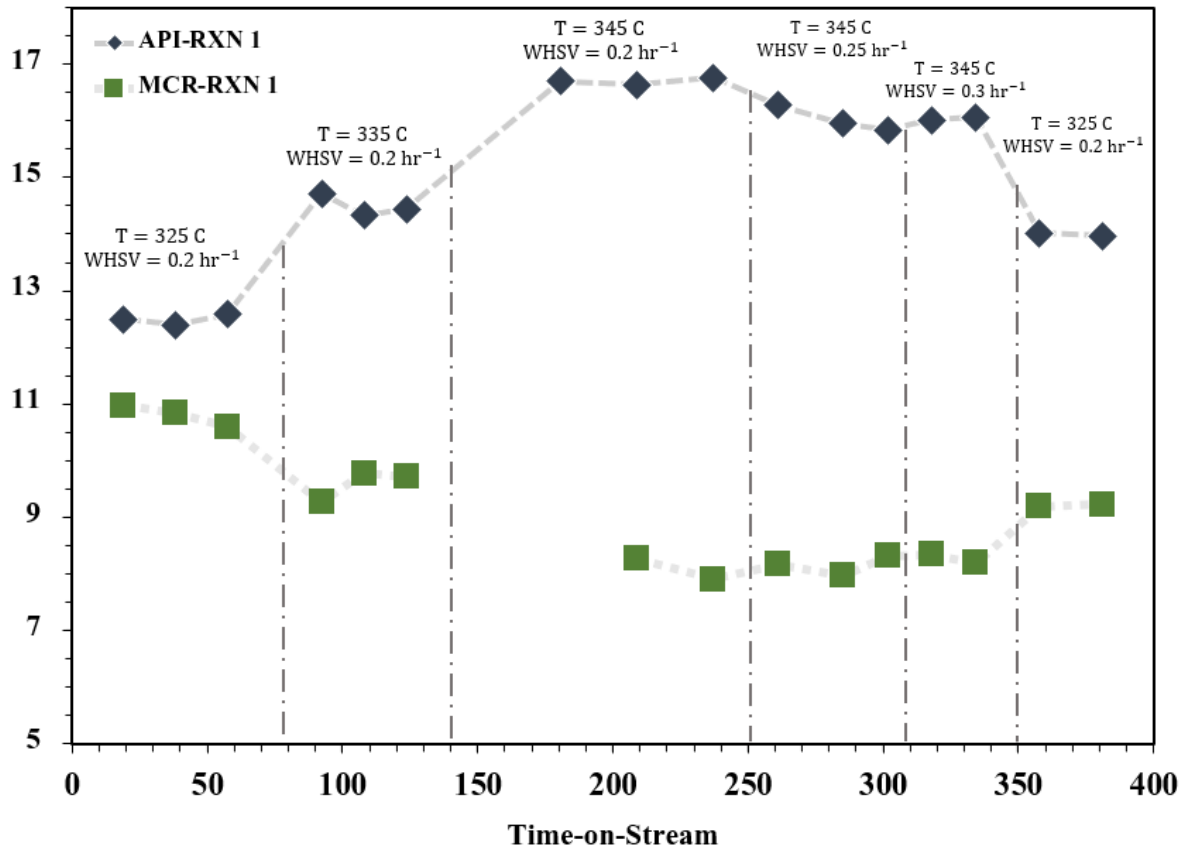

Figure 5.14 Profiles of MCR and API gravity in hydrogenated product during time on stream for RXN-1.

API and MCR values have been improved at the final hours of operation when compared to the initial values, confirming the catalyst was active throughout the reaction. Same results have been obtained for RXN-2 and all other liquid product characteristics explained in section 5.4.1. The improved properties at the end of experimental run with repeated initial operating conditions can be attributed to presence of H_2S which is produced as a result of hydrodesulfurization reaction. The presence of H_2S in hydroprocessing streams is known to be desirable for maintaining the catalyst in its active form. Our studies suggest that active metals being in their sulfide forms may improve the catalyst activity.

In summary, results of the two set of experiments proof that the specific catalyst developed and employed for mild hydro-processing of bitumen has successfully treated the whole range bitumen and has a high metal, sulfur and contaminants removal/retention capacity. That is why the catalyst activity remained constant while doing the check back test for each reaction. Therefore, it can be utilized to overcome the high level of contamination in fixed-bed processing units.

Chapter Six: Conclusions and Recommendations

6.1 Conclusions

This thesis provided an insight about modeling a new catalytic hydrotreating process performed in a TBR reactor and estimating the kinetic parameters for HDS and HDAs reactions occuring during hydrogenating of whole Athabasca bitumen. The reactor model presented, took into account the mass transfer phenomena at both gas-liquid and liquid-solid interfaces and catalyst effectiveness factors for both HDS and HDAs reactions. A non-linear regression method was adapted to estimate the unknown kinetic parameters. Once the reactions kinetics were estimated, the model was validated to simulate the bitumen hydrogenation along the reactor at the best operating condition. The primary role of bitumen hydrogenation was to obtain products with relatively low amount of sulfur, metals, asphaltenes and MCR forming component, thus ready for a steam cracking step. Results of experiments are shown in Table 6.1 and show the specific catalyst developed and employed for mild hydro-processing of bitumen has successfully treated bitumen and has a high metal, sulfur and contaminants removal/retention capacity. That is why the catalyst activity remained constant while doing the check back test for each reaction. Therefore, it can be utilized to overcome the high level of contamination in fixed-bed processing units. The major effects of the temperature and WHSV variables and their influence on the performance of the reactor can be summarized as follows. To improve the conversion for V, Ni, S, and asphaltene compounds either an increase in temperature or decrease of the WHSV can be chosen. The best conditions during the set of experiments were found to be 345°C and 0.2 hr^{-1} space velocity. However, it should be taken into account that temperatures higher than 345°C may lead to undesired products as a result of hydrocracking and on the other hand values too small for WHSV will decrease the unit capacity.

Table 6.1 Summary of experimental results for hydrogenating Athabasca bitumen.

Analysis		Athabasca Bitumen	Whole Hydrogenated Product [T=345C, WHSV=0.2 hr^{-1}]
API Gravity		9.0	16.9
Microcarbon Residue		13.83	8.08
Viscosity @ 25°C [mPa.s]		78752	1727
Metals	Sulfur Content [ppmwt.]	40673	14517
	Ni+V [ppmwt.]	253	94.2
SARA	Saturates [%wt.]	15	14.1
	Aromatics [%wt.]	48	62.5
	Resins [%wt.]	25	11.4
	Asphaltenes [%wt.]	12	5.3

The following similarities between HDS and HDAs kinetics have been observed which may be applicable for the other hydrotreating reactions as well:

The overall reaction orders obtained for HDS and HDAs occurring during hydrotreating of whole range bitumen is higher than unity. This is attributed to the grouping of components which is unavoidable due to the large number of reacting species of each component existing in feedstock. The effectiveness factor values for tested catalyst (M3), translate in a Thiele modulus greater than unity which imply that both reactions may be considered to be within strong internal diffusion limitations.

6.2 Recommendations for Future Work

The novelty of this research work is attributed to the feed stock used during the experiments, the whole range bitumen, the chemically novel catalyst and the new proposed catalytic hydro-steam cracking process which aims to reduce or eliminate the hydrogen consumption for the hydrogenation purpose in the first reactor. In order to enhance the performance of the unit it is proposed to perform longer test runs to study the catalyst de-activation kinetics and mechanism. It is also necessary to couple the continuous model with an appropriate hydrodynamic model to obtain a more precise kinetic model being able to predict the performance of the unit at commercial scales. Since bitumen as the feedstock is comprising a broad distribution of chemical species, a good approach for developing the kinetic model would be splitting each chemical lump into two groups, the less refractory fraction which is easy to react and the refractory fraction that reacts slowly to account for reactivity of species. The mechanism utilized to describe the HDAs and HDS reaction, resulted in the order of hydrogen concentrations less than 1.0 at the catalyst surface. Hence the model predicts increased conversion of sulfur and asphaltene with an increase in pressure. In order to validate the model and obtain the reaction order for hydrogen, the effect of total pressure needs to be studied in the pilot-plant while keeping the other variables constant.

References

Al Dahhan, M.H., Dudukovic, M.P. 1995. Catalyst wetting efficiency in trickle-bed reactors at high pressure. Chemical Engineering Science. Vol. 50, No. 15, pp. 2377-2389.

Alberta Innovates, March 2018. "Bitumen Partial Upgrading 2018 Whitepaper", AM0401A.

Alberta Royalty Review Advisory Panel Report, "Alberta at a Crossroads," http://www.energy.alberta.ca/Org/pdfs/ RoyaltyReportJan2016.pdf.

Alberta Oil ,"The cancellation of Voyageur leaves an uncompleted megaproject near Fort McMurray,", March 20, 2014, http://www.albertaoilmagazine.com/2014/03/economic-ruins-suncor-voyageur/; Jeremy VanLoon, "CNOOC Cutbacks at Long Lake Oil-Sands Site Caps Years of Trouble," Bloomberg, July 14, 2016, http://www.bloomberg.com/news/ articles/2016-07-14/cnooc-cutbacks-at-long-lake-oil-sands-site-caps-years-of-trouble; Kevin Birn, "Production cost and the Canadian oil sands in a lower price environment," IHS blog, February 17, 2016, http://blog.ihs.com/production-cost-andthe-canadian-oil-sands-in-a-lower-price-environment.

Ali. L.H., Abdul-Karim, E. 1986. The Oil, Origin, Composition and Technology, Al-Mosul University, Iraq.

Ali, F.A., Ghaloum, N., and Hauser, A. 2006. Structure representation of asphaltene GPC fractions derived from Kuwaiti residual oils. Energy Fuels 20 (1):231-238.

Ali, S.A. 2007. Thermodynamics of hydroprocessing reactions. In Hydroprocessing of Heavy Oils and Residua (J. Ancheyta, J.G. Speight, Eds.), CRC Press, Taylor & Francis, Boca Raton, FL, Chapter 4.

Ancheyta, J., Centeno, G., Trejo, F., Marroquin, G. 2003. Changes in asphaltene properties during hydrotreating of heavy crudes. Energy Fuels 17(5):1233-1238.

Ancheyta. J., Rana, M. S., and Furimsky, E. (2005). Hydroprocessing of heavy petroleum feeds: Tutorial. Catalysis Today, 109, pp. 3-15.

Ancheyta, J., Speight, G. 2007. Hydroprocessing of Heavy Oils and Residua. FL: CRC Press.

Asaoka, S., Nakata, S., Shlroto, Y., and Takauchl, C. 1983. “Asphattene Cracking in Catalytic Hydrotreating of Heavy Oils . Study of Changes in Asphaltene Structure during Catalytic Hydroprocessing,” pp. 242–248.

ASTM Committee D-2 on Petroleum Products, L.F. and Lubricants, 2011. Standard test method for acid number of petroleum products by potentiometric titration. ASTM International.

Banerjee, D.K. 2012. Oil Sands, Heavy Oil and Bitumen. Tulsa: PennWell Corporation.

Beuther, H., Schmid, B.K. 1963. Reaction mechanisms and rated in residue hydrodeulfurization. In proceedings of the 6th World Petroleum Congress, Frankfurt, Germany, Section 3, pp. 297-310.

Bhaskar, M., Valavarasu, G., Sairam, G., Balaraman, K. S., and Balu, K. 2004. “Three-Phase Reactor Model to Simulate the Performance of Pilot-Plant and Industrial Trickle-Bed Reactors Sustaining Hydrotreating Reactions,” pp. 6654–6669.

Brons, G. Yu, J.M. 1995. Solvent deasphalting effects on whole Cold Lake bitumen. Energy Fuels 9:641-647.

Botchwey, C., Dalai, A. K. and Adjaye, J. 2006. Simulation of a Two-Stage Micro Trickle-Bed Hydrotreating Reactor using Athabasca Bitumen-Derived Heavy Gas Oil over commercial NiMo/Al2O3 Catalyst: Effect of H2S on Hydrodesulfurization and Hydrodenitrogenation. International Journal of Chemical Reactor Engineering, 4, 1-15.

Cabrales-Navarro, F.A. 2016. Reactivity Study and Kinetic Modeling of Deasphalted Oil Upgrading via Thermal and Catalytic Cracking. PhD, University of Calgary.

Callejas, M. A.; Martinez, M. T. 2000, Hydroprocessing of Maya Residue. II. Intrinsic kinetics of the asphaltenic heteroatom and metal removal reactions, Energy & Fuels 14, 1309-1313.

Carbognani, L., Gonzalez, M. F., Pereira-Almao, P. 2007. Characterization of Athabasca Vacuum Residue and Its Visbroken Products. Stability and Fast Hydrocarbon Group-Type Distributions. Energy Fuels, 21 (3), 1631-1639. (14).

Carbognani Ortega, L.; Rogel, E.; Vien, J.; Ovalles, C.; Guzman, H.; Lopez-Linares, F.; Pereira-Almao, P. Effect of Precipitating Conditions on Asphaltene Properties and Aggregation. Energy Fuels 2015, 29 (6), 3664-3674.

Crude Oil Resources, Natural Resources Canada, 2017.

C. O. Production, “Crude Oil Production,” July 2018.

Curiale, J.A. “Distribution and Occurrence of Metals in Heavy Crude Oils and Solid Bitumen: Implications for Petroleum Exploration”; Exploration for Heavy Crude Oil and Bitumen, AAPG Res. Conf, Santa Maria, CA Oct. 29-Nov.2, 1984.

Dahl, I.M., Tangstad, E., Mostad, H.B., Andersen, K. 1996. “Effect of Hydrotreating on Catalytic Cracking of a VGO,” vol. 34, no. 4, pp. 85–90.

Dolbear, G.E. 1998. Hydrocracking: Reactions, catalysts, and processes. In Petroleum Chemistry and Refining (J.G., Speight, Ed.), Taylor & Francis, Washington, DC, Chapter 7.

Dudukovic, M.P., Larachi, F., Mills, P.L. 2002. Catalysis Review 44 (1), 123-246.

Fessenden, R.J. 1995. Organic Chemistry, Fifth Edit. Journal of Chemical Education.

Froment, G.F., Bischoff, K.B. 1990. Chemical Reactor Analysis and Design, 2nd ed. Wiley, New York.

Furimsky, E. 1983. Chemistry of catalytic hydrodeoxygenation. Catal. Rev. Sci. Eng. 25:421-458.

Furimsky, E., Massoth, F.E. 2005. Hydrodenitrogenation of petroleum. Catal. Rev. Sci. Eng. 47:297-489.

Gauthier, T., Danial Fortain, P., Merdrignac, I., Guibard, I., Quoineaud, A.-A. 2008. Studies on the evolution of asphaltene structure during hydroconversion of petroleum residues. Catal. Today 130(2-4):429-438.

Girgis, M.J., Gates, B.C. 1991. Reactivities, reaction networks, and kinetics in high-pressure catalytic hydroprocessing. Ind. Eng. Chem. Sci. 30:2021-2058.

Gioia, F., Lee, V. 1986. Effect of hydrogen partial pressure on catalytic hydrodenitrogenation of quinoline. Ind. Eng. Chem. Proc. Des. Dev. 25:918-925.

Gray, M.R., Ayasse, A.R., Chan, E.W., Veljkovic, M. 1995. Kinetics of hydrodesulfurization of thiophenic and sulfide sulfur in Athabsaca bitumen. Energy Fuels 9:500-506.

Gray, M.R.; Tykwinski, R.R.; Stryker, J.M.; Tan,X. 2011. Supramolecular assembly model for aggregation of petroleum asphaltenes. Energy Fuels 25, (7), 3125-3134.

Guibard, I., Merdrignac, I., and Kressmann, S. 2005. Characterization of refractory sulfur compounds in petroleum residue. ACS Symposium Series 895, 51-64, Washington, D.C.

Hansfors, R.C. 1964. Silica-zirconia-titania hydrocracking catalyst, U.S. Patent 3,159,588.

Hassan, A., Carbognani, L., Pereira-Almao, P. 2008. Fuel, 87, 3631-3669.

Higuerey, I., Orea, M. & Pereira, P. 2002. Estimation of Visbroken and Selective Catalytic Steam Cracked Product Stability Using IATROSCAN TLC-FID. Fuel Chemistry Division Preprints, Volumen 47(2), p. 656.

Hofmann, H., Hydrodynmics, 1977. Transport Phenomena and Mathematical Model in Trickle-Bed Reactors. Int. Chem. Eng., 17, 19.

Isoda, T., Kusakabe, K., Morooka, Sh, Mochida, I. 1998. Energy & Fuels 12, 493-502.

Jaffe, J. 1968. Co-precipitation method for making multicomponent catalysts, U.S. Patent 3,401,125.

Janessens, J.P., Elst, G., Schrikkema, E.G., Van Langeveld, A.D., Sie, S.T., Moulijin, J.A. 1996. Development of a mechanistic picture of the hydrodemettalization reaction of metallo-tetraphenylporphyrin on a molecular level. Recl. Trav. Chim. Pay-Bas. 115(11-12):465-473.

Kam, E.K.T., Al Bazzaz, H., Al Fadhli, J. 2008. Simple procedure for interpreting hydrotreating kinetic data. Ind. Eng. Chem. Res.47:8594-8601.

Kobayshi, S., Kushiyama, S., Aizawa, R., Koinuma, Y., Inoue, K., Shimizu, Y., Egi, K. 1987. Kinetic study on the hydrotreating of heavy oil. 2. Effect of catalyst pore size. Ind. Eng. Chem. Res. 26:2245-2250.

Korsten, H. and Hoffmann, U. 1996. Three-Phase Reactor Model for Hydrotreating in Pilot Trickle Bed Reactors. AIChEJournal, 42, 1350-1360.

Lal, D., Otto, F.D. Mather, A. E. 1999. Solubility of hydrogen in Athabasca bitumen. Fuel, 78, 1437-1441.

Lecrenay, E., Sakanishi, K., Mochida, I. 1997. Catalytic hydrodesulfurization of gas oil and model Sulphur compounds over commercial and laboratory-made CoMo and NiMo catalysts: activity and reaction scheme. Catal Today 39:13-20.

Le Lannic, K., Guibard, I., and Merdrignac, I. 2007. Behavior and role of asphaltenes in a two-stage fixed bed hydrotreating process. Petrol. Sci. Tech. 25 (1-2) 169-186.

Lemcoff, Cukierman, A. L., and Martínez, O. M. 2007. "Effectiveness Factor of Partially Wetted Catalyst Particles : Evaluation and Application to the Modeling of Trickle Bed Reactors Effectiveness Factor of Partially Wetted Catalyst Particles : Evaluation and Application to the Modeling of Trickle Bed Reactors," vol. 4940.

Le Page M.D. J.F., Chatila, S.G., 1992 "Resid and Heavy Oil Processing," in Resid and Heavy Oil Hydroprocessing, Technip., Paris.

Marafi, A., Fukase, S., Al-Marri, M. and Stanislaus, A. 2003. A Comparative Study of the Effect of Catalyst Type on Hydrotreating Kinetics of Kuwaiti Atmospheric Residue. Energy & Fuels, 17, 661-668..

Macias, M.J., Ancheyta, J., 2004. Simulation of an isothermal hydrodesulfurization small reactor with different catalyst particle shapes. Catalysis Today 98, 243-252.

Mehran S, Amarjeet B, Argyrios M (2007) Biodesulfurization of refractory organic sulphur compounds in fossil fuels. Biotechnol Adv 25:570-596.

Mederos, F.S., Ancheyta, J., 2007. Mathematical modeling and simulation of hydrotreating reactors: cocurrent versus countercurrent operations. Applied Catalysis A: General 332, 8-21.

Mederos, F.S., Rodriguez, M.A., Ancheyta, J., and Arce, E., "Dynamic modeling and simulation of catalytic hydrotreating reactors," Energy and Fuels, vol. 20, no. 3, pp. 936–945, 2006.

Merdrignac, I., Quoineaud, A.-A., and Gauthier, T.2006. Evolution of asphaltene structure during hydroconversion conditions. Energy Fuels 20 (5): 2028-2036.

Mochida, I., Choi, K. H., 2006. Current progress in catalysts and catalysis for hydrotreating. In Practical advances in Petroleum Processing, Volume I (C.S. Hsu, P.R. Robinson, Eds.), Springer, New York, Chapter 9.

Muske K.R., and Rawlings, J.B., "Nonlinear moving horizon state estimation," pp. 349–350.

Oil Sands Magazine, 2018.

Prins, R., De Beer, V. H. J., and Somorjai, G. A., "Structure and Function of the Catalyst and the Promoter in Co — Mo Hydrodesulfurization Catalysts Structure and Function of the Catalyst and the Promoter in Co-Mo Hydrodesulfurization Catalysts," vol. 4940, 2008.

Raia, J. C., Villalanti, D. C., Subramanian, M., & Williams, B. (2000). Application of High-Temperature Simulated Distillation to the Residuum Oil Supercritical Extraction Process in Petroleum Refining. Journal of Chromatographic Science, 38(1), 1–5.

Raid, R.C., Prausnitz, J.M., Poling, B.E., 1987. The properties of Gases & Liquids, 4th ed. McGraw-Hill, New York.

Rana, M.S., Ancheyta, J., Maity, S.K., and Rayo, P. 2007a. Hydrotreating of Maya Crude Oil.: I. Effect of support composition and its pore-diameter on asphaltene conversion. Petrol. Sci. Technol. 25 (1-2): 187-200.

Rana, M.S., Sámano, V., Ancheyta, J., and Diaz, J. A. I. 2007 "A review of recent advances on process technologies for upgrading of heavy oils and residua," Fuel, vol. 86, no. 9 SPEC. ISS., pp. 1216–1231.

Rashad, J., de Klerk, A. 2012. Desulfurization of heavy oil, Applied Petroleum Research 1:3-19.

Rodriguez, M.A., Ancheyta, J. 2004. Modeling of Hydrodesulfurization (HDS), Hydrodenitrogenation (HDN), and the Hydrogenation of aromatics (HDA) in a vacuum Gas Oil Hydrotreater. Energy & Fuels 18, 789-794.

Rodriguez-DeVecchis, V. M., Carbognani Ortega, L., Scott, C. E., & Pereira-Almao, P. 2015. Use of Nanoparticle Tracking Analysis for Particle Size Determination of Dispersed Catalyst in Bitumen and Heavy Oil Fractions. Industrial & Engineering Chemistry Research, 54(40), 9877-9886.

ROI (Revamping and Optimizing Inc.), "Partial Upgrading: Background Review in Support of National Partial Upgrading Program," October 25, 2015.

Sakornwimon, W., Sylvester, D. 1982 "Effectiveness factors for partially wetted catalysts in trickle-bed reactors" pp. 16–25, 1982.

Satterfield, C.N., 1975. “Trickle-Bed Reactors,” AIChE J., vol. 21, no. 2, pp. 209–228..

Scheele. E, 20018. Assesment of Stage 1 in a Novel Bio-Oil Upgrading Process: Catalytic Hydrotreating. University of Calgary: Calgary.

Shiflett, W. 2002. User’s guide to the chemistry, kinetics and basic engineering of hydroprocessing. 5th intern. Conf. Refin. Proc., AIChE Spring Nat. Meeting, New Orleans, March 11-14, 2002, pp. 101-122.

Shimura, M., Shiroto, Y., Takeuchi, C. (1986) Ind. Eng. Chem. Fundam., 25:330.

Speight, J.G., The Desulfurization of Heavy Oils and Residua, 2nd edm. New York, 2000.

Speight, J.G., Coal, shale, Natural Bitumen, Heavy Oil, and Peat – Vol II – Natural Bitumen (Tar Sands) and Heavy Oil.

Speight, J.G. 1999. The Chemistry and Technology of Petroleum, 3rd ed., Marcel Dekker; New York.

Stanislaus, A., Fukase, R., Koide, A., Marafi, A., Jasem, F., Absi-Halabi, M. 1999. Effect of temperature and space velocity in hydrotreating Kuwait atmospheric residue over an industrial HDM catalyst. Kuwait Istitute for Scientific Research, Report # KISR 5578, Kuwait.

Topsoe, H., Clausen, B.S., Massoth, F.E. 1996. Hydrotreating catalysis, Science and Technology 11:1-310.

Trujillo, M., 2018, Catalytic Upgrading Process of Ligno-Cellulose Derived Heavy Crude Oil. University of Calgary: Calgary.

Van Den Berg, F. G. A. et al., 2010. Method of producing a pipelineable blend from a heavy residue of a hydroconversion process. USA, Patent No. US7799206 B2.

Van Hasselt B.W., et al., 1999. “A numerical comparison of alternative three-phase reactors with a conventional trickle-bed reactor. The advantages of countercurrent flow for hydrodesulfurization,” Chem. Eng. Sci., vol. 54, no. 21, pp. 4791–4799.

Vitale, G., Frauwallner, M., Scott, C., and Pereira-Almao, P. 2011. Preparation and characterization of low-temperature nano-crystalline cubic molybdenum carbides and insights on their structures. Applied Catalysis A: 408 (1-2), 178-186.

Wammes, W.J.A., Westerterp, K.R., 1990. The influence of the reactor pressure on the hydrodynamics in a cocurrent gas-liquid trickle-bed reactor. In: Chemical engineering science. Vol. 45, No. 8. Pp. 2247-2254.

Whitehurst, D.D., Takaaki, I., and Mochida, I. 1998. Present state of the art and future challenges in the hydrodesulfurization of polyaromatic sulfur compounds. Advances in Catalysis, 42, 344-368.

Yui, S. M. 1989. Hydrotreating of bitumen-derived coker gas oil: Kinetics of hydrodesulfurization, hydrodenitrogenation , and mild hydrocracking, and correlations to predict product yields and properties. AOSTRA J. Res. 5, (3), 211-224.

APPENDIXES

APPENDIX A. RTU-1 P&ID

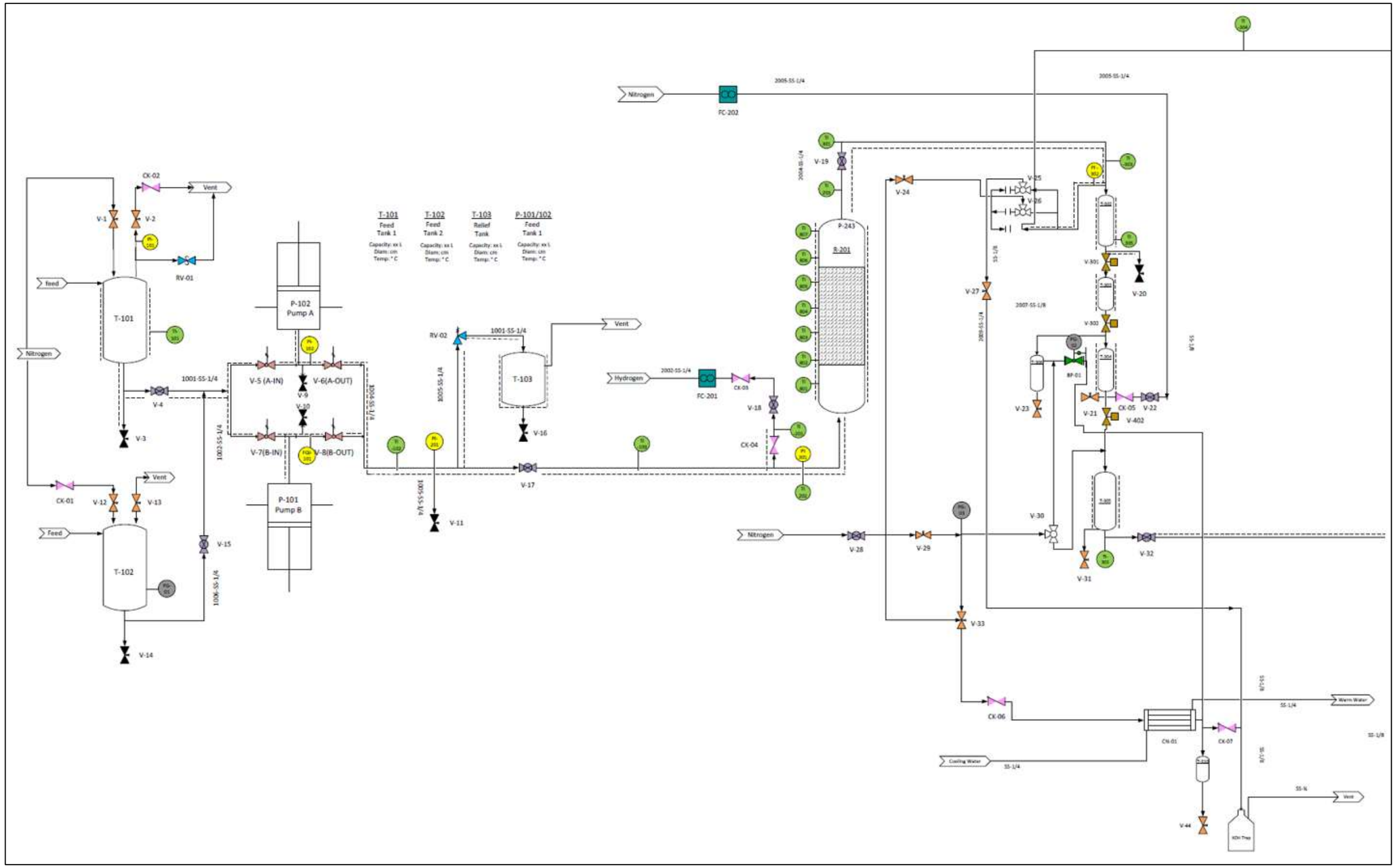

Figure A.1 Reactivity Test Unit-1

APPENDIX B. Properties Estimation Correlations

B.1 Mass Transfer coefficients

Gas–Liquid Mass Transfer Coefficients:

$$\frac{k_i^L a_L}{D_i^L} = 7\left(\frac{G_L}{\mu_L}\right)^{0.4}\left(\frac{\mu_L}{\rho_L D_i^L}\right)^{0.5}\ ,\ i = H_2, H_2S \qquad \text{B.1}$$

Liquid-Solid Mass Transfer Coefficients:

$$\frac{k_i^S}{D_i^L a_S} = 1.8\left(\frac{G_L}{a_S \mu_L}\right)^{0.5}\left(\frac{\mu_L}{\rho_L D_i^L}\right)^{1/3},\ i = H_2, H_2S, Sul, Asph \qquad \text{B.2}$$

$$k_i^S(\frac{cm}{s}), D_i^L\left(\frac{cm^2}{s}\right), a_S\left(\frac{1}{cm}\right), G_L\left(\frac{g}{cm^2 \cdot s}\right), \mu_L\left(mPa.s\right), \rho_L(\frac{g}{cm^3})\ ,\ i = H_2, H_2S, Sul, Asph$$

Molecular Diffusivities:

$$D_i^L = 8.93\times10^{-8}\frac{\upsilon_L^{0.267} T}{\upsilon_i^{0.433}\mu_L}\ ,\ i = H_2, H_2S, Sul, Asph \qquad \text{B.3}$$

$$D_i^L\left(\frac{cm^2}{s}\right), \upsilon_L \,\&\, \upsilon_i\left(\frac{cm^3}{mol}\right), T\left(K\right), \mu_L\left(mPa\cdot s\right)$$

Molar Volumes:

$$\upsilon_L = 0.285\left(\upsilon_C^L\right)^{1.048} \qquad \text{B.4}$$

$$\upsilon_i = 0.285\left(\upsilon_C^i\right)^{1.048},\ i = H_2, H_2S \qquad \text{B.5}$$

$$\upsilon_L\left(\frac{cm^3}{mol}\right), \upsilon_C^L\left(\frac{cm^3}{mol}\right), \upsilon_i\left(\frac{cm^3}{mol}\right), \upsilon_C^i\left(\frac{cm^3}{mol}\right)$$

$$\upsilon_C^L = 7.5214\times10^{-3}\left(T_{meABP}\right)^{0.2896}\left(d_{15.6}\right)^{-0.7666}\cdot MW_{crude}\cdot\frac{lb}{453.59g}\cdot\frac{28316.8cm^3}{ft^3} \qquad \text{B.6}$$

$$\upsilon_C^L\left(\frac{cm^3}{mol}\right), T_{meABP}(R), MW_{crude}(\frac{g}{mol})$$

B.2 Henry's Coefficient

$$\ln h_{H_2} = 11.92 - 0.001194 \times T - 1.166 \times \ln T \qquad \text{B.7}$$

$$\mathrm{H}_{H_2} = h_{H_2} \times \upsilon_{H_2} \qquad \text{B.8}$$

$$h_{H_2}(MPa), T(K), H_{H_2}\left(\frac{MPa \cdot cm^3}{mol}\right), h_{H_2}(MPa), \upsilon_{H_2}\left(\frac{cm^3}{mol}\right)$$

$$\mathrm{H}_{H_2S} = \frac{\upsilon_{H_2S}}{\lambda_{H_2S} \bullet \rho_L} \qquad \text{B.9}$$

$$\lambda_{H_2S} = 2.51182 - 1.40751 \times 10^{-3} T \qquad \text{B.10}$$

$$\lambda_{H_2S}\left(\frac{cm^3}{MPa \cdot g}\right), T(K)\ H_{H_2S}\left(\frac{MPa \cdot cm^3}{mol}\right), \lambda_{H_2S}\left(\frac{cm^3}{MPa \cdot g}\right), \upsilon_{H_2S}\left(\frac{cm^3}{mol}\right), \rho_L\left(\frac{g}{cm^3}\right)$$

B.3 Oil Density & Viscosity

$$\rho_{Crude} = \rho_0 + \Delta\rho_P - \Delta\rho_T \qquad \text{B.11}$$

$$\rho_L, \rho_0\ \&\ \Delta\rho_P\ \&\ \Delta\rho_T\left(\frac{lb}{ft^3}\right)$$

$$\rho_L = \rho_{Crude} \times \frac{453.59}{28316.8} \qquad \text{B.12}$$

$$\Delta\rho_P = \left[0.167 + 16.181 \times 10^{-0.0425\rho_0}\right]\left[\frac{P}{1000}\right] - 0.01 \times \left[0.299 + 263 \times 10^{-0.0603\rho_0}\right]\left[\frac{P}{1000}\right]^2 \qquad \text{B.13}$$

$$\Delta\rho_T = \left[0.0133 + 152.4\left(\rho_0 + \Delta\rho_P\right)^{-2.45}\right](T - 520) - \left[8.1 \times 10^{-6} - 0.0622 \times 10^{-0.764(\rho_0 + \Delta\rho_P)}\right](T - 520)^2 \qquad \text{B.14}$$

$$\rho_L\left(\frac{gr}{cm^3}\right),\rho_{Crude}\left(\frac{lb}{ft^3}\right),\Delta\rho_P\left(\frac{lb}{ft^3}\right),P\left(psia\right),\Delta\rho_T\left(\frac{lb}{ft^3}\right),T\left(^\circ R\right)$$

$$\mu_L = 3.141\times10^{10}\left(T-460\right)^{-3.444}\left[\log_{10}\left(API\right)\right]^a \qquad \text{B.15}$$

$$a = 10.313\left[\log_{10}\left(T-460\right)\right]-36.447 \qquad \text{B.16}$$

$$\mu_L\left(mPa\cdot s\right),T\left(^\circ R\right)$$

B.4 Characteristics of Catalyst Bed

$$a_S = \frac{6}{d_p}\left(1-\varepsilon\right) \qquad \text{B.17}$$

$$\varepsilon = 0.38+0.073\left[1+\frac{\left(\left(D_R/d_p\right)-2\right)^2}{\left(D_R/d_p\right)^2}\right] \qquad \text{B.18}$$

$$\theta = \rho_P V_g = V_g\frac{\rho_B}{1-\varepsilon} \qquad \text{B.19}$$

$$V_P = \frac{4}{3}\cdot\pi\cdot\left(\frac{d_p}{2}\right)^3 \qquad \text{B.20}$$

$$S_p = 4\cdot\pi\cdot\left(\frac{d_p}{2}\right)^2 \qquad \text{B.21}$$

$$a_S\left(\frac{1}{cm}\right),D_R\left(cm\right),\rho_P\ \&\ \rho_B\left(\frac{g}{cm^3}\right),V_P\left(cm^3\right),d_p\left(cm\right),S_P\left(cm^2\right)$$

B.5 Effectiveness Factor

$$\Phi_{Sul} = \frac{V_P}{S_P}\left[\left(\frac{n+1}{2}\right)\left(\frac{k_{HDS}C_{Sul}^{s\ (n-1)}\rho_P}{De_{Sul}}\right)\right]^{0.5} \qquad \text{B.22}$$

$$De_{Sul} = \frac{\theta}{\tau}\left(D_{Sul}^{L}\right) \quad \text{B.23}$$

$$\eta_{HDS} = \frac{\tanh \Phi_{Sul}}{\Phi_{Sul}} \quad \text{B.24}$$

$$\Phi_{Asph} = \frac{V_P}{S_P}\left[\left(\frac{e+1}{2}\right)\left(\frac{k_{HDAs} C_{Asph}^{s\ (e-1)} \rho_P}{De_{Asph}}\right)\right]^{0.5} \quad \text{B.25}$$

$$De_{Asph} = \frac{\theta}{\tau}\left(D_{Asph}^{L}\right) \quad \text{B.26}$$

$$\eta_{HDAs} = \frac{\tanh \Phi_{Asph}}{\Phi_{Asph}} \quad \text{B.27}$$

$$De_{Asph}\ \&\ De_{Sul}\left(\frac{cm^2}{s}\right), C_{Asph}^{S}\ \&\ C_{Asph}^{S}\left(\frac{mol}{cm^3}\right),$$

B.6 Flow Condition

$$\dot{\upsilon}_{Crude} = \frac{m_{cat} \times WHSV}{\rho_{bitumen} \times 60} \quad \text{B.28}$$

$$\dot{\upsilon}_{H_2} = 900 \times \dot{\upsilon}_{Crude} \quad \text{B.29}$$

$$u_L = \frac{\dot{\upsilon}_{Crude}}{A_C \times 60} \quad \text{B.30}$$

$$u_G = \frac{\dot{\upsilon}_{H_2}}{A_C \times 60} \quad \text{B.31}$$

$$G_L = \frac{\dot{\upsilon}_{Crude} \times \rho_L}{A_C \times 60} \quad \text{B.32}$$

$$\dot{\upsilon}_{Crude}\ \&\ \dot{\upsilon}_{H_2}\left(\frac{cm^3}{\min}\right), m_{cat}(g), WHSV(\frac{1}{hr}), \rho_{bitumen}\ \&\ \rho_L\left(\frac{g}{cm^3}\right), u_L\ \&\ u_G(\frac{cm}{s}), A_C\left(cm^2\right), G_L\left(\frac{g}{cm^2 \cdot s}\right)$$

APPENDIX C. Copyright Permissions

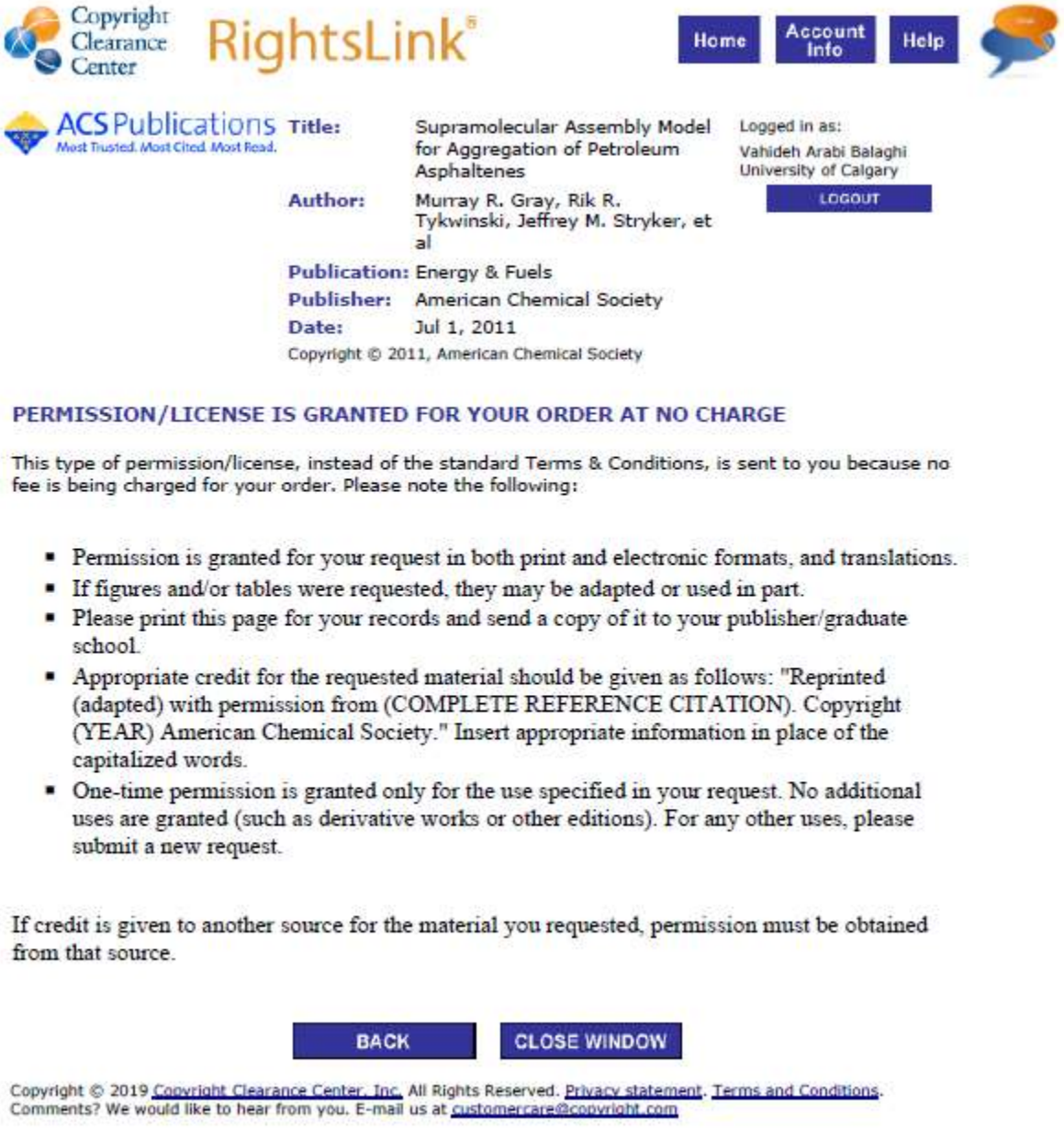

Copyright Clearance Center RightsLink®

Home | Account Info | Help

ACS Publications
Most Trusted. Most Cited. Most Read.

Title: Supramolecular Assembly Model for Aggregation of Petroleum Asphaltenes

Author: Murray R. Gray, Rik R. Tykwinski, Jeffrey M. Stryker, et al

Publication: Energy & Fuels

Publisher: American Chemical Society

Date: Jul 1, 2011

Copyright © 2011, American Chemical Society

Logged in as:
Vahideh Arabi Balaghi
University of Calgary

LOGOUT

PERMISSION/LICENSE IS GRANTED FOR YOUR ORDER AT NO CHARGE

This type of permission/license, instead of the standard Terms & Conditions, is sent to you because no fee is being charged for your order. Please note the following:

- Permission is granted for your request in both print and electronic formats, and translations.
- If figures and/or tables were requested, they may be adapted or used in part.
- Please print this page for your records and send a copy of it to your publisher/graduate school.
- Appropriate credit for the requested material should be given as follows: "Reprinted (adapted) with permission from (COMPLETE REFERENCE CITATION). Copyright (YEAR) American Chemical Society." Insert appropriate information in place of the capitalized words.
- One-time permission is granted only for the use specified in your request. No additional uses are granted (such as derivative works or other editions). For any other uses, please submit a new request.

If credit is given to another source for the material you requested, permission must be obtained from that source.

BACK | CLOSE WINDOW

Copyright © 2019 Copyright Clearance Center, Inc. All Rights Reserved. Privacy statement. Terms and Conditions.
Comments? We would like to hear from you. E-mail us at customercare@copyright.com

Copyright Clearance Center

Catalysis today

Order detail ID:	71838226
Order License Id:	4542141395168
ISSN:	0920-5861
Publication Type:	Journal
Volume:	
Issue:	
Start page:	
Publisher:	ELSEVIER BV

Permission Status: Granted

Permission type: Republish or display content

Type of use: Thesis/Dissertation

Hide details

Requestor type	Author of requested content
Format	Print, Electronic
Portion	chart/graph/table/figure
Number of charts/graphs/tables/figures	1
The requesting person/organization	Vahideh Arabi Balaghi
Title or numeric reference of the portion (s)	Fig. 8 effect of pore diameter and specific surface area on hydrotreating catalyst activities.
Title of the article or chapter the portion is from	hydroprocessing of heavy petroleum feeds: Tutorial
Editor of portion(s)	N/A
Author of portion(s)	Jorge Ancheyta, Mohan S. Rana, Edward Furimsky
Volume of serial or monograph	N/A
Page range of portion	6/13
Publication date of portion	2005
Rights for	Main product
Duration of use	Life of current edition
Creation of copies for the disabled	no
With minor editing privileges	no
For distribution to	Worldwide
In the following language(s)	Original language of publication
With incidental promotional use	no
Lifetime unit quantity of new product	Up to 499
Title	Partial Upgrading of Oilsands Bitumen and Heavy Oil: Kinetic Modeling and Reactor Design
Institution name	University of Calgary
Expected presentation date	Mar 2019

Applied Petrochemical Research

Order detail ID:	71838174
Order License Id:	4542111166021
ISSN:	2190-5525
Publication Type:	Journal
Volume:	
Issue:	
Start page:	
Publisher:	SpringerOpen

Permission Status: Granted

Permission type: Republish or display content
Type of use: Thesis/Dissertation

Hide details

Requestor type	Author of requested content
Format	Print, Electronic
Portion	chart/graph/table/figure
Number of charts/graphs/tables/figures	1
The requesting person/organization	Vahideh Arabi Balaghi
Title or numeric reference of the portion (s)	Table 3 Selected properties of two Canadian oilsands-derived bitumens in comparison with West Texas Intermediate (WTI) as a benchmark light crude oil
Title of the article or chapter the portion is from	Desulfurization of heavy oil
Editor of portion(s)	N/A
Author of portion(s)	Rashad Javadli,Arno de Klerk
Volume of serial or monograph	N/A
Page range of portion	3/17
Publication date of portion	1 March 2012
Rights for	Main product
Duration of use	Life of current and all future editions
Creation of copies for the disabled	no
With minor editing privileges	no
For distribution to	Worldwide
In the following language(s)	Original language of publication
With incidental promotional use	no
Lifetime unit quantity of new product	Up to 499
Title	Partial Upgrading of Oilsands Bitumen and Heavy Oil: Kinetic Modeling and Reactor Design
Institution name	University of Calgary
Expected presentation date	Mar 2019